

**THE STRUCTURAL, THERMAL, AND FLUID EVOLUTION OF  
THE LIVINGSTONE RANGE ANTICLINORIUM, AND ITS  
REGIONAL SIGNIFICANCE TO THE SOUTHERN ALBERTA  
FORELAND THRUST AND FOLD BELT**

by

Michael Ames Cooley

A thesis submitted to the Department of Geological Sciences and Geological Engineering

In conformity with the requirements for

the degree of Doctor of Philosophy

Queen's University

Kingston, Ontario, Canada

(November, 2007)

Copyright ©Michael Ames Cooley, 2007



View north along the Livingstone Range. Photo by R. A. Price.

## Abstract

The Livingstone Range anticlinorium (LRA) is a long (>65 km) narrow (<5 km) structural culmination that coincides with a major hanging-wall ramp across which the Livingstone thrust cuts ~1000 m up-section eastward from a regional décollement in the upper part of Devonian Palliser Formation to another regional décollement within Jurassic Fernie Formation. The presence of Precambrian basement fluids prior to thrusting and folding are recorded in the LRA by deformed jasper+/-fluorite+/-sphalerite veins, and adjacent haloes of altered, dolomitic host rock with high  $^{87}\text{Sr}/^{86}\text{Sr}$  ratios (0.7094 to 0.7100) relative to most host rocks. Basement fluids are a possible source for anomalously radiogenic strontium that occurs in the diagenetically altered Paleozoic carbonate rocks in the LRA and throughout the Western Canada Sedimentary Basin, but underlying thick shale strata such as the Exshaw Formation are also possible source. The earliest stages of thrusting deformation involved the development of distinctive chevron-style, flexural-slip thrust-propagation folds that have conspicuous blind thrust faults along their hinge zones. The hinge-zone thrust system of the Centre Peak anticline consists of a series of stacked detachment thrusts, each of which emerges from a different zone of interbed slip in the backlimb of the anticline and deflects the hinge zone eastward. Each successively lower detachment thrust dies out in the hinge zone at approximately the same stratigraphic level as an overlying detachment thrust fault that emerges from a bedding detachment zone in the backlimb. Fluid flow during thrust-propagation folding is recorded by dolomite+/-calcite veins with isotopic compositions that are similar to those of host rocks. Fluid flow occurred along faults related to thrust-propagation folding, and also along many tear faults and larger thrust faults. Veins in these fault zones have slightly higher  $^{87}\text{Sr}/^{86}\text{Sr}$  ratios relative to adjacent host rocks and are interpreted to have formed from a mixture of formation fluids and hotter basement fluids in a rock-dominated system. Oxygen isotope thermometry of four syn-folding veins indicates they precipitated at anomalously high temperatures (>250°C). The youngest episode of fluid flow along thrust faults and tear faults is recorded by calcite veins with very low  $\delta^{18}\text{O}$  values (-18 to -9‰ PDB), which are interpreted to have precipitated along faults that were active while the LRA was being transported eastward and elevated by underlying thrust faults, and cooled by infiltrating meteoric water. The conduits along which significant meteoric fluid circulation occurred are marked by visibly altered host rocks that have anomalously low  $\delta^{18}\text{O}$  values and slightly lower  $\delta^{13}\text{C}$  values relative to most host rocks.

Rapid cooling due to deep infiltration of meteoric water into the shallow brittle surface of the deforming earth is almost certainly not restricted to thrust and fold belts, nor is its thermal effect necessarily restricted to the upper few kilometers. This model for fluid flow has significant implications for predicting thermal conditions in deep metamorphic rocks that lie beneath the brittle crust, the most obvious effect being to push down the brittle/ductile transition zone, which would enhance even deeper meteoric fluid circulation and cause the deflection of underlying isotherms.

## **Co-Authorship**

Raymond A. Price

Department of Geological Sciences and Geological Engineering

Queen's University, Kingston, ON K7L 3N6

John M. Dixon

Department of Geological Sciences and Geological Engineering

Queen's University, Kingston, ON K7L 3N6

T. Kurtis Kyser

Department of Geological Sciences and Geological Engineering

Queen's University, Kingston, ON K7L 3N6

## Acknowledgements

Thanks to my wife Tina, for her understanding and patience throughout what has been, at times, a selfish endeavor, and for her word-processing prowess during the final assembly of the oh-so-many parts of this thesis. I promise her I have no intention of doing another PhD and can now devote my spare time to raising kid(s?), home renovation, camping, etc.

Thanks to Ray Price, for suggesting this very cool thesis topic and study area, and for sharing his contagious enthusiasm for the rocks of the Crowsnest Pass. I must thank Ray as well for helping me improve my writing skills with the countless revisions I have made him endure.

Thanks to John Dixon. I benefited greatly from his guidance and input during preparation for the many FRP and CSPG conferences that he encouraged me to attend, and for the final thesis revisions that were promptly returned. Unlimited deck-swabbing is definitely owed to John.

Thanks to Kurt Kyser, for his ruthless and effective editing which reduced the geochemical results section from eight pages and five figures of boring, repetitive, overly detailed data regurgitation to a concise, efficient summary in only four pages and three figures. Geochemical data presentation is both an art and a science.

Thanks to Margot McMechan for some very pointed criticisms that led me to do just a bit more re-thinking and re-writing, which resulted in making the interpretations of this thesis more solid.

Thanks to the lab techs of Q.F.I.R.; Kerry Klassen, Don Chipley and April Vuletich for their countless hours of help in the lab, from explaining analytical procedures, to running my samples, and for simply explaining how stuff works.

Thanks to Greg Cameron, Scott Conley and Kyle Larson for their excellent assistance in the field, which included cooking skills, driving skills, musical skills, and for helping prove that the Mike Cooley million-step weight-loss plan really works.

## **Statement of Originality**

I hereby certify that all of the work described within this thesis is the original work of the author.

Any published (or unpublished) ideas and/or techniques from the work of others are fully acknowledged in accordance with the standard referencing practices.

Michael Ames Cooley

November, 2007

# Table of Contents

Abstract.....	iii
Co-Authorship .....	v
Acknowledgements.....	vi
Statement of Originality.....	vii
Table of Contents.....	viii
List of Figures.....	xi
List of Tables .....	xix
Chapter 1 Introduction.....	1
1.1 Regional Geological Summary .....	1
1.2 Structural geology of the LRA.....	3
1.3 Fluid flow in the LRA.....	4
1.4 Summary of conclusions.....	5
1.5 References.....	6
Chapter 2 Chevron-style, flexural-slip thrust-propagation folding, Livingstone Range anticlinorium, southern Alberta Foothills, Canada. ....	9
2.1 Abstract.....	9
2.2 Introduction.....	11
2.3 Stratigraphy of the southern Livingstone Range.....	16
2.4 Structural Geology of the southern Livingstone Range.....	19
2.4.1 <i>Overview</i> .....	19
2.5 Cross-strike discontinuities (tear faults or lateral thrust ramps) .....	31
2.5.1 <i>Interpretation</i> .....	31
2.6 Transverse Zones of Intense Fracturing and Minor Faulting.....	32
2.6.1 <i>Observations</i> .....	32
2.6.2 <i>Interpretation</i> .....	34
2.7 Detachment Thrust Faults.....	35
2.7.1 <i>Observations</i> .....	35
2.7.2 <i>Interpretation; significance of detachments in the LRA</i> .....	44
2.8 The Centre Peak Anticline thrust-propagation fold .....	45
2.8.1 <i>Observations</i> .....	45
2.8.2 <i>Interpretation; Evolution of the Centre Peak anticline</i> .....	49
2.8.3 <i>Deformation model of the Centre Peak anticline</i> .....	51

2.8.4	<i>Fracture analysis of the Centre Peak anticline</i> .....	55
2.9	Cataclastic Flow.....	59
2.10	Conclusions.....	60
2.11	Acknowledgements.....	63
2.12	References.....	64
Chapter 3	Stable-isotope geochemistry of syntectonic veins in the Livingstone Range anticlinorium and their significance to the thermal and fluid evolution of the southern Canadian Foreland Thrust and Fold Belt.....	67
3.1	Abstract.....	67
3.2	Introduction.....	69
3.3	Geological Setting.....	72
3.4	Structural Geology of the southern Livingstone Range.....	73
3.4.1	<i>Southern part of the study area (Green, Morin and Caudron Creeks)</i> .....	80
3.4.2	<i>Central part of the study area (Daisy Creek area)</i> .....	81
3.4.3	<i>North part of the study area (Pocket Creek area)</i> .....	86
3.4.4	<i>Descriptions of Veins</i> .....	89
3.5	Isotope Geochemistry.....	95
3.5.1	<i>Analytical Methods</i> .....	95
3.5.2	<i>Results</i> .....	97
3.6	Interpretation.....	107
3.6.1	<i>Pre-thrusting dolomitization and diagenesis</i> .....	107
3.6.2	<i>Pre-thrusting hydrothermal fluids</i> .....	109
3.6.3	<i>Early syn-thrusting formation fluid flow +/- basement fluids</i> .....	112
3.6.4	<i>Late syn-thrusting meteoric fluid flow and vein formation</i> .....	116
3.7	Regional Implications of the Isotopic Data.....	118
3.7.1	<i>Regional dolomitization and infiltration of basement fluid</i> .....	118
3.7.2	<i>Pre-thrusting hot thermal event</i> .....	119
3.7.3	<i>Initial syn-thrusting fluid flow</i> .....	119
3.7.4	<i>Regional syn-thrusting meteoric fluid infiltration</i> .....	120
3.8	Conclusions.....	124
3.9	Acknowledgements.....	126
3.10	References.....	127
Chapter 4	Conclusions and recommendations for further work.....	133

4.1	Structural geology conclusions .....	133
4.2	Isotope-geochemistry Conclusions .....	135
4.3	Summary of Hydrocarbon Exploration Significance .....	138
4.4	Recommendations for further work .....	140
4.4.1	<i>Analogue modelling of bedding-detachment thrust-propagation folding</i> .....	140
4.4.2	<i>Direct dating of veins (and deformation) using Sm-Nd in fluorite.</i> .....	141
4.4.3	<i>Fluid inclusion study of veins.</i> .....	141
4.4.4	<i>Recognition and documentation of major conduits of meteoric fluid circulation.</i>	
	141	
4.5	References.....	142

## List of Figures

Figure 2-1. Regional geological setting of the study area at the south end of the Livingstone Range, southern Alberta foothills. Cross section X X' is modified from Price (cross section of Fernie map, in preparation). Cross section Y Y' is modified from an unpublished 1999 cross section of Paul Mackay..... 13

Figure 2-2. Geologic map of the study area. The LRA comprises generally north-trending segments that are separated by regularly-space cross-strike discontinuities. Most are tear faults marked by abrupt changes in fold plunges and dextral offsets of folds, but the southern one (Rock Creek discontinuity) may be a blind tear fault or lateral ramp. The location of this map is shown in Figure 2-1. Map units are the same as those in Figure 2-3. The cross section locations depicted in this figure are for sections illustrated in Figure 2-5. Contoured equal area plots of poles to bedding in equal area projection from the lower hemisphere, plotted using GEORient© 9.1 (R. J. Holcombe, University of Queensland)..... 15

Figure 2-3. Carboniferous stratigraphy of the study area. A schematic east-west section showing stratigraphic relationships of the Crowsnest Pass area is presented in A (modified from Norris, 1993). B is a composite stratigraphic section of the formations that were mapped and measured in the study area. Map units are explained in the legend in Figure 2-4. .... 17

Figure 2-4. Geologic map of the southern part of the study area..... 20

Figure 2-5. Cross sections through the Livingstone Range anticlinorium. The locations of cross sections are shown in Figure 2-2 and on maps in Figures 2-4 (sections A-A' to E-E'), Figure 2-7 (sections F-F' and G-G') and Figure 2-8 (sections H-H', I-I' and J-J'). .... 21

Figure 2-6. View southward at Centre Peak anticline on the northeast side of Centre Peak. Banff Formation is juxtaposed over the upper part of Turner Valley Member along a thrust that cuts up through the forelimb of the anticline. This fault merges along strike to the north with the Ernst Creek thrust, which dies out southward in the core of the Centre Peak anticline (see Figures 2-4 and 2-7)..... 25

Figure 2-7. Geologic map of the Daisy Creek area. The legend for this map is the same as Figure 2-8. .... 26

Figure 2-8. Geologic map of the northern part of the study area. .... 27

Figure 2-9. View south at the folds and related thrust faults along the north slopes of Thunder Mountain..... 30

Figure 2-10. Photographs of transverse zones of intense fracturing and minor faulting in the LRA. *A* – vertical air photo of the Cross anticline at Caudron Creek. The east-west trending gullies mark the locations of transverse east-west zones of fracturing and faulting that cut Turner Valley Member limestone in the core of the anticline at regularly-spaced (~150 metre) intervals, but –note that they do not extend into the overlying Mount Head dolomite and shale. *B* - view to the west at the core of the Centre Peak anticline south of Morin Creek. The black arrows mark the locations of transverse zones of fracturing and faulting that cut through the east limb. The dashed line marks the surface trace of the thrust fault that lies along the hinge zone of the anticline. *C* - view to the west at intensely fractured limestone within a transverse zone of fracturing and faulting. White arrow points along the main fault contact where photo *D* was taken. The handle of the rock hammer in the circle at lower centre of photo is 33 cm long. *D* – the white arrow points along a steeply dipping vein of black hydrocarbon residue that formed along a transverse fault surface, a common feature in zones of transverse fracturing and faulting. View is to the west. Pencil is 14 cm long. .... 33

Figure 2-11. View south at the core of the Centre Peak anticline as exposed on the south side of the Green Creek canyon. The planar limbs of the anticline are separated by a composite, east-verging thrust fault that extends along the hinge zone. The lower segment, at the level of Green Creek, is a near-vertical thrust fault that is sub-parallel with the steep bedding in the micrite unit of the Banff Formation (Cbm) in the forelimb of the anticline but cuts up-section through the sub-horizontal bedding of the grainstone unit (Cbg) and micrite unit (Cbm) in the hinge zone. Approximately 150 metres above the creek, this cross-cutting, sub-vertical fault is interpreted to die out within the hinge zone of the anticline within the lower part of the Turner Valley Member (Clvtv). This fault is overlapped by a thrust that emerges from a bedding detachment ~20 metres below the top of the Banff Formation, deflects the hinge zone eastward as it truncates the Turner Valley Member (Clvtv) in its footwall, and then curves upward into the core of the Centre Peak anticline as it cuts up-section through the Turner Valley Member (Clvtv) in its hanging-wall as it becomes sub-parallel with the bedding in its footwall. The footwall and hanging-wall cut-offs of the top of the Banff Formation along this thrust fault, which are marked by X and X', respectively, have been offset ~250 metres along this fault. These structural relationships have been projected northward into section A-A' in Figure 2-5. .... 38

Figure 2-12. (following page) View south at the upper part of the core of the Centre Peak anticline exposed in the Green Creek canyon. A - A network of sub-vertical and bedding-

parallel thrust faults deforms the upper part of the Turner Valley Member (Clvtv) within the upper forelimb. Extension faults (dotted lines) offset bedding in the core of the anticline. Thrust displacements also occur in the hinge zone and in the backlimb, forming duplex structures that thicken the fold hinge. Individual marker beds within this fault network, such as a distinctive brown weathering fine grained dolomitic limestone in the upper part of the Turner Valley Member (Clvtv-b), are represented by discontinuous elongate blocks ‘floating’ within a matrix of highly faulted and brecciated host rock fragments. B - The detachment thrust fault that emerges from the backlimb ~20 metres below the top of the Banff Formation (Cbm) dies out upward within the zone of intense faulting in the upper part of the forelimb..... 39

Figure 2-13. (following page) View north at the core of the Centre Peak anticline as exposed on the north side of the Green Creek canyon. The planar fold limbs are separated by a composite, east-verging thrust fault that extends along the hinge zone of the anticline. This fault consists of three distinct segments, two of which emerge from bedding-parallel detachment zones in the backlimb of the anticline (upper photo), deflect the hinge zone of the anticline, and then curve upward, cutting up-section to form a ramp through the beds in its hanging-wall. The structurally lowest fault segment, which is steeply west-dipping to vertical (lower photo), juxtaposes a ramp that cuts through the grainstone unit (Cbg) and micrite unit (Cbm) of the top of the Banff Formation in the hanging-wall with overturned and steeply dipping micrite unit (Cbm) and Turner Valley Member (Clvtv) in the footwall, that have been deformed by minor antithetic folds. This lower hinge-zone thrust is overlapped (upper photo) by a thrust that emerges from a bedding-parallel detachment in the lower part of the micrite unit (Cbm); and this middle hinge-zone thrust is, in turn, overlapped by a upper thrust that emerges from a bedding-parallel detachment in the lower part of the Turner Valley Member (Clvtv), The conspicuous bedding-parallel detachment thrust that occurs ~20 metres below the top of the Banff Formation on the south side of Green Creek (Figure 2-11) dies out in the core of the anticline between the middle and upper detachment thrusts on the north side of the creek. .... 41

Figure 2-14. View south at the core of the Centre Peak anticline as exposed along the south side of Morin Creek canyon. In the lower core of the anticline, a steeply west-dipping thrust fault juxtaposes the west-facing grainstone unit (Cbg) of the backlimb over the upper part of the micrite unit (Cbm) in the east-facing overturned forelimb. An overlying thrust fault that emerges from a bedding detachment just above the bottom of the Turner Valley Member

(Clvtv) in the backlimb of the fold truncates most of the Turner Valley Member (Clvtv) along its footwall. Near the skyline this detachment thrust curves upward and juxtaposes a hanging-wall ramp along which it steeply cuts up section through most of the Turner Valley Member (Clvtv) with a footwall “flat” that cuts sub-parallel to bedding, cutting the contact between uppermost Turner Valley Member and lowermost Mount Head Formation. A thrust fault that offsets the Misty Formation (Cm) and the lower part of the Fernie Formation (Jf) in the steeply dipping west limb of the Green Creek syncline dies out downward within the Etherington Formation (Ce) in the core of the syncline..... 43

Figure 2-15. Proposed kinematic evolution of the Centre Peak anticline, based on cross section A-A’ in Figure 2-5. .... 50

Figure 2-16. Other thrust-propagation fold models. *A* is from Jamieson (1987) showing how fold shape is related to fault ramp angle, fold intelimb angle and degree of thickening or thinning of the forelimb. *B* is from Williams and Chapman (1983) defining displacement and distance of offset of marker beds. *C* is from Wickham (1995) showing a simple thrust-propagation fold that has growth strata accumulating during fold development. *D* is from Suppe and Medwedeff showing a simple thrust-propagation fold growing self-similarly. In all of these models the tip line of the thrust is still within the area of the model and the fold has not been detached from its footwall. .... 54

Figure 2-17. (Following page) Fracture orientation data from the Centre Peak anticline plotted in equal area stereographic projection from the lower hemisphere with the bedding plane horizontal (the poles to the fractures have been rotated about the local axis of folding, together with the pole to bedding, to compensate the rotation of the bedding during folding). The forelimb (east limb) of the fold contains transverse zones of fracturing and minor faulting and also flexural-slip-related back-thrusts that involve highly variable fracture patterns adjacent to fault surfaces. Areas in the forelimb that are not adjacent to faults exhibit simpler fracture patterns (e.g. Stations M687A and M687B). Stereonet images were generated using the program GEORient© 9.1 (R. J. Holcombe, University of Queensland). 56

Figure 3-1. Regional geological setting of the study area (shown in Figure 2) at the south end of the Livingstone Range, southern Alberta foothills. Map modified from Wheeler and McFeely (1991) and Price (map of Fernie area, in preparation). Cross section X X’ modified from Price (cross section of Fernie area, in preparation). Cross section Y Y’ modified from unpublished cross section of Paul Mackay. .... 74

Figure 3-2. Geologic map of the study area. Thin dashed lines are thrust faults. Thick dashed lines are tear faults. The location of this map is shown in Figure 3-1. Map units are the same as those in Figure 3-3 and Figure 3-4. The Livingstone Range anticlinorium comprises five straight segments that are separated by regularly spaced cross-strike discontinuities. Bedding orientations within each of the five segments are shown in stereographic projections from the lower hemisphere. ....	76
Figure 3-3. Geologic map of the southern half of the Livingstone Range anticlinorium study area (based on 1:20000 geological mapping, 2000, 2001, 2002). Sample localities for geochemical analysis are labelled on the map and discussed in the text. ....	77
Figure 3-4. Geologic cross sections through the southern half of the LRA study area. The locations of cross sections and symbols for geochemical samples are shown on Figure 3-3.	78
Figure 3-5. View south at the core of the Centre Peak anticline, a typical chevron-style thrust-propagation fold in the LRA. The thin solid lines represent stratigraphic contacts. Stratigraphic units (Cbg, Cbm, Clvtv, Clvtv-b and Cmh) are described in the legend in Figure 3-3. The x and x' mark the top of the Banff Formation which has been offset by approximately 250 metres by a thrust fault that propagated out of the back limb of the fold. Thrust faults are represented by thick dashed lines. ....	79
Figure 3-6. (following page) Photographs of transverse faults in the LRA. <i>A</i> – vertical air photo of the Cross anticline at Caudron Creek. The east-west trending gullies mark the locations of transverse fault zones that cut through Turner Valley Member limestone at regularly spaced intervals in the anticlinal core. Note that most gullies do not extend into the overlying Mount Head Formation. <i>B</i> - view westward at the east limb of the Centre Peak anticline south of Morin Creek. The black arrows mark the locations of transverse faults that cut through the east limb. The dashed line marks the surface trace of the hinge of the anticline core. <i>C</i> - view westward at intensely fractured limestone within a transverse fault zone visible in Figure 3-6B. Dashed white line with arrows points along the main fault contact. The circle at lower centre of photo outlines a 33 cm-long hammer for scale. <i>D</i> is a view to the west at a vertical transverse fault surface at lower centre of photo containing black hydrocarbon residue, a common feature of fault zones. Pencil for scale is 14 cm long. ....	82
Figure 3-7. Geologic map of the Daisy Creek area. The legend for this map is on Figure 3-3. Sample localities for geochemical analysis are labelled on the map and discussed in the text. ....	84

Figure 3-8. Cross section E E' and profile section F F' through the Daisy Creek fault system. Profile section F F' is a view down to the west at a plane that strikes north and dips 45 degrees eastward. The locations of the sections are shown on Figure 3-7. Sample localities for geochemical analysis are labelled on profile section F F' ..... 85

Figure 3-9. Geologic map of the northern part of the study area. Three east-west tear faults are associated with a dextral deflection of the LRA at Pocket Creek. Sample localities for geochemical analysis are labelled on the map and discussed in the text. .... 87

Figure 3-10. Cross sections G G' and H H'. The locations of the sections are shown on Figure 3-9. .... 88

Figure 3-11. (following page) Photographs of hydrothermal veins that pre-date thrusting and folding. *A* – The flat surface facing the field of view is an east-dipping bedding surface cut by orthogonal hydrothermal veins with narrow alteration haloes in surrounding siltstone (Sample locality 374, Figure 3-3). Inset microphotographs in *A* show thinly-banded jasperoid chert cut by younger calcite. *B* - view northward at west-dipping Etherington Formation. The hammer lies on an irregular bedding surface along which brecciated hydrothermal vein fragments are cemented by calcite as shown in detail in the inset photo in the lower right corner (Sample locality 441, Figure 3-7). *C* - view southward at a west-dipping bedding-parallel hydrothermal vein cut by a near-vertical stylolitic surface. Inset microphotographs show euhedral dolomite crystals included in jasperoid chert (Sample locality 470, Figure 3-7). *D* - view eastward at a west-dipping bedding surface of dolomitic mudstone near the top of the Livingstone Formation. Three steeply dipping, en-echelon hydrothermal veins lie along an ESE-trending sinistral-sense shear zone (Sample locality 490, Figure 3-9). .... 90

Figure 3-12. (following page) Veins associated with fault zones in the LRA. *A* - view northward at the footwall of the Daisy Creek back thrust. Down-dip trending slickenlines are defined by white calcite encrusting the fault surface. *B* - view westward at calcite veins (black dashed line) that lie along the surface of the Daisy Creek back thrust, where Turner Valley Member of Livingstone Formation (Clvtv) has been thrust over Etherington Formation (Ce). *C* - view northward at an oriented sample of micritic limestone of Lower Turner Valley showing thrust-sense sigmoidal en-echelon calcite veins that developed in a duplex structure in the core of the Centre Peak anticline at Morin Creek. *D* - polished slab of dolomitic limestone and chert of the micrite unit of the top of the Banff Formation cut by two generations of calcite veins. The inset photo in *D* is a close-up view of the younger vein set

which contains dolomite, calcite and quartz. *E* - view westward at the outcrop where the sample in photo *D* was taken. This fractured rock occurs within a duplex structure in the core of the Centre Peak anticline at Green Creek. *F* - view southward at a transverse fault zone marked by breccia and massive white calcite veining that cuts through Upper Mount Head Formation in Caudron Creek. .... 93

Figure 3-13.  $\delta^{18}\text{O}$  versus  $\delta^{13}\text{C}$  values of host rock samples collected from the LRA study area. Host rocks from the top member of the Mount Head Formation and younger units have  $\delta^{13}\text{C}$  values that are consistently lower than those of older units. Three host rock samples with  $\delta^{18}\text{O}$  values  $<-10\text{‰}$  are from thrust fault zones where host rocks have been recrystallized. The shaded box represents proposed Mississippian Seawater carbonate composition, where the  $\delta^{18}\text{O}$  range is based on Killingly (1983) and Muehlenbachs (1998) and the  $\delta^{13}\text{C}$  range is based on Veizer et al. (1999). .... 98

Figure 3-14.  $\delta^{18}\text{O}$  versus  $\delta^{13}\text{C}$  values of carbonate veins collected from different types of structures in the LRA study area. The majority of veins associated with thrust-propagation folding have compositions that lie within the range of host rock compositions, represented by the box with the dashed outline. The shaded box represents proposed Mississippian Seawater carbonate composition, where the  $\delta^{18}\text{O}$  range is based on Killingly (1983) and Muehlenbachs (1998) and the  $\delta^{13}\text{C}$  range is based on Veizer et al. (1999). .... 102

Figure 3-15.  $^{87}\text{Sr}/^{86}\text{Sr}$  ratios versus  $\delta^{18}\text{O}$  values of veins and host rocks from the LRA. Hydrothermally altered host rocks (circles) have the highest  $^{87}\text{Sr}/^{86}\text{Sr}$  ratios. Tie lines connect veins with their associated host rocks. The shaded box representing ideal Mississippian Seawater carbonate composition is based on Killingly (1983) and Muehlenbachs (1998) for  $\delta^{18}\text{O}$  and Veizer et al. (1999) for  $^{87}\text{Sr}/^{86}\text{Sr}$ . All veins and host rocks have high  $^{87}\text{Sr}/^{86}\text{Sr}$  ratios relative to proposed Mississippian seawater carbonate values reported by Veizer et al. (1999). .... 106

Figure 3-16. The thermal and fluid evolution in the LRA deduced from  $\delta^{18}\text{O}$  values of host rocks and veins. .... 108

Figure 3-17. Paragenetic sequence of sedimentation, tectonic events and fluid/veining events in the LRA. .... 111

Figure 3-18. Hypothetical sequential palinspastic reconstruction of a composite balanced cross section showing the thermal, fluid, and deformation history of the southern Canadian Front Ranges and Foothills. Cross section X X' is modified from R. A. Price (cross section of Fernie map, in preparation). Cross section YY' is modified from an unpublished cross

section of Paul Mackay. Cross section locations are shown on Figure 3-1. All ages are approximate, and are based on the assumption that initial movement of Livingstone thrust occurred at ~64Ma (see text for discussion). ..... 117

Geologic Map and Cross-Sections of the southern Livingstone Range

Back Pocket

## List of Tables

Table 1. Isotopic compositions of host rocks and veins collected from the LRA. $\delta^{18}\text{O}$ and $\delta^{13}\text{C}$ values are reported relative to VPDB. Host rocks are denoted by sample numbers that end with R, Rcal, or Rdol. Vein sample numbers end with V, V1, V2, etc, where V2 indicates a younger cross-cutting vein set. Three hydrothermal vein samples are mentioned in the text but were not analyzed (374, 441, 470).....	99
Table 2. Apparent equilibration temperatures and coeval water compositions calculated from $\delta^{18}\text{O}$ values of calcite, dolomite +/- quartz in veins in fault zones in the Centre Peak anticline. The error associated with the temperature calculation is approximately +/-50 °C, which represents a range in $\delta^{18}\text{O}$ values for coeval water of +1.7/-2.3‰ for calcite/water, and +1.9/-2.5‰ for dolomite/water (*).	103

# Chapter 1 Introduction

## 1.1 Regional Geological Summary

The Foothills and Rocky Mountains of southwestern Alberta form the eastern margin of the Cordilleran foreland thrust and fold belt. The thrust and fold belt is a northeast-tapering accretionary wedge comprising sedimentary strata that have been scraped off the under-riding Laurentia craton and transported eastward with the over-riding Intermontane terrane, which is a tectonic collage of oceanic volcanic arc and sedimentary rocks that was obducted over and accreted to the western margin of Laurentia during Late Jurassic to Paleocene convergence between Laurentia and subduction zones along its western margin (Monger and Price, 1979; Price, 1981; Price, 1994).

The structure of the accretionary wedge is dominated by east-verging listric thrust faults that flatten with depth and merge into a basal décollement situated just above the contact between the sedimentary cover and underlying Paleoproterozoic basement (Bally et al., 1966). The “thin skinned” (Rodgers, 1963; Gwinn, 1964) style of deformation involved extensive sheets of Neoproterozoic to Jurassic miogeoclinal to cratonic platform sedimentary rocks that accumulated prior to the thrusting, Late Jurassic to Paleocene foreland basin clastic rocks that accumulated over the cratonic platform rocks during the thrusting, and, southwest of the study area, a very thick sequence of Mesoproterozoic rocks that accumulated in an intra-continental rift basin and are overlain by the cratonic platform and miogeoclinal rocks. These supracrustal rocks have been displaced eastward and stacked in an imbricate arrangement along the interleaved thrust faults.

In the Foothills belt of the southern Canadian Rocky Mountains the main level of exposure is the foreland-basin deposits. In the eastern Main Ranges and Front Ranges it is mainly the deeper levels of thrust sheets that are exposed (Bally et al., 1966, Dahlstrom, 1970). Most thrust sheets have undergone significant deformation; they have passed over fault-bend folds

(Suppe, 1983) and have been folded as a result of displacements on underlying younger, deeper thrust faults (Douglas, 1950; Dahlstrom, 1970; Price 1981). Duplex structures are common along most thrust faults (Boyer and Elliot, 1982; Mitra, 1986), and parts of thrust sheets have been locally deformed by tear faults or lateral thrust ramps (Douglas 1958, Dahlstrom, 1970, Price, 2001).

Thrust-propagation folding is a particular style of deformation that occurs at the “leading edges” of thrust sheets or at the tip lines of thrust faults as they propagate through stratified sedimentary rock. As a thrust fault propagates stratigraphically up-section through a thrust-propagation fold, the rate of fault propagation is less than the rate of displacement, and fold shortening compensates for the deficit in thrust propagation (Dahlstrom, 1970; Suppe and Medwedeff, 1990). Thrust-propagation folds are rarely exposed at surface, except at the lateral terminations of thrust faults (Boyer, 1986), because the “leading edges” of thrust sheets are usually eroded away, or they are deeply buried.

In the foothills of the southern Canadian foreland thrust and fold belt the “leading edge” of the Livingstone thrust sheet is very well exposed along strike for more than 30 km in the Livingstone Range anticlinorium (LRA). The LRA provides an unique opportunity to study a part of a thrust sheet that is normally eroded away, or that is deeply buried and difficult to study except through drilling or seismic imaging. The LRA is an important analogue for the type of hydrocarbon reservoirs that are currently being explored for, or exploited, in the subsurface of foreland thrust and fold belts.

## **1.2 Structural geology of the LRA**

Thrust-propagation folding was an important deformation process during thrusting and folding in the LRA. Thrust-propagation folds in the LRA are recognized by the displacement gradients along thrust faults that die out in the cores of anticlines. The blind thrusts were identified in the LRA by Douglas (1950) and illustrated by Price in Douglas et al. (1970) but the nature and timing of their formation had not been studied in detail. A principal focus of this research was to document the geometry of the thrust-propagation folds in the LRA and to elucidate the mechanisms that were at work during thrust-propagation folding. The Centre Peak thrust-propagation anticline, which is the best-exposed structure in the LRA, was the main focus of detailed mapping. Geological mapping of the LRA was conducted over 3 field seasons (2000, 2001 and 2002) at a scale of 1:10,000. Fieldwork included detailed examination and measurement of stratigraphic sections through Upper Paleozoic and Lower Jurassic strata, and extensive sampling of the orientations of bedding, fractures, veins, faults, slickensides and kinematic indicators, and collecting samples that record various fluid-rock interactions during the depositional and structural evolution of the area. Detailed mapping was supplemented by documentation of deformation at all scales, ranging from thin section petrography, detailed observations made from hand samples and outcrops, to observations made in large exposures in canyon walls and air photo analysis. Field stations were located using geographic positioning system (GPS) observations, triangulation on topographic base maps, and 1:50000 scale aerial photographs. Geological data were plotted on 1:10000 scale digital data topographic maps in UTM coordinates, datum NAD 83, Zone 11.

Chapter 2 of this thesis, which is a summary of the structural geology of the Livingstone Range study area and a detailed description and interpretation of the Centre Peak anticline, has been submitted as a paper to the American Association of Petroleum Geology Bulletin.

### **1.3 Fluid flow in the LRA**

Within the history of deformation of every foreland thrust and fold belt there are concurrent thermal and fluid-flow histories that are integral parts of the tectonic evolution. Fluid flow transmits heat, facilitates faulting, and transports potentially economic minerals and hydrocarbons.

Hitchon (1984) proposed that regions of elevated topography that developed during thrusting and folding in the southern Canadian Cordillera provided the hydraulic head that drove deep circulation of meteoric water that cooled the rocks. This theory is supported by apatite fission track data from above and below the Lewis thrust in southern Alberta that indicate that the Lewis thrust sheet cooled rapidly soon after thrusting began (Osadetz et al., 2004). An additional focus of this project was to determine if there is evidence for an influx of cool meteoric fluids into the Livingstone thrust sheet during thrusting.

During thrusting and folding in the LRA there were discrete episodes of fluid flow, as shown by the presence of veins along many fault zones. Within the LRA, deformation associated with the formation of many carbonate and quartz veins can be linked unequivocally to displacements on specific thrust faults, tear faults, and minor faults. Cross-cutting relationships observed between many vein sets provide relative age constraints between different fluid flow events. An important objective of this study was to investigate the isotope geochemistry of syntectonic veins in the LRA and deduce the sources of fluids that were flowing in the structures at different stages of thrusting and folding.

The ultimate goal of this part of the study was to combine fluid source information, isotope geothermometry of veins and thermal data from nearby coal to establish a thermal, fluid, and tectonic history for the LRA, and to correlate this with the thermal and fluid evolution of the

southern Canadian Foreland Thrust and Fold Belt. This topic forms Chapter 3 of this thesis, which has been submitted as a separate paper to AAPG Bulletin.

#### **1.4 Summary of conclusions**

During the course of this study several important conclusions have been made regarding how the thrust-propagation folds and other structures in the LRA formed, when they formed and the types of fluids that were flowing through the structures at various times throughout their evolution. Chapter 4 of this thesis contains a summary of the conclusions made within the previous two chapters, as well as a separate section discussing conclusions that have particular significance for hydrocarbon exploration. Also included in Chapter 4 are recommendations for further work.

## 1.5 References

- Bally, A. W.; Gordy, P. L.; Stewart, G. A., 1966. Structure, seismic data, and orogenic evolution of southern Canadian Rocky Mountains. *Bulletin of Canadian Petroleum Geology*, v.14, no.3, p. 337-381.
- Boyer, S. E., 1986. Styles of folding within thrust sheets: examples from the Appalachian and Rocky Mountains of the U.S.A. and Canada. *Journal of Structural Geology*, v. 8, Nos. 3/4, p. 325-339
- Boyer, S. E. and Elliott, D., 1982. Thrust systems. *AAPG Bulletin*, v.66, no.9, p.1196-1230.
- Dahlstrom, C. D. A., 1970, Structural geology in the eastern margin of the Canadian Rocky Mountains: *Bulletin of Canadian Petroleum Geology*, v. 18, p. 332-406.
- Douglas, R. J. W., 1950, Callum Creek, Langford Creek and Gap map-area, Alberta, *Geological Survey of Canada Memoir 255*, 124 p.
- Douglas, R. J. W., 1958. Mount Head map-area, Alberta. *Geological Survey of Canada Memoir 291*, 241 p.
- Douglas, R. J. W.; Gabrielse, H.; Wheeler, J. O.; Stott, D. F.; Belyea, H. R., 1970. Geology and economic minerals of Canada, ed. 5, *Economic Geology Report - Geological Survey of Canada*, vol.1, pp.366-488, 1970
- Gwinn, V. E., 1964. Thin-skinned tectonics in the Plateau and northwestern Valley and Ridge provinces of the Central Appalachians. *Geological Society of America Bulletin*, v. 75, no. 9, p. 863-900.

- Hitchon, B., 1984. Geothermal gradients, hydrodynamics, and hydrocarbon occurrences, Alberta, Canada. American Association of Petroleum Geologists Bulletin, v.68, p.713-743.
- Mitra, S. 1986. Duplex structures and imbricate thrust systems: geometry, structural position, and hydrocarbon potential. American Association of Petroleum Geologists Bulletin, v. 70, p. 1087-1112.
- Monger, J. W. H.; Price, R. A., 1979. Geodynamic evolution of the Canadian Cordillera; progress and problems. Canadian Journal of Earth Sciences, v.16, 3, p.771-791.
- Osadetz, K. G., Kohn, B. P., Feinstein, S., and Price, R. A., 2004. Foreland belt thermal history using apatite fission-track thermochronology: Implications for Lewis thrust and Flathead fault in the southern Canadian Cordilleran petroleum province, in Swennen, R., Roure, F., and Granath, J. W., eds., Deformation, fluid flow, and reservoir appraisal in foreland fold and thrust belts: AAPG Hedberg Series, No. 1, American Association of Petroleum Geologists, Tulsa, U.S.A.,p. 21–48.
- Price, R. A., 1981. The Cordilleran foreland thrust and fold belt in the southern Canadian Rocky Mountains, in McClay, K. R., and Price, N. J., eds., Thrust and nappe tectonics, The Geological Society of London, p. 427-448.
- Price, R. A., 1994. Cordilleran tectonics and the evolution of the Western Canada sedimentary basin, in Mossop, G. D., and Shetsen, I., eds., Geological Atlas of Western Canada: Calgary, Canadian Society of Petroleum Geologists/Alberta Research Council, p. 13-24.
- Price, R. A., 2001. An evaluation of models of kinematic evolution of thrust and fold belts: structural analysis of a transverse fault zone in the Front Ranges of the Canadian Rockies north of Banff, Alberta. Journal of Structural Geology, v. 23, p. 1079 - 1088.
- Rodgers, J., 1963. Mechanics of Appalachian foreland folding in Pennsylvania and West Virginia. AAPG Bulletin v. 47; no. 8; p. 1527-1536

Suppe, J., 1983. Geometry and kinematics of fault-bend folding. *American Journal of Science*, v. 283, no. 7, p. 684-721

Suppe, J., and Medwedeff, D. A., 1990. Geometry and kinematics of fault-propagation folding. *Ecologiae Geologicae Helvetiae*, v. 83, p. 409-454.

## **Chapter 2 Chevron-style, flexural-slip thrust-propagation folding, Livingstone Range anticlinorium, southern Alberta Foothills, Canada.**

Michael A. Cooley, Raymond A. Price, John M. Dixon & T. Kurtis Kyser  
Queen's University, Kingston, Ontario, Canada

### **2.1 Abstract**

The Livingstone Range anticlinorium (LRA) is a long (>65 km) narrow (<5 km) structural culmination that coincides with a major hanging-wall ramp across which the Livingstone thrust cuts ~1000 m up-section eastward from a regional décollement in the upper part of Devonian Palliser Formation to another regional décollement within the Jurassic Fernie Formation. This ramp includes minor ramps and flats within Carboniferous rocks that are controlled by locally important detachments in the lower part of the Banff Formation, at the top of the Banff Formation, and near the base of the Turner Valley Member of the Livingstone Formation. The anticlinorium consists mainly of chevron-style, flexural-slip thrust-propagation folds that have conspicuous blind thrust faults along their hinge zones. The distinctive pattern of ramp-flat thrusting that occurs along the hinge zone thrust system of the asymmetric chevron-style Centre Peak anticline consists of a series of stacked detachment thrusts, each of which emerges from a different zone of interbed slip in the backlimb of the anticline and deflects the hinge zone eastward. Each detachment thrust consists of two contrasting segments. The lower segment, which is parallel to bedding in the less steeply dipping backlimb of the fold, juxtaposes a hanging-wall flat with a footwall ramp. The upper segment, which is sub-parallel with the

steeply-dipping forelimb, juxtaposes a hanging-wall ramp with what roughly approximates an overturned footwall flat. Each successively lower detachment thrust dies out in the hinge zone at approximately the same stratigraphic level as an overlying detachment thrust fault that emerges from a bedding detachment zone in the backlimb. Displacement along each successively higher bedding detachment thrust is interpreted to have occurred after the displacement on the underlying thrust. The highest bedding detachment thrust, which formed last and terminates in the core of a concentric, parallel, flexural-slip fold, records the arrested growth of the anticline. Displacements on the detachment thrusts were kinematically integrated with rotation of fold limbs and with inter-bed slip within the fold limbs. The result is a distinctive chevron-style of flexural-slip thrust-propagation folding. Deformation during thrust propagation and related folding involved a form of cataclastic flow in which individual blocks of rock delimited by networks of faults, joints and sheared bedding surfaces underwent major translation and rotation with little or no internal deformation. Pressure solution and vein formation were widespread but minor components of the deformation. Multiple sets of cross-cutting calcite and/or dolomite and/or hydrocarbon veins associated with faults and fractures provide evidence of intermittent reactivation and intermittent fluid migration along fault zones.

## 2.2 Introduction

The Foothills and Rocky Mountains of southwestern Alberta form the eastern margin of the Cordilleran foreland thrust and fold belt. The thrust and fold belt is a northeast-tapering accretionary wedge comprising sedimentary strata that have been scraped off the under-riding Laurentia craton and transported eastward with the over-riding Intermontane terrane, which is a tectonic collage of oceanic volcanic arc and sedimentary rocks that was obducted over and accreted to the western margin of Laurentia during Late Jurassic to Paleocene convergence between Laurentia and subduction zones along its western margin (Monger and Price, 1979; Price, 1981; Price, 1994).

The structure of the accretionary wedge is dominated by east-verging listric thrust faults that flatten with depth and merge into a basal décollement situated just above the contact between the sedimentary cover and underlying Paleoproterozoic basement (Bally et al., 1966). Thrust-propagation and fault-bend folds developed during the thrusting. Older thrust faults have been folded along with underlying strata by displacements on younger, deeper thrust faults (Douglas, 1950; Dahlstrom, 1970; Price 1981). The displaced and deformed rocks include the Belt-Purcell strata, which accumulated in a Mesoproterozoic intracontinental rift (Price and Sears, 2001; Sears and Price, 2003); the Neoproterozoic to Jurassic Cordilleran miogeocline, which accumulated along the western rifted continental margin of Laurentia; the platform cover on Laurentia, which is the lateral equivalent of the miogeocline; and the synorogenic foreland basin deposits that accumulated in front of the advancing accretionary wedge and were partly incorporated in it. In the Front Ranges imbricate sheets of cratonic platform carbonate strata form conspicuous linear mountain ranges. In the Foothills, thinner imbricate slices of foreland basin siliciclastic strata

form more subdued topography, but with isolated linear mountain ranges underlain by local culminations that expose Paleozoic platformal carbonate rocks.

The Livingstone Range anticlinorium (LRA) is a long (65 km) narrow (<5km wide) north- to northwest-trending horizontally plunging structural culmination of Carboniferous platformal carbonate rock that stands above the surrounding deformed Jurassic and younger foreland basin strata of the Foothills belt. At the north end, the anticlinorium terminates along the east side of the broad domal Plateau Mountain culmination; at the south end it terminates abruptly as south-plunging conical folds just north of the Crowsnest Pass Highway (Figure 2-1).

The LRA coincides with a major hanging-wall ramp across which the Livingstone thrust cuts ~1000 m up-section from a regional décollement in lime mudstones of the upper part of Devonian Palliser Formation to another regional décollement within marine shale of the Jurassic Fernie Formation. The matching footwall cutoff is located more than 30 kilometres to the west, under the Lewis thrust sheet (Price, 1981, 1994).

A distinctive characteristic of the LRA is the presence of steeply dipping east-verging blind thrust faults that extend along the hinge zones of most anticlines. These were identified by Douglas (1950) and illustrated by Price (in Douglas et al., 1970); however, they do not appear on the 1:50,000-scale geological map and structure sections of the southern part of the Livingstone range by Norris (1993). Each blind thrust separates outward-facing planar fold limbs that merge above the tip line of the thrust as a concentric parallel fold. The resulting chevron-style flexural-slip thrust-propagation fold differs significantly from the fault-propagation fold models outlined by Dahlstrom (1969 and 1970), Williams and Chapman (1983), Jamieson (1987), Suppe and Medwedeff (1990), Wickham (1995), and Allmendinger (1998).

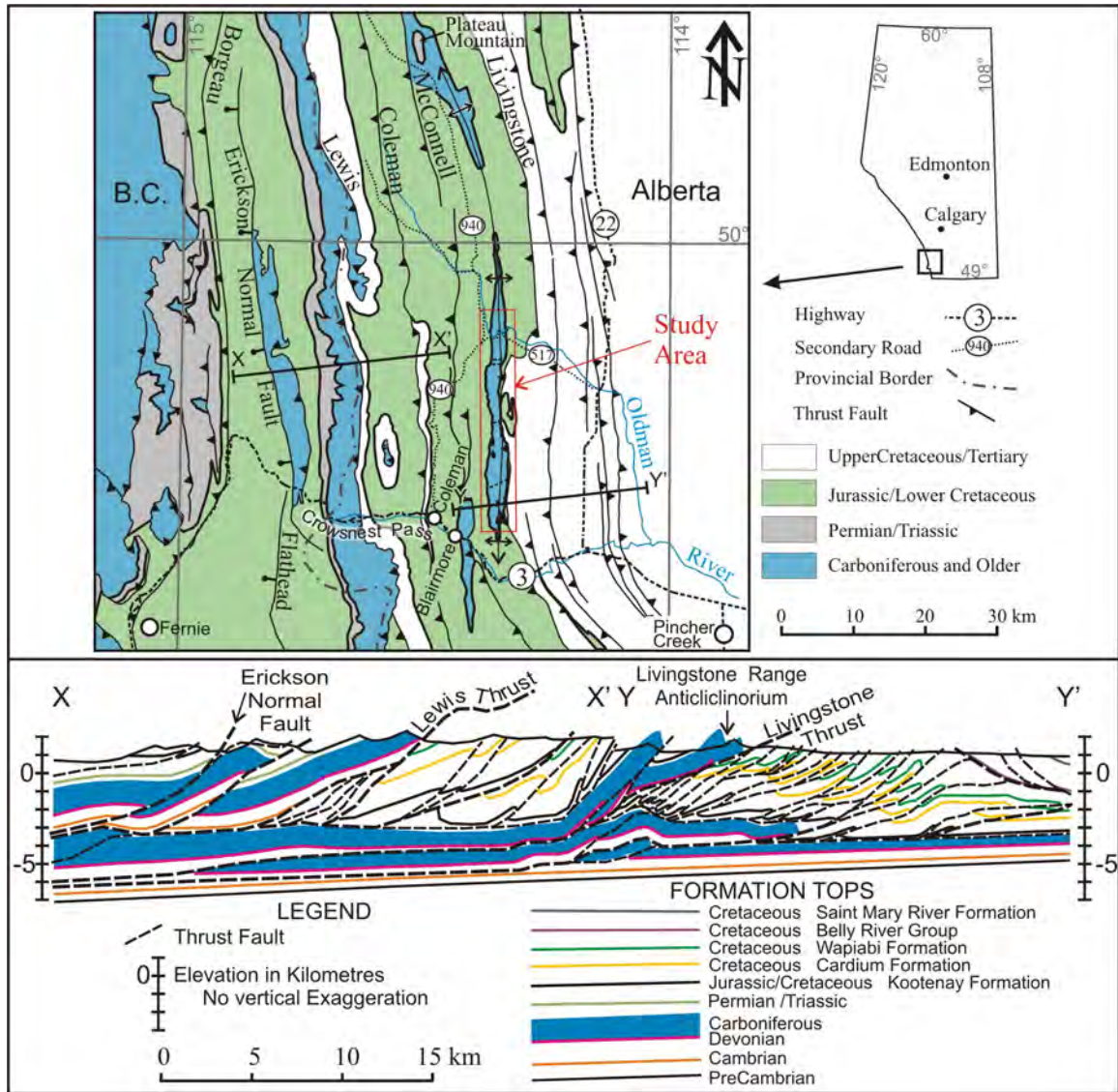


**Figure 2-1.** Regional geological setting of the study area at the south end of the Livingstone Range, southern Alberta foothills. Cross section X X' is modified from Price (cross section of Fernie map, in preparation). Cross section Y Y' is modified from an unpublished 1999 cross section of Paul Mackay.

The internal structure of the anticlinorium varies along strike as individual anticlines emerge, increase in size, and die out (Figure 2-2). These changes are generally gradual, but locally they occur abruptly across cross-strike discontinuities (Figure 2-2). Most discontinuities coincide with east- or northeast-trending “tear faults” or transverse thrust ramps. The Rock Creek discontinuity (Figure 2-2), which is marked by the northeast alignment of abrupt changes in plunge of several folds, probably marks an underlying transverse thrust ramp. Because of these along-strike changes, the number of anticlines in different segments of the LRA varies from one to three.

During the formation of the Livingstone Range anticlinorium, the Carboniferous carbonate rocks underwent brittle deformation that was conspicuously discontinuous and inhomogenous at the scale of an individual outcrop (Price, 1967). The folding involved small displacements along and across a myriad array of small contraction and extension faults, inter-bed shear zones, and joints. These brittle fractures bounded individual blocks of rock that underwent large translation and rotation with little or no internal deformation. The overall result was a form of cataclastic flow analogous to the deformation of a masonry wall in which individual blocks retain their original shape, but not their original orientation and location (cf Wojtal, 1986; Ismat and Mitra, 2005). Substantial dilation occurred during the deformation, and precipitation of calcite, dolomite, and quartz in dilatant fracture zones was a widespread but minor component of the deformation. Some fractures contain veins, or their surfaces are coated with carbonate or quartz druze; they record extension and dilation between adjacent blocks; some are stylolitic pressure solution surfaces that mark compression and convergence between adjacent blocks; some are shear surfaces along which vein minerals have been precipitated in the lee of asperities. The geochemistry of the vein minerals, which provides important information about the nature

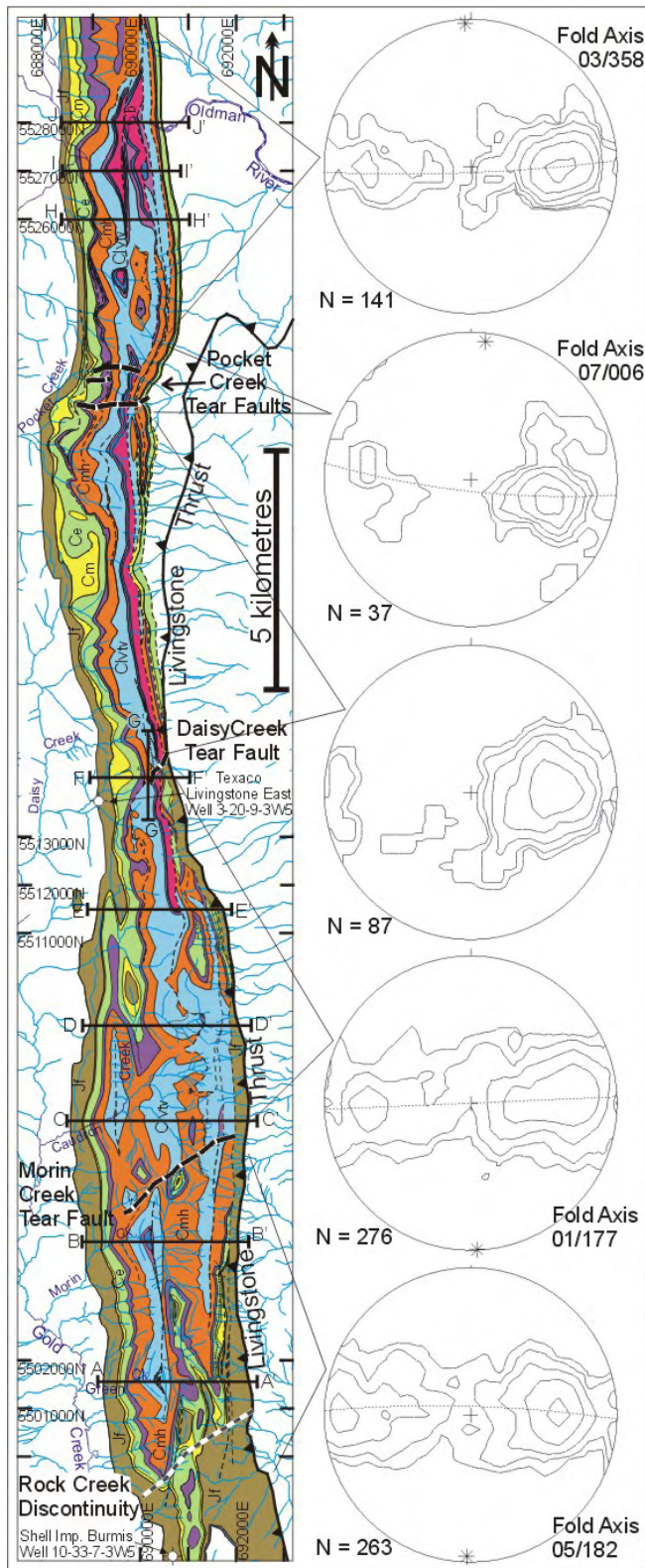


**Figure 2-2.** Geologic map of the study area. The LRA comprises generally north-trending segments that are separated by regularly-space cross-strike discontinuities. Most are tear faults marked by abrupt changes in fold plunges and dextral offsets of folds, but the southern one (Rock Creek discontinuity) may be a blind tear fault or lateral ramp. The location of this map is shown in Figure 2-1. Map units are the same as those in Figure 2-3. The cross section locations depicted in this figure are for sections illustrated in Figure 2-5. Contoured equal area plots of poles to bedding in equal area projection from the lower hemisphere, plotted using GEOrient© 9.1 (R. J. Holcombe, University of Queensland).

and evolution of the fluids that were flowing through the fractures, is discussed in Chapter 3.

This research entailed three field seasons of detailed geological mapping at 1:10,000 scale. Field work also included detailed examination and measurement of stratigraphic sections through Upper Paleozoic and Lower Jurassic strata, extensive sampling of the orientations of bedding, fractures, veins, faults, slickensides and kinematic indicators. Detailed mapping was supplemented by documentation of deformation at all scales of observation ranging from thin section petrography, detailed observations made from hand samples and outcrops, to observations made in large exposures in canyon walls and air photo analysis.

### **2.3 Stratigraphy of the southern Livingstone Range**

The southern Livingstone Range anticlinorium comprises Upper Devonian to Middle Jurassic cratonic platform strata that are overlain by Late Jurassic and younger foreland basin deposits. Strata that were mapped in detail in the LRA are presented in the stratigraphic column in Figure 2-3.

The basal ~150 metres of the Livingstone thrust sheet is not exposed at surface but it has been intersected by many oil exploration wells, including two in the study area (Figure 2-2, Texaco Livingstone East 3-20-9-3W5, and Shell Imperial Burmis 10-33-7-3W5). It also has been imaged on seismic reflection profiles in areas to the north and west of the study area (Deline, 2003). The lowest unit in the thrust sheet comprises ~60 metres of Palliser Formation Upper Devonian lime mudstone. This upper part of the Palliser Formation overlies a major regional décollement along the Livingstone thrust (Price, 1981). The Palliser Formation is overlain by ~10 metres of Upper Devonian-Lower Mississippian black shale of the Exshaw Formation, an

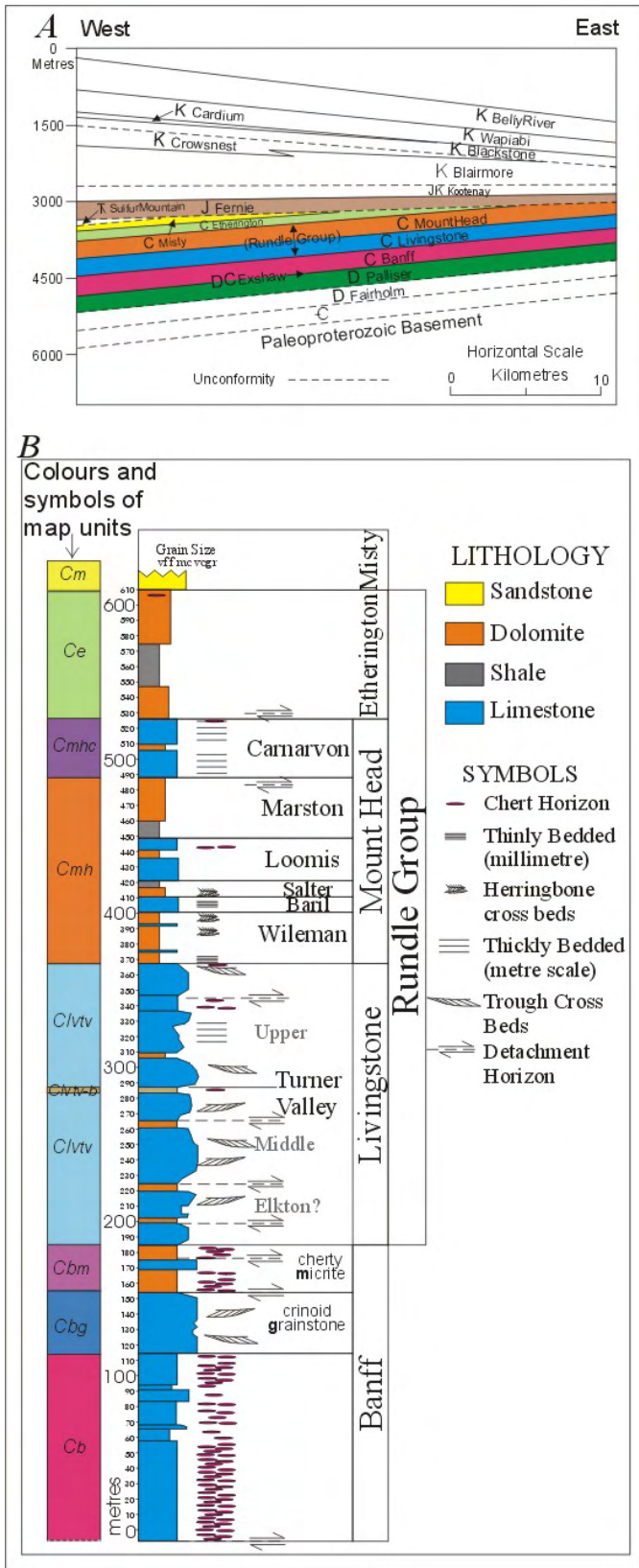


**Figure 2-3.** Carboniferous stratigraphy of the study area. A schematic east-west section showing stratigraphic relationships of the Crowsnest Pass area is presented in A (modified from Norris, 1993). B is a composite stratigraphic section of the formations that were mapped and measured in the study area. Map units are explained in the legend in Figure 2-4.

important hydrocarbon source rock (Obermajer et al., 1997). The overlying Banff Formation consists of ~320 metres of Lower Mississippian argillaceous silty and cherty limestone. Only the upper ~230 metres of the Banff Formation is exposed in the study area. The lower ~150 metres consists of dark grey, cherty, argillaceous and silty limestone. This is overlain by two conspicuous and laterally consistent marker units; a lower unit that consists of ~45 metres of coarse crinoidal grainstone and an overlying unit of ~60 metres of lime mudstone with pale chert horizons. The overlying Livingstone Formation comprises ~230 metres of predominantly coarse crinoidal grainstone and packstone and minor interbedded lime mudstone and dolomitic mudstone with rare thin shaly layers. The upper ~205 metres of the Livingstone Formation is tentatively identified as the Turner Valley Member. The Mount Head Formation, which overlies the Livingstone Formation, ranges in thickness from 130 to 190 metres. It includes three members dominated by fine-grained silty dolomite and shale (Wileman, Salter and Marston Members) that are interlayered with three members that consist mainly of lime mudstone (Baril, Loomis and Carnarvon Members). The Carnarvon Member is a distinctive conspicuously bedded dark grey lime mudstone marker unit that forms the uppermost ~40 metres of the Mount Head Formation. The overlying ~83 metre interval of Upper Mississippian Etherington Formation comprises interbedded fine-grained dolomitic mudstone, shale, siltstone and sandy limestone. The Livingstone, Mount Head, and Etherington Formations comprise the Mississippian Rundle Group, which is overlain by ~40 metres of Pennsylvanian quartz arenite of the Misty Formation of the Spray Lakes Group. The Jurassic Fernie Formation, which is poorly exposed along the margins of the anticlinorium and within a few synclines, is predominantly shale with minor interbedded wacke. The poor exposures precluded measuring stratigraphic sections through this unit. The Fernie Formation is the youngest Formation mapped during this study. The Upper Jurassic 'Passage beds' at the top of the Fernie Formation represent the first occurrence of coarser-grained westerly-derived sediments shed from the emerging Cordillera. They are the

oldest unit in the foreland basin succession. The Fernie Formation is overlain by the coal-bearing Jurassic/Cretaceous Kootenay Formation.

## **2.4 Structural Geology of the southern Livingstone Range**

### **2.4.1 Overview**

The Livingstone Range anticlinorium is an array of linked, en-echelon, thrust-propagation, chevron-style folds involving the Devonian-Carboniferous platformal carbonate rocks and overlying Mesozoic siliciclastic foreland basin deposits (Figure 2-2). Each chevron-style anticline is associated with a foreland-verging thrust fault that dies out upward into the core of the fold. These blind thrusts separate steeply dipping planar east-facing forelimbs from less steeply dipping west-facing planar backlimbs (Figures 2-2, 2-4, and 2-5). Above the tip lines of the blind thrust faults, which generally lie near the top of the Livingstone Formation, the strata in the cores of the anticlines outline concentric, parallel folds. Other minor thrust faults die out downward into the cores of concentric parallel synclines (Figures 2-2, 2-4, and 2-5). The structure of the Livingstone Range anticlinorium changes along strike as individual anticlines emerge, increase in size, and die out (Figure 2-2). One to three anticlines occur in individual cross sections. The changes are generally gradual, but locally they occur abruptly across cross-strike discontinuities that coincide with lateral thrust ramps or with northeast-trending tear faults that are kinematically linked to slip on the underlying Livingstone thrust. The four cross-strike discontinuities that occur in the study area (Figure 2-2) separate the LRA into five distinct segments, four of which were mapped in detail during this study.

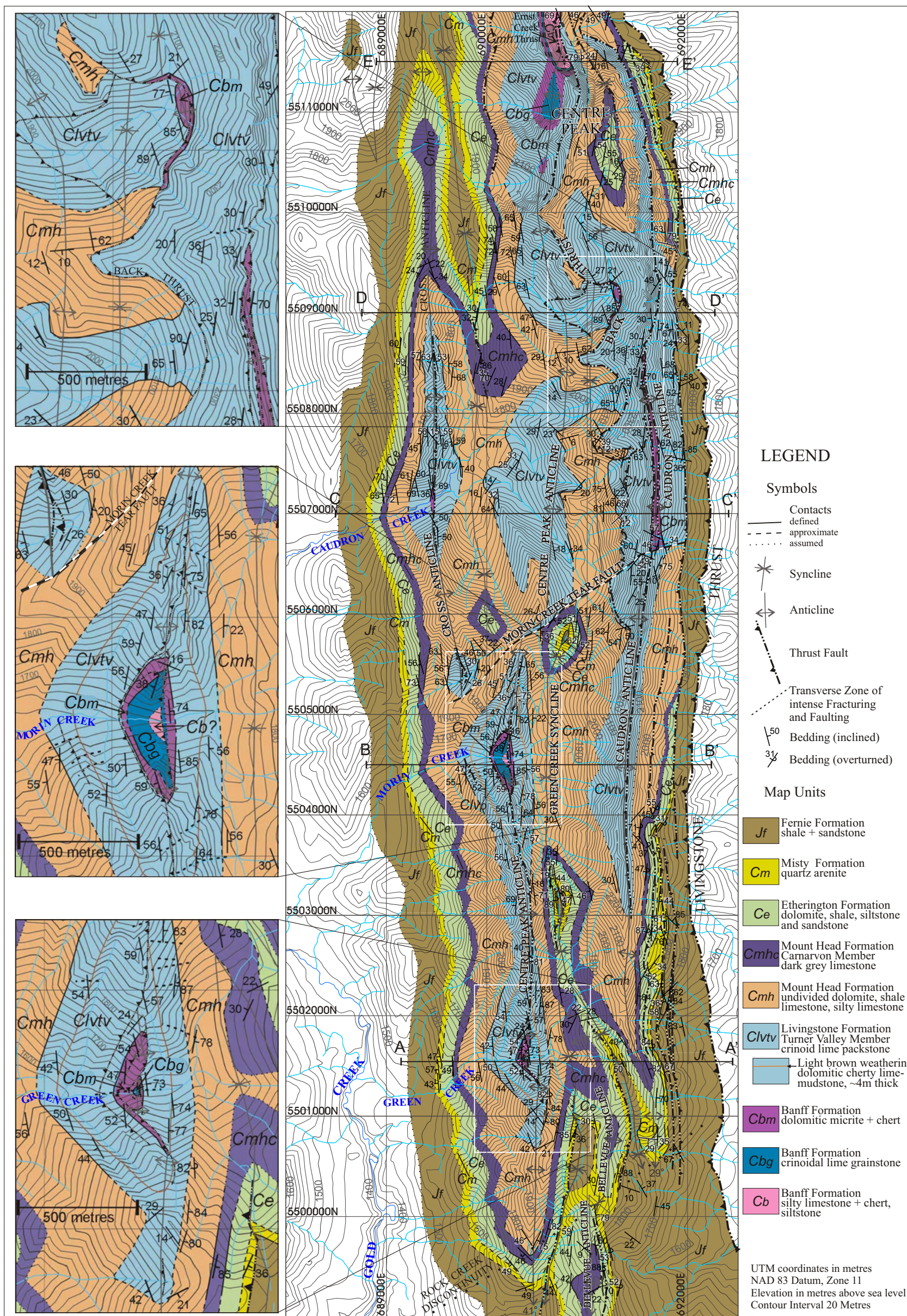
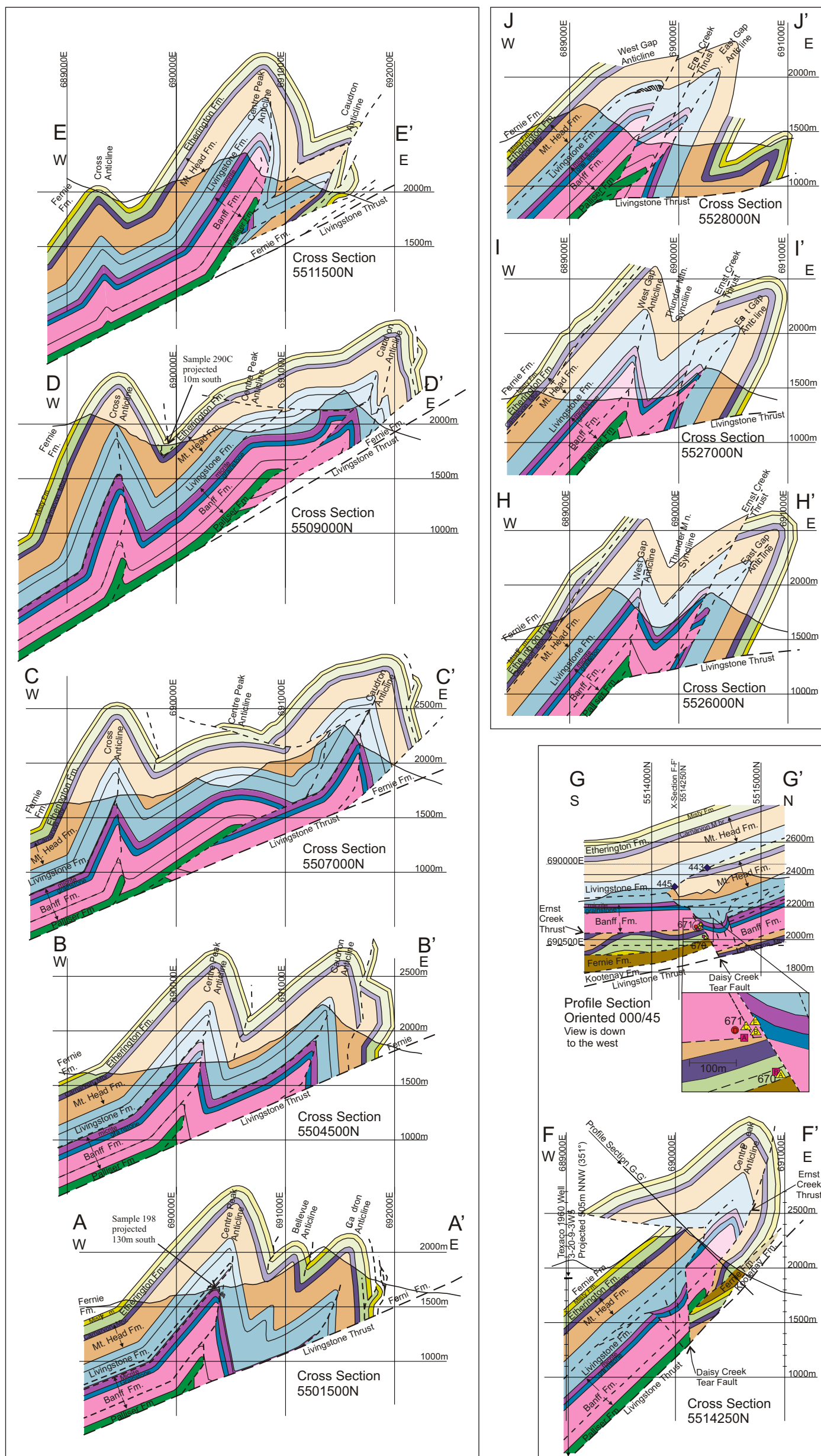


Figure 2-4. Geologic map of the southern part of the study area.



**Figure 2-5.** Cross sections through the Livingstone Range anticlinorium. The locations of cross sections are shown in Figure 2-2 and on maps in Figures 2-4 (sections A-A' to E-E'), Figure 2-7 (sections F-F' and G-G') and Figure 2-8 (sections H-H', I-I' and J-J').

The Green Creek/Morin Creek segment, which is at the southern end of the study area and is easily accessible (Figures 2-2 and 2-4), is particularly informative because it provides excellent exposures of the core of the anticlinorium along the deep canyons occupied by these two creeks. The south end of this segment is delimited by the northeast-trending Rock Creek discontinuity, which is marked by abrupt changes in plunge of three anticlines. These are, from west to east: the Centre Peak anticline, the Belleview anticline, and the Caudron anticline. The Centre Peak anticline has a relatively horizontal plunge between Morin Creek and Green Creek, but immediately south of Green Creek the plunge changes abruptly to 25 degrees south. Two kilometres south of Green Creek the plunge increases to 41 degrees and the anticline terminates southward as a conical fold at the western end of the Rock Creek discontinuity (Figure 2-4). The Belleview anticline is the dominant structure of the southernmost part of the LRA. North of Green Creek the Belleview anticline dies out northward as a north-plunging conical chevron fold (Figure 2-5, section A-A'), but south of Green Creek it maintains a relatively horizontal plunge. However, 1.3 kilometres south of Green Creek, a conspicuous 200 metre dextral jog in the Bellevue anticline marks the location of the Rock Creek discontinuity. The Caudron anticline has a relatively horizontal plunge at Morin Creek, but it plunges gently southward at Green Creek. One kilometre south of Green Creek the plunge of the Caudron anticline abruptly increases to approximately 29 degrees south and the anticline terminates as a south-plunging conical fold at the eastern end of the Rock Creek discontinuity. The Centre Peak anticline and Caudron anticline extend northward as far as the northeast-trending, steeply dipping Morin Creek tear fault where they are offset dextrally ~250 metres and ~130 metres, respectively. The culmination of the Centre Peak anticline occurs mid-way between the Rock Creek discontinuity and the Morin Creek tear fault. The anticline plunges gently northward on the south side of the Morin Creek tear fault.

The Centre Peak segment of the LRA, which extends from the Morin Creek tear fault to the Daisy Creek tear fault, contains three anticlines. These are, from west to east: the Cross anticline, the Centre Peak anticline, and the Caudron anticline. The Cross anticline is narrow, straight, and 6-7 kilometres long, with a culmination at Caudron Creek (Figure 2-4). South of the culmination, the anticline terminates abruptly against the Morin Creek tear fault; north of the culmination it plunges gently northward and dies out 2 km northwest of Centre Peak as a conical fold within the Fernie Formation (Figure 2-4). The morphology of the Centre Peak anticline changes abruptly where it is offset dextrally ~250 m across the Morin Creek tear fault. South of the tear fault the interlimb angle is ~55 degrees and the anticline closes with an angular hinge at the top of the Livingstone Formation at an elevation of ~2250 metres. Below this level there is a thrust fault along its hinge zone (Figure 2-5, cross section B-B'). North of the Morin Creek tear fault the closure at the top of the Livingstone Formation is at ~1900 metres elevation, and the fold is open and concentric with no thrust fault in the hinge zone (Figure 2-5, cross section C-C'). The Centre Peak anticline extends northward as an open fold to the vicinity of Centre Peak where it changes into a tight chevron fold with planar limbs and with an east-verging thrust fault cutting up through the forelimb (Figure 2-5, cross sections D-D' and E-E'). The Caudron anticline is offset dextrally ~130 m across the Morin Creek tear fault, but the structural style is the same on both sides – a tight chevron fold with an east-verging thrust fault in the hinge zone. However, the structural style changes significantly along strike to the north. On the north side of the Morin Creek tear fault a west-verging back thrust emerges in the upper backlimb of the fold, forming the “roof thrust” of an eastward-tapering thrust wedge that has been displaced toward the core of the Caudron anticline (Figure 2-5, cross sections C-C' and D-D'). The “floor thrust” of this wedge, which carries the top of the Banff Formation in its hanging-wall in the core of the Caudron anticline on the north side of Morin Creek tear fault (Figure 2-4), is interpreted to be the eastern part of a thrust splay from the underlying Livingstone thrust that cuts up-section at a low angle to

bedding from the Palliser Formation to the Lower Livingstone Formation. The hanging-wall and footwall ramps of this hypothetical fault combine to form the broad, open Centre Peak anticlinal fault-bend fold (Figure 2-5, cross sections C-C' and D-D'). This thrust is interpreted to die out in the core of the Caudron anticline east of the branch line of the overlying back thrust that merges with it. The back thrust that forms the roof of the wedge can be traced northward to UTM 5509800N (Figure 2-4), where it dies out in the eastern limb of the Centre Peak anticline, southwest of Centre Peak. Northward from cross section D-D' (Figures 2-4 and 2-5), the east-verging thrust fault that emerges from the axial zone of the Caudron anticline progressively overrides the east limb of the fold. On the eastern flank of Centre Peak the Livingstone Formation forming the western limb of the Caudron anticline is juxtaposed over rocks of the Upper Mount Head Formation and Etherington Formation that form the overturned eastern limb of the anticline (Figure 2-4, section E-E' of Figure 2-5, and Figure 2-6). North of Centre Peak, where only the deeper levels of the LRA are exposed, the hinge zones of both the Centre Peak anticline and the Caudron anticline are represented by simple west-dipping thrust faults on either side of the Centre Peak syncline (Figures 2-4, 2-6 and 2-7; section E-E' of Figure 2-5).

The Ernst Creek thrust, which underlies the Centre Peak anticline, is a major structure that has been traced northward 20 km from Centre Peak to where it dies out in the core of an anticline at the north end of the study area (Figures 2-4, 2-6, 2-7 and 2-8). Northward from the north side of Centre Peak (UTM 5512500N in Figure 2-7) where the thrust that emerges from the hinge zone of the Centre Peak anticline merges with the Ernst Creek thrust, to the Daisy Creek tear fault, the structure of the LRA is mainly dominated by the west-dipping homoclinal panel in the hanging-wall of the Ernst Creek thrust (Figure 2-7).



**Figure 2-6.** View southward at Centre Peak anticline on the northeast side of Centre Peak. Banff Formation is juxtaposed over the upper part of Turner Valley Member along a thrust that cuts up through the forelimb of the anticline. This fault merges along strike to the north with the Ernst Creek thrust, which dies out southward in the core of the Centre Peak anticline (see Figures 2-4 and 2-7).

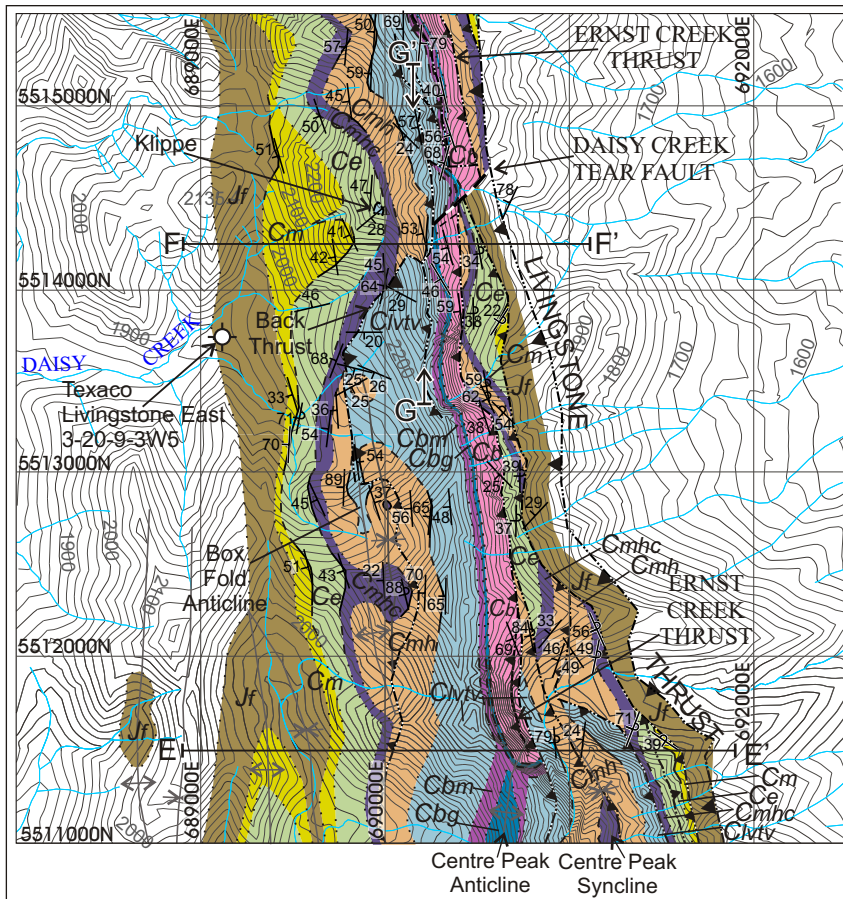
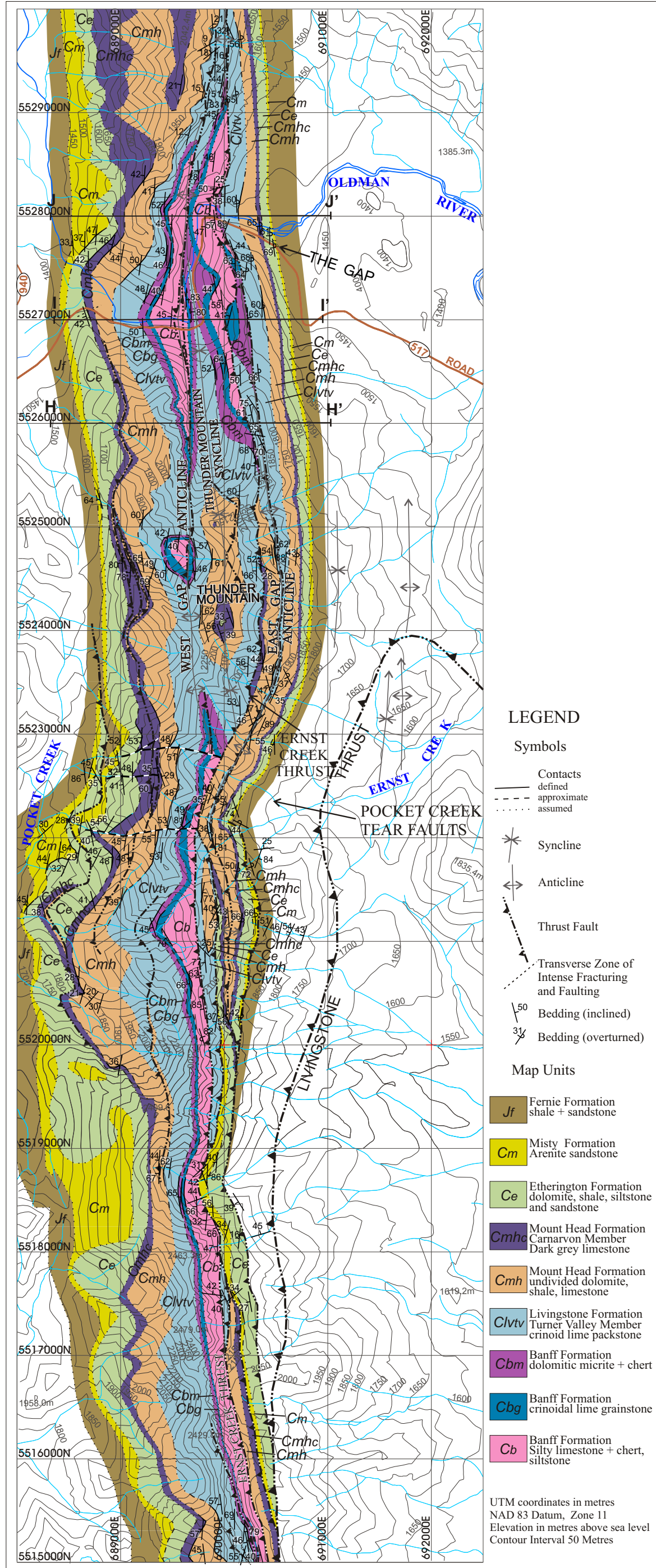


Figure 2-7. Geologic map of the Daisy Creek area. The legend for this map is the same as Figure 2-8.

Figure 2-8. Geologic map of the northern part of the study area.



The steeply-dipping, northeast-striking Daisy Creek tear fault (Figure 2-7) is marked by ~ 160 m of dextral offset of the Ernst Creek thrust. It appears to abut the underlying Livingstone thrust and to have formed in conjunction with slip along the Livingstone thrust. However, upward, the Daisy Creek tear fault abuts a detachment zone within the upper part of the Livingstone Formation that forms the floor of an eastward-tapering thrust wedge that has delaminated the Livingstone Formation (Figure 2-5, cross section F-F' and profile section G-G'). The back thrust forming the roof of the wedge juxtaposes the Livingstone Formation over the Carnarvon Member of the Mount Head Formation and the Etherington Formation. A small klippe of Livingstone Formation occurs above the Etherington Formation at the ridge crest, ~200 metres north of cross section F-F' (Figure 2-7). The back thrust dies out rapidly southward within the upper part of the Livingstone Formation in the core of a small box anticline (Figure 2-7).

In the segment of the LRA that extends northward from the Daisy Creek tear fault to the Pocket Creek tear faults, the structure of the LRA is dominated by the Ernst Creek thrust (Figures 2-7 and 2-8). The west-dipping, north-trending homoclinal panel of Banff Formation and Rundle Group strata in the hanging-wall of the thrust forms the backlimb of the anticlinorium. The thin thrust slices and attenuated folds of Misty, Etherington, Mount Head and upper Livingstone strata in the footwall of the Ernst Creek thrust form the forelimb.

The Pocket Creek tear faults comprise three steeply dipping, map-scale, east-west trending, transverse faults (Figures 2-2 and 2-8). They occur within a conspicuous transverse, east-west trending dextral monoclinial flexure that has been superimposed on the entire LRA. The flexure, which is ~1500 m-wide and has an amplitude of ~ 800 m, is situated west of the nose of an underlying north-plunging anticline that involves the Livingstone thrust as well as the Mesozoic rocks in its footwall (Figure 2-8). This anticline is part of a group of folds that deformed the Livingstone thrust and were related to displacements on thrusts that developed below the Livingstone thrust (Douglas, 1950, Figure 14). The two largest tear faults end

downward against the Ernst Creek thrust, and appear to have been linked kinematically to displacement on it (Figure 2-8). The other smaller tear fault ends downward against a minor thrust that repeats part of the Mount Head Formation within the Ernst Creek thrust slice. All three faults die out upward within the Etherington Formation. Overlying strata, including a minor east-verging backlimb thrust that repeats part of the Etherington and Misty Formations, have been folded by dextral displacement on the southern tear fault. The three tear faults, as a group, deformed at least one minor thrust within the LRA, and they involved small displacements that were linked to displacements on other thrusts within the LRA. The tear faulting evidently occurred during the development of the superimposed dextral transverse monoclinial flexure, and was associated with minor reactivation of pre-existing minor thrusts within the LRA.

In the segment of the LRA that extends from the Pocket Creek area northward to the northern edge of the study area, the structure of the LRA is dominated by the Ernst Creek thrust and by the two thrust-propagation anticlines that occur on either side of it, namely, the West Gap anticline and the East Gap anticline (Figures 2-8 and 2-9). The Ernst Creek thrust, which juxtaposes the Banff Formation over Rundle Group strata along the west limb of the East Gap anticline is separated from the West Gap anticline by the Thunder Mountain syncline. Both anticlines have planar limbs and both contain east-verging thrust faults along their hinge zones (Figures 2-8 and 2-9 and sections H-H', I-I' in Figure 2-5). The thrust fault along the hinge zone of the West Gap anticline dies out ~2.5 km south of The Gap near Thunder Mountain, in the hinge of the West Gap anticline, at the stratigraphic level of the lower part of the Turner Valley Member (Figures 2-8 and 2-9). However, at The Gap, where the length of the common limb linking the West Gap anticline to the Thunder Mountain syncline decreases northward, this hinge-zone thrust transforms northward into a simple east-verging thrust within the homoclinal panel in

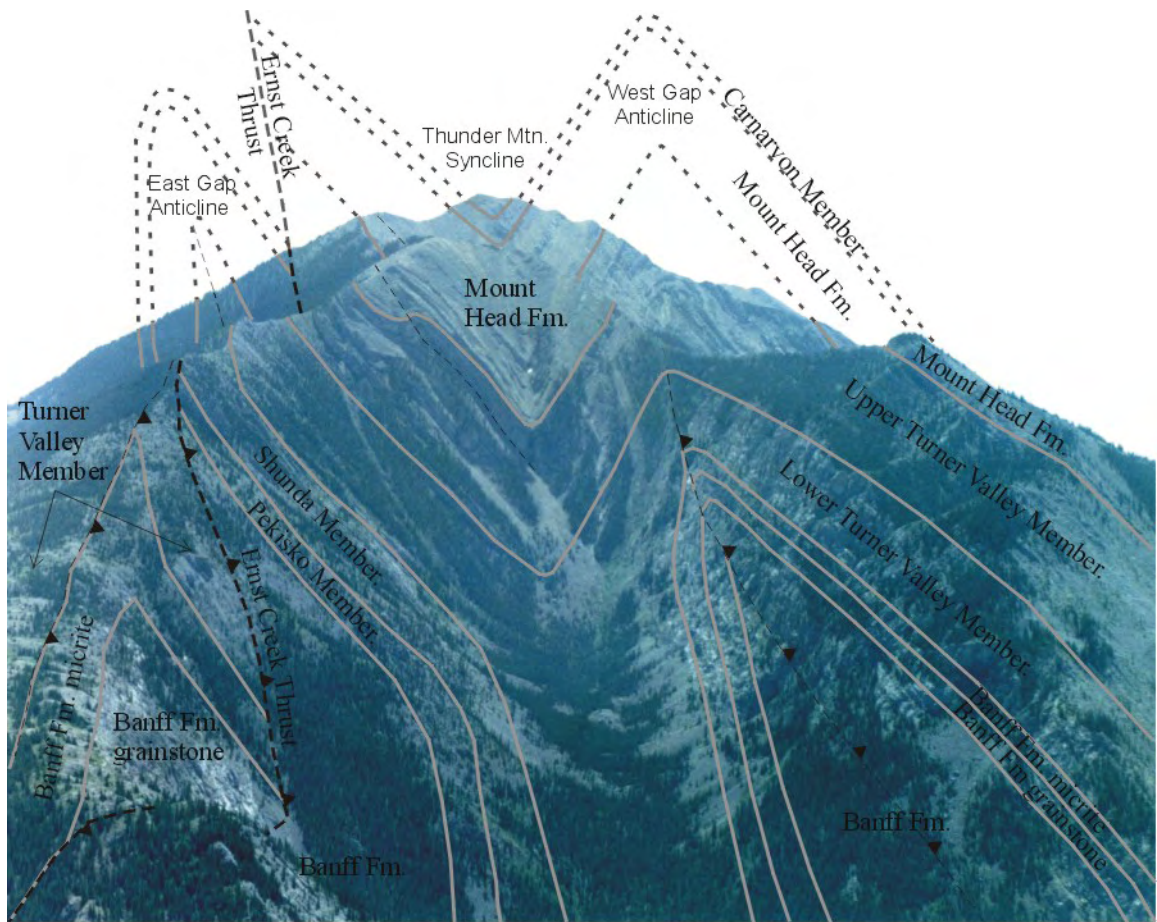


Figure 2-9. View south at the folds and related thrust faults along the north slopes of Thunder Mountain.

the hanging-wall of the Ernst Creek thrust (Figure 2-5, sections I-I' and J-J', and Figure 2-8). The thrust fault along the hinge zone of the East Gap anticline has been traced southward >7 km from The Gap to UTM 5520000N where it juxtaposes steeply west-dipping Carnarvon Member with overturned east-facing Etherington Formation (Figure 2-8). Near The Gap this "hinge-zone" thrust is overlapped northward by the Ernest Creek thrust, which juxtaposes west-dipping Banff Formation over overturned east facing Turner Valley Member (Figure 2-8). North of The Gap both the Ernest Creek thrust and the overlying thrust that emerges northward from the hinge of the West Gap anticline die out in the hinge of a simple east-verging asymmetric thrust-propagation anticline (Figure 2-8 and Douglas, 1950).

## **2.5 Cross-strike discontinuities (tear faults or lateral thrust ramps)**

### **2.5.1 Interpretation**

Based on geological relationships described above, the Morin Creek tear fault and Daisy Creek tear fault are interpreted to be pre-existing northeast-trending faults that became reactivated as tear faults or lateral ramps during thrusting and folding. At deeper structural levels, the Rock Creek discontinuity is probably the same type of reactivated fault structure, but at its present level of erosion the only evidence for the underlying tear fault are the abrupt changes in fold trends and plunges. These structures are interpreted to have been active prior to the deposition of the Early Carboniferous Mount Head Formation because both the Morin Creek tear fault and the Daisy Creek tear fault cut up through the Livingstone Formation but not into the overlying Mount Head Formation. Evidence of their original movement was not observed along these structures, possibly due to later fault reactivation obscuring previous kinematic indicators. On the west side

of the LRA at Morin Creek, the upper part of the Mount Head Formation strikes north-south across the tear fault with no apparent offset or evidence of folding (Figure 2-4). The Daisy Creek tear fault cuts vertically through the Livingstone Formation and older strata, but it links upwards with a back thrust within the middle to upper part of the Livingstone Formation (Figure 2-5, profile section G G' and Figure 2-7). The northeast trend of these faults is parallel with the east-trending shortening direction of the thrusting and folding deformation and therefore they are ideally oriented to have been reactivated during thrusting and folding. The pre-existing fault that formed the Morin Creek tear fault may continue to the southwest and form the lateral ramp that marks the abrupt northward termination of the Turtle Mountain anticline (Figure 2-1), as mapped by Norris (1983). The Pocket Creek tear faults clearly differ fundamentally from the other three cross-strike discontinuities because they are east-west striking and formed within a conspicuous transverse, east-west trending dextral monoclinial flexure that has been superimposed on the entire LRA by underlying younger thrust-related structures.

## **2.6 Transverse Zones of Intense Fracturing and Minor Faulting**

### **2.6.1 Observations**

Regularly-spaced, east-west to east-northeast striking, steeply dipping zones of intense fracturing and minor faulting transect the north-south striking limbs and hinge zones of folds within the LRA in the vicinity of Green Creek, Morin Creek and Caudron Creek (Figure 2-4, Figure 2-10A). The transverse zones of intense fracturing, which have a regular spacing of approximately 150 metres and commonly contain one or more discrete, but discontinuous fault

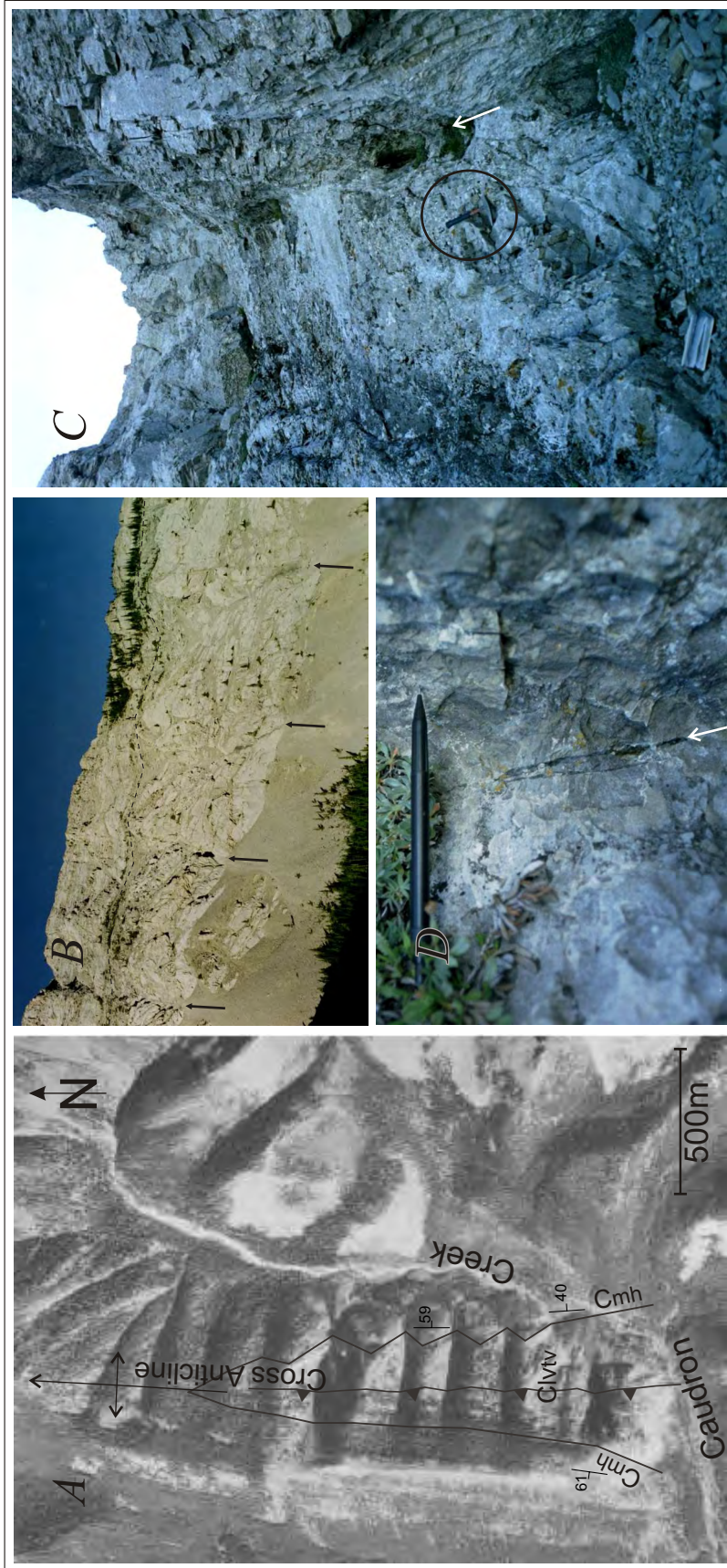


**Figure 2-10.** Photographs of transverse zones of intense fracturing and minor faulting in the LRA. **A** vertical air photo of the Cross anticline at Caudron Creek. The east-west trending gullies mark the locations of transverse east-west zones of fracturing and faulting that cut Turner Valley Member limestone in the core of the anticline at regularly-spaced (~150 metre) intervals, but note that they do not extend into the overlying Mount Head dolomite and shale. **B** - view to the west at the core of the Centre Peak anticline south of Morin Creek. The black arrows mark the locations of transverse zones of fracturing and faulting that cut through the east limb. The dashed line marks the surface trace of the thrust fault that lies along the hinge zone of the anticline. **C** - view to the west at intensely fractured limestone within a transverse zone of fracturing and faulting. White arrow points along the main fault contact where photo **D** was taken. The handle of the rock hammer in the circle at lower centre of photo is 33 cm long. **D** the white arrow points along a steeply dipping vein of black hydrocarbon residue that formed along a transverse fault surface, a common feature in zones of transverse fracturing and faulting. View is to the west. Pencil is 14 cm long.

surfaces appear to be restricted mainly to the Livingstone Formation and are commonly marked by gullies that form conspicuous erosional features in the steeper slopes and cliffs (Figure 2-10A, B). The fracture zones are generally wider and more strongly deformed in the forelimbs of the folds than in the backlimbs. Fault offsets are commonly 1 metre or less and the sense of displacement varies from one fault to the next. Some individual faults terminate abruptly against bedding surfaces, but are aligned with other faults that occur several metres away. Slickenlines and slickenfibres are rare, but where preserved are generally parallel with the bedding. Solid black hydrocarbon residues are common on fault surfaces and in fractures (Figure 2-10D). In a few transverse fracture zones, multiple sets of cross-cutting calcite and/or dolomite and/or hydrocarbon veins provide evidence of intermittent reactivation of the transverse fracture zones.

### **2.6.2 Interpretation**

The transverse zones of intense fracturing and minor faulting appear to have formed during flexural-slip folding by reactivation of a set of pre-existing steeply dipping, east-west-trending mega-joints that had developed preferentially within the Livingstone Formation. The bedding-parallel slickenlines and slickenfibres, and the discontinuous development of aligned faults within individual fracture zones, indicate that the fractures were reactivated in conjunction with inter-bed slip during flexural-slip folding. Propagation of inter-bed slip along individual bedding surfaces during flexural-slip folding evidently was interrupted by the pre-existing transverse fractures. Some inter-bed slip may have been transformed into strike-slip within the transverse fracture zones, some may have been transformed back into inter-bed slip at another stratigraphic level on the opposite side of the fracture zone, and some displacement may have been dissipated within the dense network of fractures within the transverse zone. If inter-bed slip

occurred at different times throughout the thrust-propagation folding process, as episodic propagation of discrete dislocations along individual bedding horizons, small increments of interbed slip would have been transferred into transverse fracture zones at various times and at various stratigraphic levels, producing a complex pattern of superimposed intense fracturing and small dextral and sinistral bedding-parallel shear. The transverse zones of intense fracturing and minor faulting are analogous to concentrations of dislocations that build up during dislocation-creep in crystalline materials (e.g. Hobbs et al., 1976). These intermittently reactivated fractured zones may have been important conduits for fluid migration before, during and after thrusting and folding; moreover, they provide a good example of the types of small-scale structures that may be important pathways for hydrocarbon migration and accumulation.

## **2.7 Detachment Thrust Faults**

### **2.7.1 Observations**

Interbed shear and detachment thrust faulting were important processes at work during thrust-propagation folding in the LRA. Evidence of bedding-parallel shear is widespread in the study area. It ranges from polished and slickensided bedding surfaces to small detachment thrust faults that emerge from interbed shear zones and offset adjacent beds. Detachment thrust faults range in scale from minor features with displacements of less than a few metres, to regional features that have controlled the ramp-flat geometry of the Livingstone thrust sheet as first recognized by Douglas (1950). Some of the more conspicuous thrust detachment horizons are identified in the stratigraphic column of Figure 2-3. Two stratigraphic horizons have been identified as preferred zones of regional detachment in the study area. The lowermost, which occurs ~60 metres below the top of the Devonian Palliser Formation forms an extensive regional

detachment at the base of the Livingstone thrust sheet. It has been intersected in two nearby exploration wells (Figure 2-2, Texaco Livingstone East 3-20-9-3W5, and Shell Imperial Burmis 10-33-7-3W5), and is well-established by regional borehole data and local seismic reflection imaging (Price, 1981; Deline, 2003). A locally important thrust detachment zone occurs ~140 metres below the top of the Banff Formation. It is conspicuous between Centre Peak and the north end of the study area where it controls the location of the hanging-wall of the Ernst Creek thrust and of an overlying thrust that dies out in the hinge zone of the West Gap anticline (Figures 2-2, 2-4, 2-6, 2-7 and cross sections E-E' and F-F' of Figure 2-5). In the subsurface this detachment thrust horizon is interpreted to underlie the west limb of the Caudron anticline, and to control parts of the hinge zones of the Centre Peak anticline and the Cross anticline (Figure 2-5, sections A-A', B-B', C'C' and D-D'). Other important detachment thrust horizons occur near the top of the Banff Formation. Detachment thrusting at this stratigraphic level generally occurs within the upper 20 metres of the Banff Formation; however, detailed mapping has shown that overlapping detachment horizons also occur in the lower part of the Turner Valley Member (Figures 2-11, 2-12, 2-13, and 2-14 and detailed maps of Figure 2-4). South of Green Creek (Figure 2-11 and section A-A' of Figure 2-5) a detachment occurs ~ 20 metres below the top of the Banff Formation and extends into the hinge zone of the Centre Peak anticline; however, north of Green Creek (Figure 2-13) detachment thrusts also emerge from two other overlapping detachment horizons, one in the lower part of the cherty and dolomitic micrite unit that forms the top of the Banff Formation, and the other in the lower part of the Turner Valley Member (see detailed map of the Green Creek canyon in Figure 2-4). At Morin Creek a detachment thrust that emerges from near the base of the Turner Valley Member truncates the steeply dipping strata of the forelimb and extends into the hinge zone of the Centre Peak anticline (see Figure 2-14, detailed map of Morin Creek area in Figure 2-4, and cross section B-B' of Figure 2-5). In the Caudron Creek area, a detachment ~ 20 metres below the top of the Banff Formation forms the

hanging-wall of the back thrust between Centre Peak anticline and Caudron anticline (detailed map of Caudron Creek in Figure 2-4, and cross section D-D' of Figure 2-5). These documented occurrences of detachments have guided interpretations of the subsurface structure of the LRA shown in Figure 2-5.

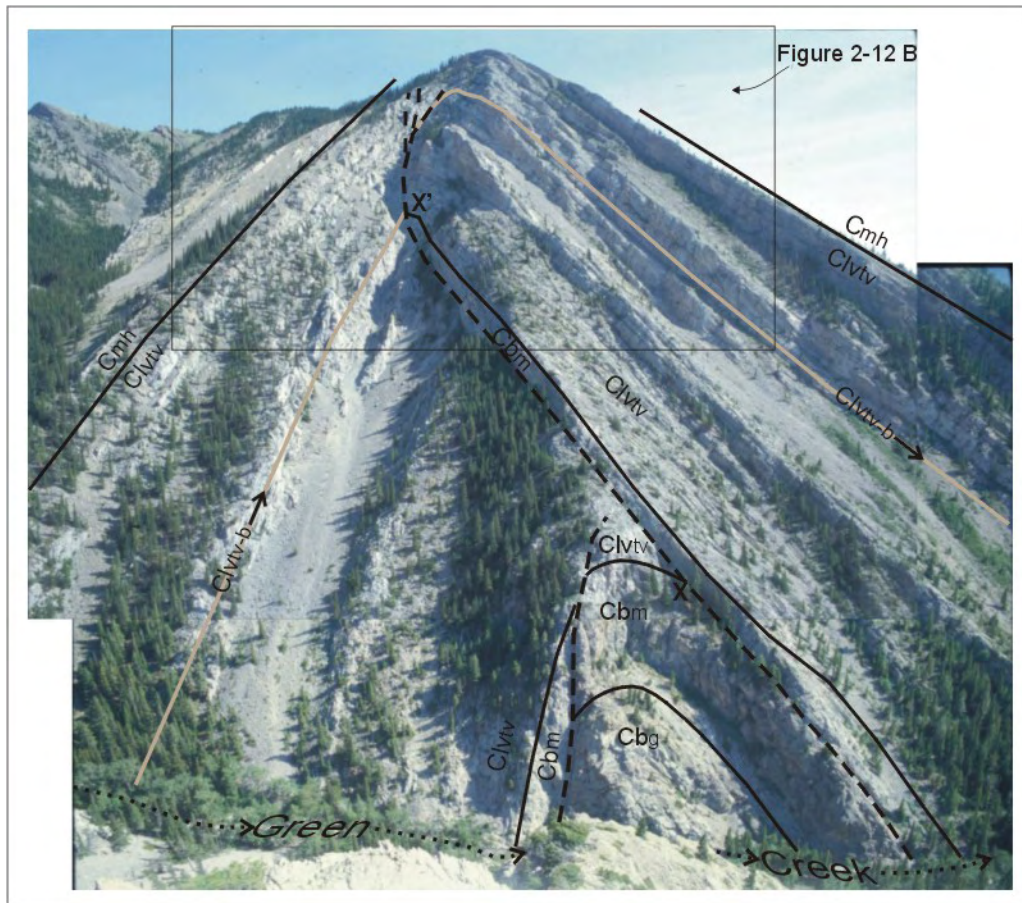


**Figure 2-11.** View south at the core of the Centre Peak anticline as exposed on the south side of the Green Creek canyon. The planar limbs of the anticline are separated by a composite, east-verging thrust fault that extends along the hinge zone. The lower segment, at the level of Green Creek, is a near-vertical thrust fault that is sub-parallel with the steep bedding in the micrite unit of the Banff Formation (Cbm) in the forelimb of the anticline but cuts up-section through the sub-horizontal bedding of the grainstone unit (Cbg) and micrite unit (Cbm) in the hinge zone. Approximately 150 metres above the creek, this cross-cutting, sub-vertical fault is interpreted to die out within the hinge zone of the anticline within the lower part of the Turner Valley Member (Clvtv). This fault is overlapped by a thrust that emerges from a bedding detachment ~20 metres below the top of the Banff Formation, deflects the hinge zone eastward as it truncates the Turner Valley Member (Clvtv) in its footwall, and then curves upward into the core of the Centre Peak anticline as it cuts up-section through the Turner Valley Member (Clvtv) in its hanging-wall as it becomes sub-parallel with the bedding in its footwall. The footwall and hanging-wall cut-offs of the top of the Banff Formation along this thrust fault, which are marked by X and X', respectively, have been offset ~250 metres along this fault. These structural relationships have been projected northward into section A-A' in Figure 2-5.

**Figure 2-12.** (following page) View south at the upper part of the core of the Centre Peak anticline exposed in the Green Creek canyon. A - A network of sub-vertical and bedding-parallel thrust faults deforms the upper part of the Turner Valley Member (Clvtv) within the upper forelimb. Extension faults (dotted lines) offset bedding in the core of the anticline. Thrust displacements also occur in the hinge zone and in the backlimb, forming duplex structures that thicken the fold hinge. Individual marker beds within this fault network, such as a distinctive brown weathering fine grained dolomitic limestone in the upper part of the Turner Valley Member (Clvtv-b), are represented by discontinuous elongate blocks 'floating' within a matrix of highly faulted and brecciated host rock fragments. B - The detachment thrust fault that emerges from the backlimb ~20 metres below the top of the Banff Formation (Cbm) dies out upward within the zone of intense faulting in the upper part of the forelimb.

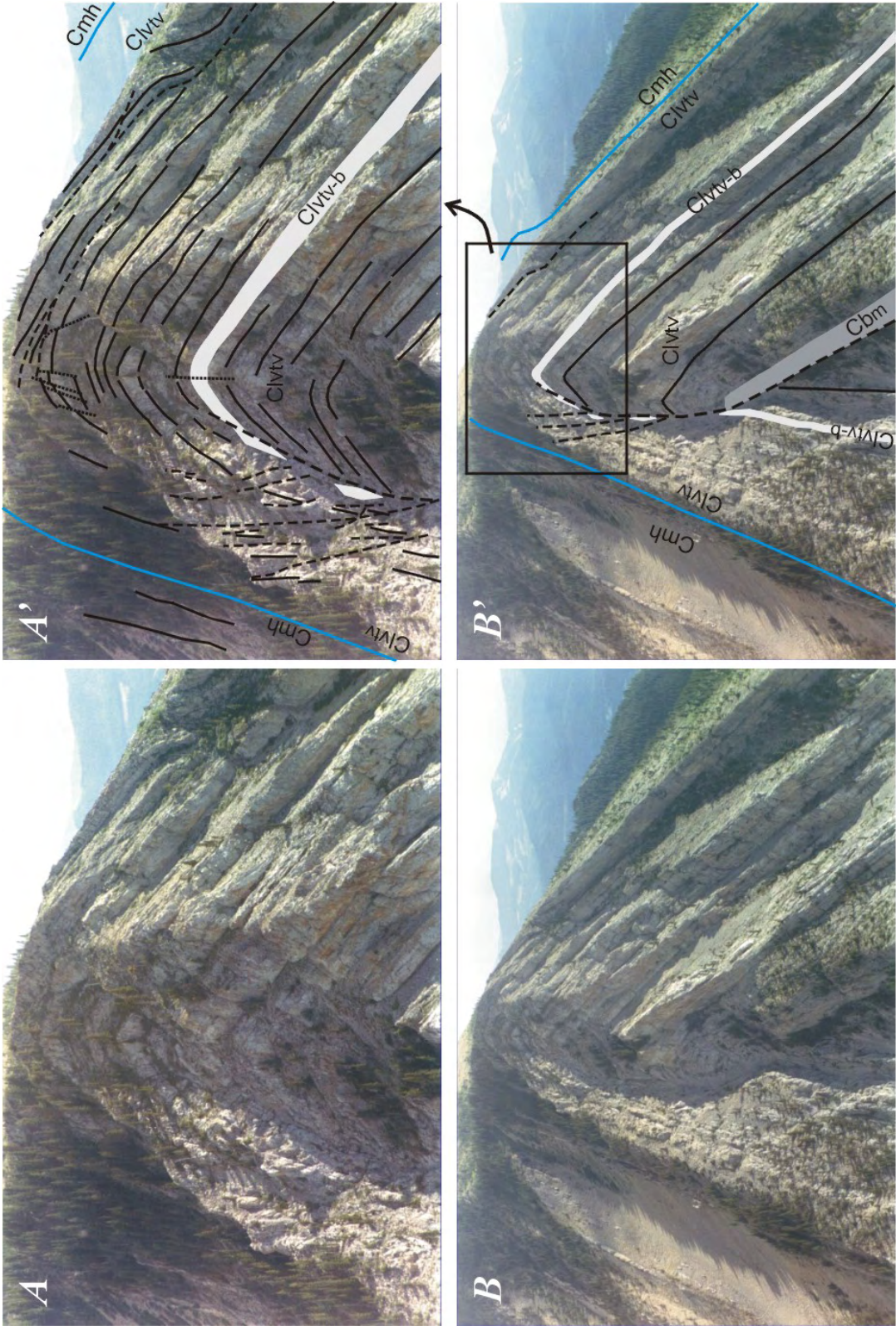


**Figure 2-12**

**Figure 2-13.** (following page) View north at the core of the Centre Peak anticline as exposed on the north side of the Green Creek canyon. The planar fold limbs are separated by a composite, east-verging thrust fault that extends along the hinge zone of the anticline. This fault consists of three distinct segments, two of which emerge from bedding-parallel detachment zones in the backlimb of the anticline (upper photo), deflect the hinge zone of the anticline, and then curve upward, cutting up-section to form a ramp through the beds in its hanging-wall. The structurally lowest fault segment, which is steeply west-dipping to vertical (lower photo), juxtaposes a ramp that cuts through the grainstone unit (Cbg) and micrite unit (Cbm) of the top of the Banff Formation in the hanging-wall with overturned and steeply dipping micrite unit (Cbm) and Turner Valley Member (Clvtv) in the footwall, that have been deformed by minor antithetic folds. This lower hinge-zone thrust is overlapped (upper photo) by a thrust that emerges from a bedding-parallel detachment in the lower part of the micrite unit (Cbm); and this middle hinge-zone thrust is, in turn, is overlapped by a upper thrust that emerges from a bedding-parallel detachment in the lower part of the Turner Valley Member (Clvtv), The conspicuous bedding-parallel detachment thrust that occurs ~20 metres below the top of the Banff Formation on the south side of Green Creek (Figure 2-11) dies out in the core of the anticline between the middle and upper detachment thrusts on the north side of the creek.

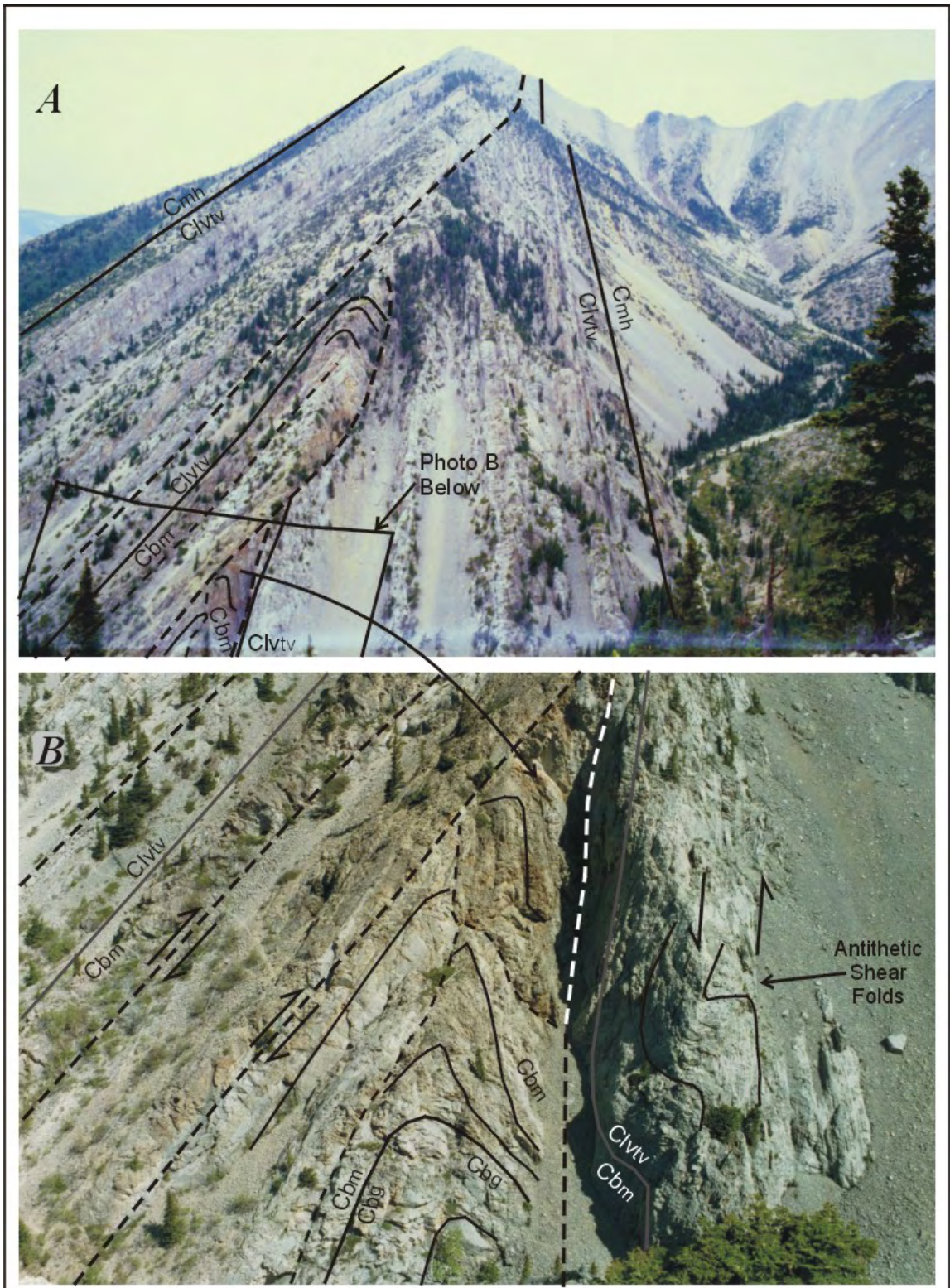


Figure 2-13



**Figure 2-14.** View south at the core of the Centre Peak anticline as exposed along the south side of Morin Creek canyon. In the lower core of the anticline, a steeply west-dipping thrust fault juxtaposes the west-facing grainstone unit (Cbg) of the backlimb over the upper part of the micrite unit (Cbm) in the east-facing overturned forelimb. An overlying thrust fault that emerges from a bedding detachment just above the bottom of the Turner Valley Member (Clvtv) in the backlimb of the fold truncates most of the Turner Valley Member (Clvtv) along its footwall. Near the skyline this detachment thrust curves upward and juxtaposes a hanging-wall ramp along which it steeply cuts up section through most of the Turner Valley Member (Clvtv) with a footwall “flat” that cuts sub-parallel to bedding, cutting the contact between uppermost Turner Valley Member and lowermost Mount Head Formation. A thrust fault that offsets the Misty Formation (Cm) and the lower part of the Fernie Formation (Jf) in the steeply dipping west limb of the Green Creek syncline dies out downward within the Etherington Formation (Ce) in the core of the syncline.

### **2.7.2 Interpretation; significance of detachments in the LRA**

The Livingstone Range Anticlinorium is a far-travelled, hanging-wall-ramp anticline. It developed as a thrust-propagation fold while the Livingstone thrust fault was propagating up-section eastward through Paleozoic strata that occupied the interval between a lower regional detachment near the top of the Devonian Palliser Formation and a higher regional detachment within the Jurassic Fernie Formation (Douglas, 1950; Price, 1981). In the Green Creek area the forelimb of the Caudron anticline is interpreted to have developed above the main ramp along which the Livingstone thrust propagated upward from the detachment within the Banff Formation to that in the Fernie Formation (Figure 2-5, cross sections B-B', C-C', D-D'). South of the Morin Creek tear fault and north of Green Creek the forelimb of the Centre Peak anticline is interpreted to have developed above a ramp along which the Livingstone thrust propagated upward from the regional detachment in the Palliser Formation to the overlying detachment within the Banff Formation (Figure 2-5, section B-B'). Between Morin Creek and Green Creek the Livingstone thrust cuts up-section southward in its hanging-wall from the detachment in the lower part of the Banff Formation to the detachment near the top of the Banff Formation (compare cross sections A A' and B-B' in Figure 2-5). The part of the Centre Peak anticline that lies north of Morin Creek tear fault and south of Centre Peak is interpreted to have developed above a minor thrust that splays from the underlying Livingstone Thrust (Figure 2-5, cross sections C-C' and D-D'). The Cross anticline is interpreted to be a thrust-propagation fold that formed above a splay from the underlying Livingstone thrust, which accommodated part of the ~700 metres of additional shortening on the north side of the Morin Creek tear fault.

## **2.8 The Centre Peak Anticline thrust-propagation fold**

### **2.8.1 Observations**

The Centre Peak anticline is illustrative of the thrust-propagation folds in the LRA, and its internal structure is well exposed in the transverse canyons of Green Creek and Morin Creek (Figure 2-4). The limbs of the anticline are remarkably planar. In the hinge zone of the anticline, at creek-level on the south side of Green Creek canyon (Figure 2-11), a near-vertical thrust fault separates the west-facing backlimb from the east-facing forelimb. The thrust truncates bedding in the upper part of the coarse lime grainstone unit of the upper part of the Banff Formation that outline the anticlinal hinge, but it is sub-parallel with bedding in cherty dolomitic micrite of the top of the Banff Formation in the steeply dipping to locally overturned forelimb (Figure 2-11, and Section A-A' of Figure 2-5). Stratigraphic separation across this fault decreases upward as it cuts up-section in its hanging-wall more steeply than in its footwall. Approximately 150 metres above the creek, this cross-cutting, sub-vertical fault appears to die out in the hinge zone of the anticline within lime grainstone of the lower part of the Turner Valley Member (Figure 2-11, and Section A-A' of Figure 2-5). Immediately above this location a conspicuous detachment thrust emerges from the backlimb of the anticline along a bedding detachment in the upper part of the micrite unit of the Banff Formation. This detachment thrust is parallel with the bedding in its hanging-wall, but it cuts up-section eastward in its footwall, truncating the underlying Turner Valley Member strata in the forelimb of the anticline (Figure 2-11 and Section A-A' of Figure 2-5). At the highest levels in the structure, the detachment thrust becomes steeper and concave to the west (Figures 2-11 and 2-12). As it cuts up-section in its hanging-wall from the bedding detachment in the micritic unit of the top of Banff Formation through the lower part of the Turner Valley Member, it becomes sub-parallel to the steeply dipping strata in the uppermost Turner Valley

Member in its footwall; thrust displacement decreases and the fault terminates in the core of the anticline below an unbroken fold hinge in the upper part of the Turner Valley Member (Figure 2-12A). The dip separation between the footwall and hanging-wall cut-offs of the top of the Banff Formation indicates that thrust displacement is ~ 250 metres at that stratigraphic level in the structure (Figure 2-11 and Section A-A' of Figure 2-5). However, the dip separation, and the displacement, decrease rapidly up-dip as the thrust cuts up-section, first in its footwall and then in its hanging-wall before dying out within a narrow zone of intense faulting in the upper part of the forelimb (Figure 2-12). A network of sub-vertical, bedding-parallel and subhorizontal extension faults deform the rocks in the upper forelimb and in the core of the fold (near the top of the photograph in Figure 2-12A). Individual marker beds within this fault network are represented by discontinuous elongate blocks 'floating' within a matrix of highly faulted and brecciated host rock fragments (Figure 2-12A).

The same basic pattern of chevron-style folding is displayed in the Centre Peak anticline on the steep slopes along the north side of Green Creek, but with some significant minor variations (Figure 2-13). In the core of the anticline at creek level a near-vertical thrust fault juxtaposes the grainstone unit and overlying tightly folded micritic unit of the Banff Formation in the hanging-wall with the upper part of the micrite unit of the Banff Formation in the footwall (Figure 2-13B). Asymmetric minor folds in the nearly vertical east-facing strata of the micrite unit of the Banff Formation and Turner Valley Members in the footwall are kinematically congruent with the sense of interbed shear for the flexural-slip folding (Figure 2-13B). As this near-vertical thrust fault cuts up-section along its hanging-wall, displacement decreases upwards, and is almost to zero where the fault abuts an overlying thrust fault that emerges from a bedding-parallel detachment within the lower part of the micrite unit of the Banff Formation in the backlimb of the fold (Figure 2-13A). As this detachment thrust cuts up-section through the steeply dipping Turner Valley Member in its footwall it deflects the hinge zone of the Centre Peak

anticline ~50 m eastward (Figure 2-13A) to where it curves upward to become steeply dipping and sub-parallel with the beds in its footwall as it cuts up-section through the micrite unit of the Banff Formation in the east limb of an anticline in its hanging-wall. Displacement on this thrust decreases upward and it is interpreted to die out in the hinge zone of the anticline just below the level at which a higher thrust emerges from a bedding detachment zone in the lower part of the Turner Valley Member. This higher bedding detachment thrust deflects the hinge zone of the Centre peak anticline ~150 m eastward as it cuts up-section eastward through the steeply dipping beds in its footwall (Figure 2-13A). Its tip line has been eroded away but clearly was higher than the base of the Mount Head Formation (Figure 2-13A). The detachment in the upper part of the micrite unit of the Banff Formation that is so conspicuous in the Centre Peak anticline on the south side of Green Creek canyon is still discernable ~20 metres below the top of the Banff Formation on the north side, but displacement on it appears to die out northward (Figure 2-13A).

Additional details in the pattern of chevron-style folding in the Centre Peak anticline are seen on the steep slopes along the south side of Morin Creek (Figures 2-4 and 2-14). In the core of the anticline, near creek-level in Morin Creek canyon, a near-vertical thrust fault juxtaposes the lower part of the grainstone unit of the upper part of the Banff Formation in the west-facing limb with the upper part of the micrite unit of the top of the Banff Formation in the east-facing limb. The stratigraphic separation across this thrust decreases abruptly southward as it cuts up-section through the beds in its hanging-wall (Figure 2-14). Just above where the thrust seems to die out within the micrite unit of the Banff Formation, it is overlapped by a higher thrust that emerges from a bedding detachment zone near the base of the Turner Valley Member (Figure 2-14). This detachment thrust deflects the hinge zone of the anticline ~200 metres eastward as it cuts up-section eastward along its footwall to the top of the Turner Valley Member, where it abruptly curves upward, cutting up-section in its hanging-wall and becoming sub-parallel to the bedding in

its footwall. At the skyline in Figure 2-14, the thrust fault cuts into the lower part of the Mount Head Formation in its footwall.

There is widespread evidence of inter-bed slip in the Centre Peak anticline. Polished bedding surfaces, many with slickenlines that plunge down-dip, occur in both limbs; and locally small thrust faults that emerge from inter-bed shear zones extend into overlying strata. Evidence of inter-bed slip is particularly conspicuous in the backlimb close to the core of the anticline where bedding detachment faults are linked up-dip to duplex-structures that attenuate the anticline along the hinge zone (Figure 2-12A). The stretching in the hinge zone is especially concentrated in the forelimb where thrust faults cut up along the hinge zone (Figure 2-12A).

The distinctive pattern of ramp-flat thrusting that occurs along the hinge zone thrust system of the asymmetric chevron-style Centre Peak anticline consists of a series of stacked detachment thrusts, each of which emerges from a different zone of interbed slip in the backlimb of the anticline and deflects the hinge zone. Each detachment thrust consists of two contrasting segments. The lower segment, which is parallel to bedding in the less steeply dipping backlimb of the fold, juxtaposes a hanging-wall flat with a footwall ramp. The upper segment, which is sub-parallel with the steeply-dipping forelimb, juxtaposes a hanging-wall ramp with what roughly approximates an overturned footwall flat. Each successively higher detachment thrust dies out in the hinge zone at approximately the same stratigraphic level from which an overlying detachment thrust fault emerges from a bedding detachment zone in the backlimb (Section A A' of Figure 2-5). The uppermost thrust fault dies out in the hinge zone of the anticline.

### ***2.8.2 Interpretation; Evolution of the Centre Peak anticline***

The well-documented configuration of the asymmetric chevron fold and its hinge-zone thrust system places tight constraints on the interpretation of the kinematics and mechanics of the Centre Peak anticline. In this fold, interbed slip was unevenly distributed throughout the fold limbs; extra interbed slip occurred along successive, discrete bedding detachment thrusts that propagated into the hinge zone of the anticline, resulting in an axial surface with conspicuous jogs. These bedding detachment thrusts may be analogous to limb thrusts of Ramsay (1974), which tend to form at the bases of thicker, more competent strata within chevron fold limbs.

The bedding detachment thrusts in the Centre Peak anticline are discontinuous along strike; they die out where they are overlapped by bedding plane detachments in adjacent stratigraphic levels (compare Figures 2-11 and 2-13). The fold shape is relatively consistent along strike, which indicates that the total interbed slip must have remained relatively constant along strike.

Successively higher bedding detachment thrusts deflect the hinge zone eastward and therefore displacement along them is interpreted to have occurred after the displacement on the underlying thrust. The highest bedding detachment thrust, which formed last and terminates in the core of a concentric, parallel, flexural-slip fold, records the arrested growth of the anticline. It provides an actualistic model for the configuration/geometry of the structure prior to the development of each of the underlying detachment thrusts that deflect the hinge zone. This sequence of deformation is modelled in Figure 2-15 as a series of cross-sections that represent stages in the development of the structural interpretation shown in the cross section A-A' in Figure 2-5. The reconstruction uses kink band migration and conservation of bedding thickness.

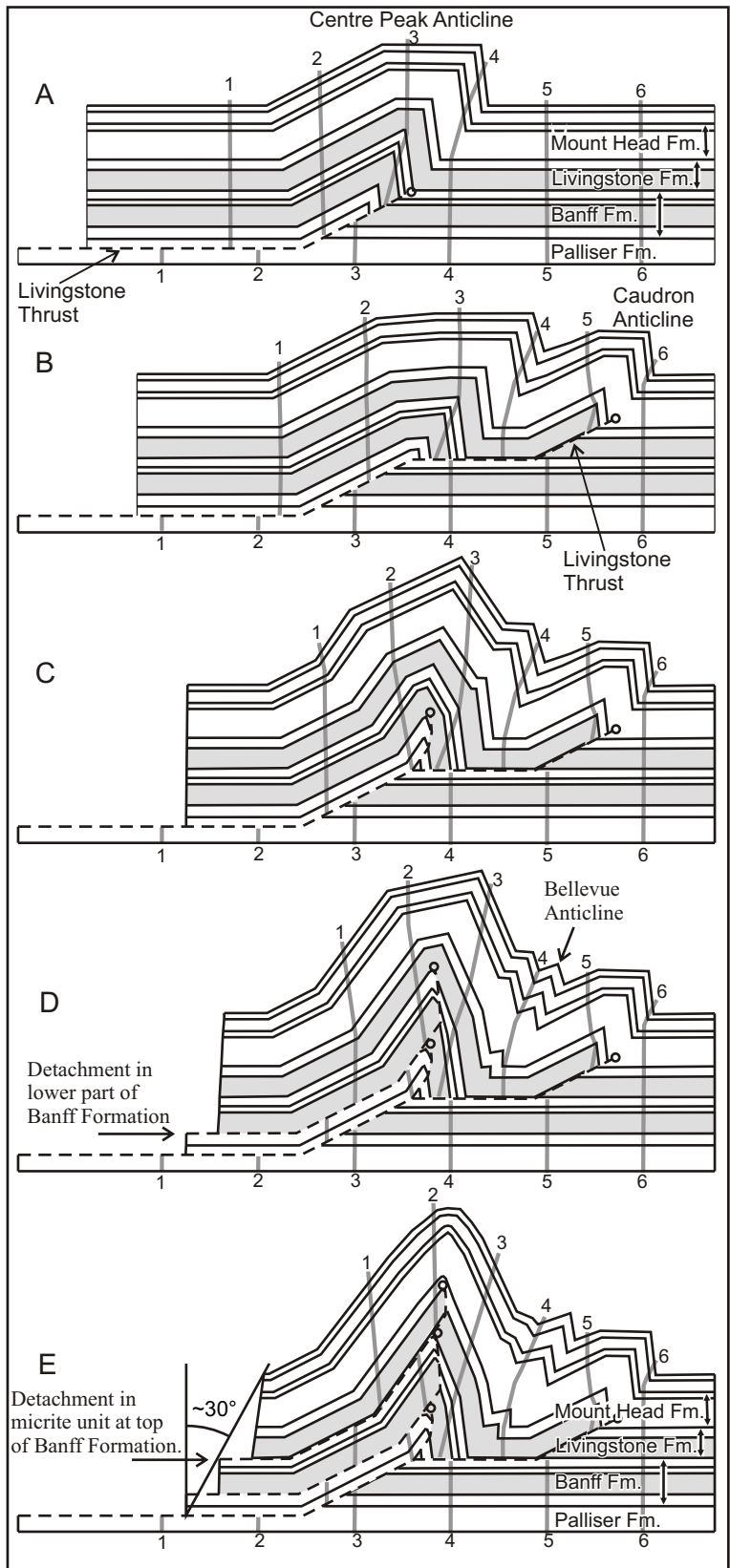


**Figure 2-15.** Proposed kinematic evolution of the Centre Peak anticline, based on cross section A-A' in Figure 2-5. Light grey lines are original vertical material lines that track relative displacement.

### ***2.8.3 Deformation model of the Centre Peak anticline***

The initial stage in the evolution of the Centre Peak anticline involved the propagation of the Livingstone thrust up a ramp from the regional detachment in the upper part of the Palliser Formation, through the Banff Formation and into the lower part of the Livingstone Formation (Figure 2-15 A). The “first-generation” thrust-propagation fold (Al Saffar, 1993) that developed during this stage has a structural style similar to that described by Williams and Chapman (1983), Jamieson (1987), and Suppe and Medwedeff (1990). A décollement breakthrough (Suppe and Medwedeff, 1990) occurred when the Livingstone thrust was deflected into a bedding detachment in the micrite unit near the top of the Banff Formation, and the simple “first-generation” thrust-propagation fold was displaced passively eastward (Figure 2-15B). The Livingstone thrust then propagated upward from the detachment in the micrite unit of the top of the Banff Formation and into the overlying Livingstone Formation, above which the Caudron thrust-propagation anticline began to develop (Figure 2-15B). At this stage, propagation of the Livingstone thrust up the ramp beneath the emerging Caudron anticline is interpreted to have stalled temporarily when displacement along the Livingstone thrust became diverted into the hinge zone of the Centre Peak anticline (Figure 2-15 B). A “second-generation” thrust-propagation fold (Al Saffar, 1993) developed within the Centre Peak anticline as a new thrust branched upward from the Livingstone Thrust at the top of the footwall ramp, cutting upward from the detachment in the Palliser Formation through the core of the “first-generation” fault-propagation fold (Figure 2-15 C). This new thrust juxtaposed the Palliser detachment in its hanging-wall over the truncated, steeply dipping Palliser Formation and Banff Formation strata in its footwall. As the new thrust propagated upward, simultaneous limb rotation and antithetic interbed slip within fold limbs caused fault cut-offs to lengthen, and shortening due to thrusting transformed into shortening by

flexural-slip folding. The secondary fault-propagation folding caused the hinge of the initial anticline to migrate upward, and thus may have lengthened the forelimb (Figure 2-15 C). The new thrust died out in the hinge zone of the anticline within the lower part of the Banff Formation. As the secondary thrust fault stopped propagating, a new thrust fault emerged from the detachment horizon in the lower part of the Banff Formation in the backlimb of the anticline; it propagated upward through the steeply dipping grainstone unit of the upper part of the Banff Formation in the forelimb, and displaced the anticlinal hinge eastward and upward. As it died out in the upper part of the micrite unit of the top of the Banff Formation (Figure 2-15 D), a third thrust fault emerged from the backlimb of the anticline from a detachment horizon near the tip line of the underlying thrust fault. It also displaced the anticlinal hinge eastward and upward as it propagated up-section through the steeply-dipping forelimb of the anticline into the upper part of the Turner Valley Member, where it terminated in the core of the anticline. At this stage the evolution of the Centre Peak anticline was arrested, preserving the relationships between flexural-slip folding and thrust-propagation. Subsequent to the deformation sequence outlined in Figure 2-15, thrust-propagation folding would have resumed within the Caudron anticline when the Livingstone thrust continued to propagate up-section through the Paleozoic strata before flattening out within a décollement in the Jurassic Fernie Formation. The Bellevue anticline, which is interpreted to be a simple, low amplitude chevron fold that propagated northward at the stage of fold development shown in Figure 2-15 D, lies between the Centre Peak anticline and the Caudron anticline in cross section A A' (Figure 2-5).

The cumulative bedding-parallel shear recorded by thrusts emerging from detachment horizons in the backlimb of the Centre Peak anticline is approximately 30 degrees (Figure 2-15 E). This provides an indication of the top-to-the-east bedding-parallel shear that was likely distributed throughout the Carboniferous strata within the Livingstone thrust sheet in the region to the west of the Livingstone Range.

During each step in the evolution of the Centre Peak anticline, external rotation of the fold limbs was accommodated by antithetic inter-bed slip within them. As the back limb underwent top-to-the-west rotation there was synchronous antithetic top-to-the-east interbed shear within the back limb. This may be expressed in part by the conspicuous offsets along thrusts that emerge from bedding detachment horizons. As the forelimb underwent top-to-the-east rotation there was synchronous top-to-the-west shear within the forelimb. This is illustrated by minor folds within the forelimb in Green Creek (Figure 2-13B). The amount of interbed shear was not symmetrical between the two fold limbs of the Centre Peak anticline. Extra interbed shear was localized along the bedding detachment horizons in the back limb, which was responsible for the upward propagation of the hinge-zone thrust system, the consequential upward growth of the anticline, and the formation of the conspicuous jogs in the hinge zone. The interpreted evolution of the Centre Peak anticline as shown in Figure 2-15 involved migration of kink bands. This is especially evident during later stages of fold tightening where two kink bands migrated upwards through each limb, resulting in the fold tightening to its final interlimb angle of  $\sim 60^\circ$  (Figure 2-15C, D, E). The intense deformation evident in the forelimb of the Centre Peak anticline may be evidence of the migration of a kink band through this part of the fold.

The Centre Peak anticline provides an actualistic model for the elucidation of the kinematics and mechanics of the evolution of the other chevron folds in the LRA that also have thrust faults along their hinge zones. These include the Caudron anticline, Cross anticline and the East and West Gap anticlines. The tight chevron folds in the LRA represent a relatively high level of strain (horizontal shortening and vertical thickening) of the Carboniferous carbonate rocks.

The detachment thrust faults that occur within the back limb of the Centre Peak anticline, and the conspicuous jogs in the axial surface that occur where these detachment thrusts deflect the hinge zone, are features that are not included in many models of thrust-propagation folding (Dahlstrom, 1969 and 1970; Williams and Chapman, 1983; Jamieson, 1987; Suppe and

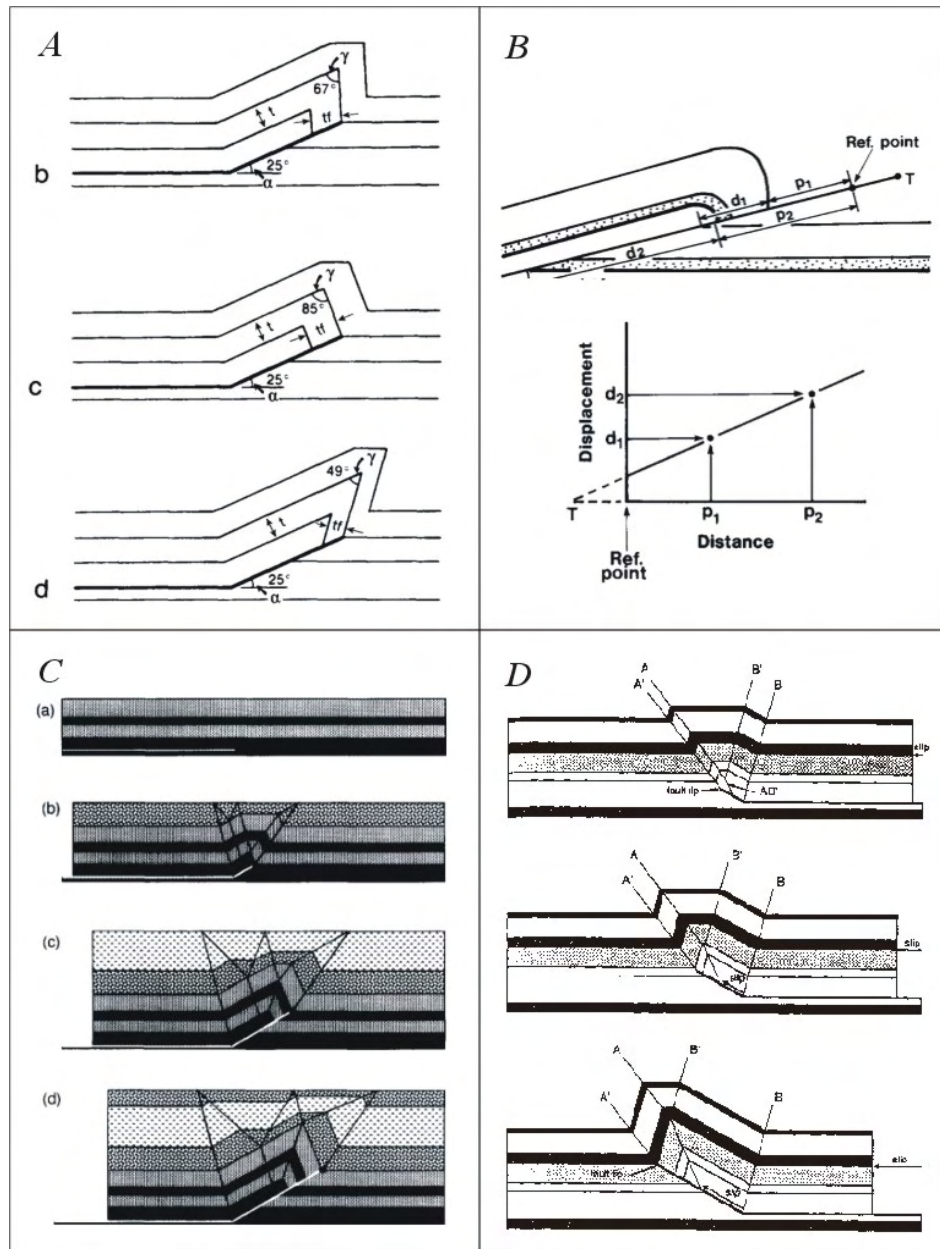


**Figure 2-16.** Other thrust-propagation fold models. *A* is from Jamieson (1987) showing how fold shape is related to fault ramp angle, fold intelimb angle and degree of thickening or thinning of the forelimb. *B* is from Williams and Chapman (1983) defining displacement and distance of offset of marker beds. *C* is from Wickham (1995) showing a simple thrust-propagation fold that has growth strata accumulating during fold development. *D* is from Suppe and Medwedeff showing a simple thrust-propagation fold growing self-similarly. In all of these models the tip line of the thrust is still within the area of the model and the fold has not been detached from its footwall.

Medwedeff, 1990; Wickham, 1995; and Allmendinger, 1998) (Figure 2-16). Although some models of thrust-propagation folds that are based on kink-band migration (Jamieson, 1987; Suppe and Medwedeff, 1990) do involve interbed slip, these models show much less than that shown in the Centre peak anticline. The Centre Peak anticline evolved further than the stages of deformation shown by most models of thrust-propagation folding (Figure 2-16).

#### **2.8.4 *Fracture analysis of the Centre Peak anticline***

Fracture orientations were measured in the Livingstone Formation at six localities in the backlimb of the Centre Peak anticline and at ten localities in the forelimb (Figure 2-17). The data from each locality have been rotated to restore the local fold axis to horizontal and then rotated about the local fold axis to restore bedding to horizontal. Three of the localities in the backlimb at Green Creek are from unpublished measurements made in 1963 by R. A. Price. At most localities a few dominant fracture sets are obvious, but locally there is substantial dispersion in fracture orientations. Fractures are generally more numerous and variable in the forelimb of the Centre Peak anticline than in the backlimb. In both limbs, fracture orientation patterns are highly variable from one locality to another. However, north-south trending bedding-normal fractures (b-c joints) are common. At one locality (Figure 2-17, Locality M687) the dominant fracture sets apparent in one stratigraphic unit (Locality M687A) differ conspicuously from those within an adjacent stratigraphic unit (Locality M687B). At most localities within the zone of transverse fracturing (Figure 2-17, localities M131, M686, M688, M689, M693) there is a conspicuous steeply dipping, east-west trending dominant fracture set. The intensity of fracturing and variability in orientation diminish abruptly away from the zones of transverse fracturing.

**Figure 2-17. (Following page) Fracture orientation data from the Centre Peak anticline plotted in equal area stereographic projection from the lower hemisphere with the bedding plane horizontal (the poles to the fractures have been rotated about the local axis of folding, together with the pole to bedding, to compensate the rotation of the bedding during folding). The forelimb (east limb) of the fold contains transverse zones of fracturing and minor faulting and also flexural-slip-related back-thrusts that involve highly variable fracture patterns adjacent to fault surfaces. Areas in the forelimb that are not adjacent to faults exhibit simpler fracture patterns (e.g. Stations M687A and M687B). Stereonet images were generated using the program GEORient© 9.1 (R. J. Holcombe, University of Queensland).**

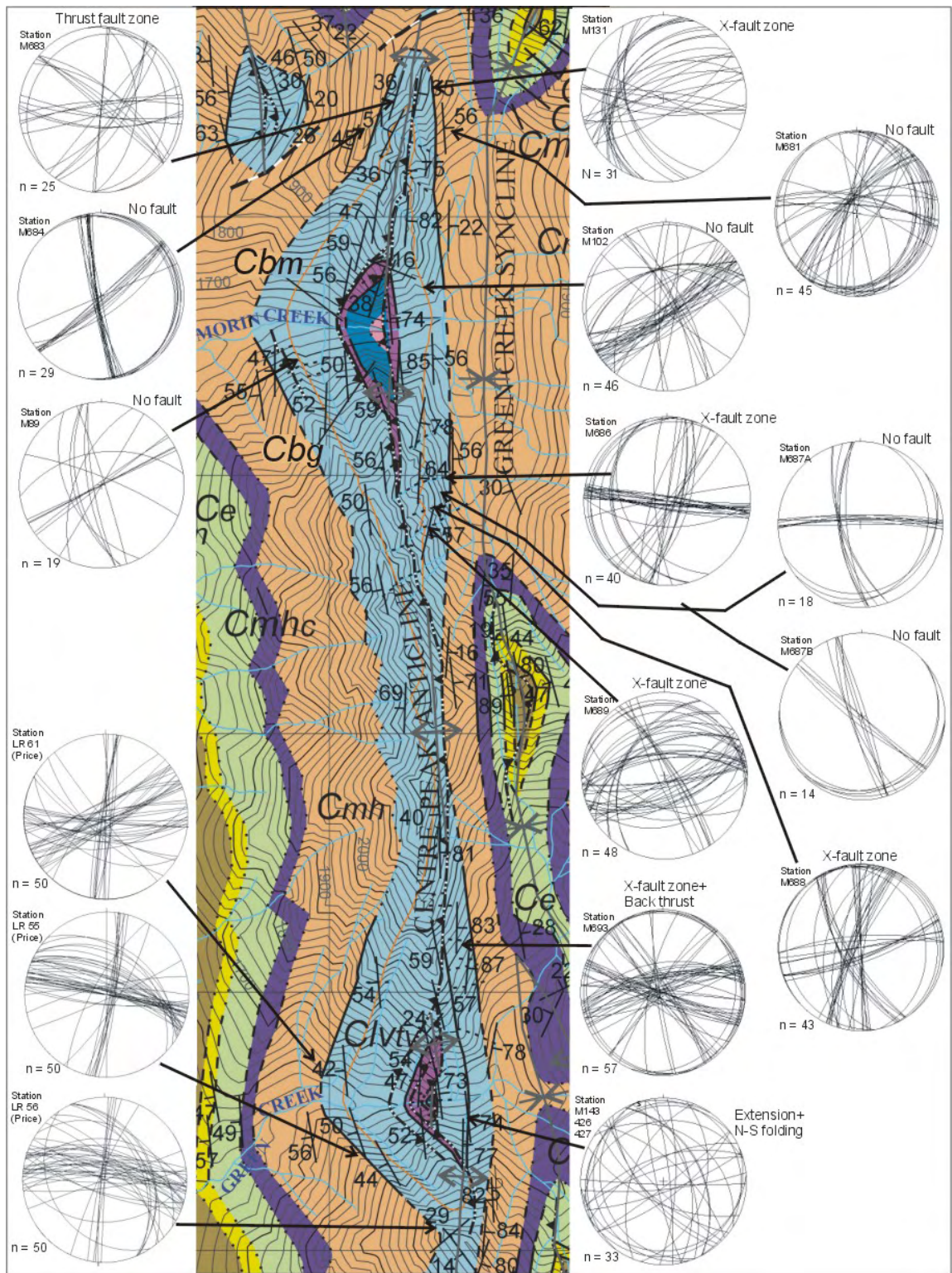


Figure 2-17

#### **2.8.4.1 Interpretation**

The generally more intense fracture development in the forelimb relative to the backlimb of the Centre Peak anticline can be attributed to deformation of the forelimb during propagation of thrusts along the hinge zone of the fold. Transverse fracture zones, minor back thrust faults and extension faults are more extensive in the forelimb than in the backlimb. The contrasting fracture patterns between adjacent stratigraphic units at Location M687 (Figure 2-17), which is in the forelimb but isolated from fracture zones, suggest that individual segments of the stratigraphic section separated by bedding detachment zones may have deformed independently. The along-strike variability in fracture development evident in Figure 2-17 illustrates the importance of the transverse fracture zones. These fracture zones have the greatest complexity of fracture orientations and hence would have been the most favourable conduits for fluid migration, an interpretation that is supported by the prevalence of hydrocarbon residues in the fractures and faults within them.

## 2.9 Cataclastic Flow

Strata within the Centre Peak anticline have been subjected to several deformation events during their translation from relatively undisturbed subhorizontal beds, to their present position within the chevron fold of the Centre Peak anticline. In addition to thrust-propagation folding, the Centre Peak anticline was affected by fault bend folding as it travelled through the footwall syncline and then the footwall anticline of the ramp through the Paleozoic strata, and then again as it travelled up a ramp within Mesozoic strata. Deformation within the rock mass included displacements along and across networks of thrust faults, extension faults and other shear fractures that cut across bedding. These discrete displacement discontinuities bound individual blocks of rock that underwent major translation and rotation with only very minor internal deformation. There is generally little evidence of penetrative strain. Even the finest details of sedimentary and fossil structures are well preserved within the fracture-bound blocks. This style of deformation, which is analogous to deformation in a granular or blocky aggregate in which individual fragments are free to move relative to one another along their bounding surfaces (Price, 1967), is an example of “cataclastic flow” (cf. Wojtal, 1986; Ismat and Mitra, 2005). Slickenlines provide evidence of the direction and sense of shear displacements along small extension faults, contraction faults, shear joints and bedding. Surface markings and crystal druze on joints, faults and bedding planes provide evidence of dilation between blocks. Pressure solution and stylolitization on some fractures and precipitation of carbonate and quartz in dilatant zones along other fractures were widespread but minor features of the deformation (Price, 1967). Cataclastic flow was most intense and conspicuous in the hinge zone of the Centre Peak anticline where beds are offset and stretched near the tip lines of bedding detachment faults that propagated out of the back limb (Figure 2-12). In this location, extension faults cut previously

formed thrusts, implying that the local stress state within the fold hinge changed from an earlier episode of compression to extension during later stages of folding.

## **2.10 Conclusions**

The Livingstone Range anticlinorium is a detached and displaced hanging-wall-ramp thrust-propagation fold. It developed as the eastward propagating Livingstone thrust cut upward through ~1000 m of well bedded, shallow-water, Upper Paleozoic carbonate strata to form a ramp between extensive regional detachments in the lime mudstones of the upper part of the Upper Devonian Palliser Formation and in the marine shales of the Jurassic Fernie Formation. The anticlinorium consists of an array of linked, asymmetric flexural-slip chevron folds that contain distinctive blind hinge-zone thrust systems.

The distinctive pattern of ramp-flat thrusting that forms the hinge zone thrust system of the asymmetric chevron-style Centre Peak anticline consists of a series of stacked detachment thrusts, each of which emerges from a different zone of interbed slip in the backlimb of the anticline and deflects the hinge zone. The distinctive hinge-zone thrust system of the Centre Peak anticline separates the moderately dipping, planar, west-facing backlimb from the steeply dipping, planar, east-facing forelimb. Each detachment thrust consists of two contrasting segments. The lower segment, which is parallel to bedding in the less steeply dipping backlimb of the fold, juxtaposes a homoclinal, west-facing structural panel above a hanging-wall flat with an east-facing footwall ramp. The upper segment, which is sub-parallel with the steeply-dipping forelimb, juxtaposes a hanging-wall ramp with what roughly approximates an overturned footwall flat. Each successively lower detachment thrust dies out upward in the hinge zone at

approximately the same stratigraphic level from which an overlying thrust fault emerges from a bedding detachment zone in the backlimb (Section A A' of Figure 2-5). Successively higher bedding detachment thrusts deflect the hinge zone eastward and therefore displacement along them must have occurred after the displacement on the underlying thrust. The highest bedding-detachment thrust, which formed last and terminates in the core of a concentric, parallel, flexural-slip fold, records the arrested growth of the anticline. It provides an actualistic model for the configuration/geometry of the structure prior to the development of each of the underlying detachment thrusts that deflect the hinge zone.

The initial stages of thrust-propagation folding in the Centre Peak anticline may have resembled models described by Dahlstrom, (1969 and 1970); Williams and Chapman (1983) Jamieson (1987), Suppe and Medwedeff (1990), Wickham (1995), and Allmendinger (1998) (Figure 2-16). However, the folds in the LRA underwent additional deformation that involved the propagation of thrust faults that emerged from bedding detachment zones in the back limb and cut up along the hinge zones. This additional thrust-propagation folding caused the fold hinges to tighten to an interlimb angle of ~60 degrees and lengthened the fold limbs, which essentially doubled the size of the anticlines and resulted in a distinctive style of chevron folding.

The cumulative bedding-parallel shear recorded by thrusts emerging from detachment horizons in the backlimb of the Centre Peak anticline is approximately 30 degrees (Figure 2-15 E). This provides an indication of the top-to-the-east bedding-parallel shear that was likely distributed throughout the Carboniferous strata within the Livingstone thrust sheet in the region to the west of the Livingstone Range.

Locally important detachments occur in the lower part of the Banff Formation, in the micrite unit at the top of the Banff Formation, and near the base of the Turner Valley Member of the Livingstone Formation. Most of the individual chevron-style thrust-propagation folds in the anticlinorium formed above the minor ramps that developed along the hanging-wall of the

Livingstone thrust as it propagated up-section from one bedding-parallel detachment to another. Notable exceptions are the tight chevron-style Cross anticline which formed above a thrust splay that branched upward from the Livingstone thrust, and one short segment of the Centre Peak anticline that formed a broad open fault-bend fold.

Along-strike changes in the structure of the Livingstone Range anticlinorium are generally gradual, but locally they occur abruptly across cross-strike discontinuities. These are associated with dextral tear faults (or lateral thrust ramps) that are kinematically linked to slip on the Livingstone thrust. The Morin Creek and Daisy Creek tear faults, which die out upward near the top of the Livingstone Formation, may have originated as east-northeast-trending steeply dipping structures that were active prior to deposition of the Mount Head Formation, and were subsequently reactivated as tear faults during thrusting and folding. The Pocket Creek tear faults, which trend east-west and cut through Mount Head Formation and younger strata, are interpreted to have formed much later when a dextral transverse fault-bend fold flexure was superimposed on the anticlinorium as the Livingstone thrust sheet was being transported eastward on underlying thrusts.

Broad anticlinal culminations occur between the cross-strike discontinuities in the Livingstone Range anticlinorium. The relationships between the locations of cross-strike discontinuities and fold culminations may provide actualistic models for interpreting deeply-buried prospective petroleum reservoir structures, which commonly are difficult to interpret with seismic reflection imaging.

The abundant fractures that occur along the Centre Peak anticline in the Green Creek/Morin Creek area have relatively heterogeneous orientations and do not show a consistent pattern that can be related simply to folding. Fracture patterns are instead dominated by east-west trending transverse zones of intense fracturing that cut through fold limbs and that formed during reactivation of a widely spaced (~150 metres) pre-existing joint set. The transverse fracture zones

and extension faults are especially well developed within Livingstone Formation strata in the forelimbs of the anticlines in the LRA, which would have made this the most permeable part of the structure during hydrocarbon migration and trapping when the LRA was still deeply buried. These transverse structures do not extend up into the overlying shale-bearing Mount Head Formation, which may have served as a seal that prevented the upward migration of fluids.

The LRA is a well-exposed analogue to similar, buried hanging-wall ramp anticlines such as the Turner Valley anticline, which is a prolific hydrocarbon-bearing structure that underlies the foothills ~40 km south of Calgary.

## **2.11 Acknowledgements**

This research has been supported by NSERC research grants to Raymond Price, John Dixon and Kurt Kyser. We gratefully acknowledge the financial assistance of the sponsors of the Fold Fault Research Project. Field work benefited greatly from the field assistance of Greg Cameron, Scott Conley and Kyle Larson. We are grateful for the constructive criticisms of Margot McMechan. Digital topography was provided at nominal cost by AltaLIS Ltd., and access to well logs was provided by Nexen.

## 2.12 References

- Allmendinger, R. W., 1998. Inverse and forward modelling of trishear fault-propagation folds. *Tectonics*, v. 17, p. 640-656.
- Al Saffar, M., 1993. Geometry of fault-propagation folds: method and application. *Tectonophysics*, v. 223, p. 363-380.
- Bally, A. W.; Gordy, P. L.; Stewart, G. A., 1966. Structure, seismic data, and orogenic evolution of southern Canadian Rocky Mountains. *Bulletin of Canadian Petroleum Geology*, v.14, no.3, p. 337-381.
- Dahlstrom, C. D. A., 1969. Balanced cross sections: *Canadian Journal of Earth Sciences*, v. 6, p. 743-757.
- Dahlstrom, C. D. A., 1970, Structural geology in the eastern margin of the Canadian Rocky Mountains: *Bulletin of Canadian Petroleum Geology*, v. 18, p. 332-406.
- Deline, D.W., 2003. Investigation of a sub-surface lateral ramp in the southern Canadian Rocky Mountains (Crowsnest Pass area, S.W. Alberta) using 3-D seismic interpretation and physical analog modeling. Unpublished M.Sc. Thesis, Queen's University, Kingston, ON, Canada.
- Douglas, R. J. W., 1947. Preliminary map, Gap, Alberta, Paper - Geological Survey of Canada, p. 47-23.
- Douglas, R. J. W., 1950, Callum Creek, Langford Creek and Gap map-area, Alberta, Geological Survey of Canada Memoir 255, 124 p.
- Douglas, R. J. W.; Gabrielse, H.; Wheeler, J. O.; Stott, D. F.; Belyea, H. R., 1970. Geology and economic minerals of Canada, ed. 5, Economic Geology Report - Geological Survey of Canada, vol.1, pp.366-488, 1970
- Fleuty, M. J., 1964. The description of folds. *Proceedings of the Geologists' Association*, v.75, Part 4, p.461-492.
- Hobbs, B. E., Means, W. D. and Willians, P. F. 1976. *An outline of structural geology*. Wiley, New York

- Ismat, Z., and Mitra, G., 2005, Folding by cataclastic flow: evolution of controlling factors during deformation: *Journal of Structural Geology*, v. 27, no. 12, p. 2181-2203.
- Jamison, W. R., 1987, Geometric analysis of fold development in overthrust terranes: *Journal of Structural Geology*, v. 9, no. 2, p. 207-219.
- Norris, D. K., 1993. Geology and structure cross-sections, Blairmore (west half), Alberta, Geological Survey of Canada Map, 1829A, scale 1:50000.
- Obermajer, M., Stasiuk, L. D., Fowler, M. G., Osadetz, K., 1997. A comparative examination of organic geochemistry and petrology of Upper Devonian to Early Mississippian epicontinental black shales from Canada. *AAPG Bulletin*, vol.81, no.9, pp.1560-1561.
- Price, R A, 1967. The tectonic significance of mesoscopic subfabrics in the southern Rocky Mountains of Alberta and British Columbia. *Canadian Journal of Earth Sciences* v. 4, no. 1, p.39-70.
- Price, R. A., 1981. The Cordilleran foreland thrust and fold belt in the southern Canadian Rocky Mountains, in McClay, K. R., and Price, N. J., eds., *Thrust and nappe tectonics*, The Geological Society of London, p. 427-448.
- Price, R. A., and Sears, J. W., 2001. A preliminary palinspastic map of the Mesoproterozoic Belt/Purcell Supergroup, Canada and U.S.A.: Implications for the tectonic setting and structural evolution of the Purcell anticlinorium and the Sullivan deposit, in Lydon, J. W., Slack, J. F., Höy, T., and Knapp, M., eds., *The Sullivan deposit and its geological environment*, Geological Association of Canada, Mineral Deposits Division, MDD Special Volume No. 1, p. 43-63.
- Price, R. A., 1994. Cordilleran tectonics and the evolution of the Western Canada sedimentary basin, in Mossop, G. D., and Shetsen, I., eds., *Geological Atlas of Western Canada*: Calgary, Canadian Society of Petroleum Geologists/Alberta Research Council, p. 13-24.
- Price, R. A., Osadetz, K. A., Kohn, B. P., Feinstein, S., 2001. Deep refrigeration of an evolving thrust and fold belt by enhanced penetration of meteoric water; the Lewis thrust sheet, southern Canadian Rocky Mountains. *Abstracts with Programs - Geological Society of America*, v. 33 (6), p. 52.
- Ramsay, J. G., 1967. *Folding and fracturing of rocks*. New York, McGraw-Hill Book Co. (Internat. Ser. Earth and Planetary Sci.)

- Ramsay, J. G., 1974. Development of chevron folds. *Geological Society of America Bulletin*, v. 85, no. 11, p. 1741-1754.
- Sears, J. W., and Price, R. A., 2003, Tightening the Siberian connection to western Laurentia: *Geological Society of America Bulletin*, v. 115, no. 8, p. 943–953.
- Suppe, J., and Medwedeff, D. A., 1990. Geometry and kinematics of fault-propagation folding. *Eclogae Geologicae Helvetiae*, v. 83, p. 409-454.
- Suppe, J., 1983. Geometry and kinematics of fault-bend folding. *American Journal of Science*, v. 283, no.7, p.684-721.
- Wheeler, J. O. and McFeely, p., 1991. Tectonic Assemblage Map of the Canadian Cordillera and adjacent parts of the United States of America; Geological Survey of Canada, Map 1712A, scale 1:20000000.
- Wickham, J., 1995, Fault displacement-gradient folds and the structure at Lost Hills, California (U.S.A.): *Journal of Structural Geology* v. 17, no. 9, p. 1293-1302.
- Williams, G., and Chapman, T., 1983, Strains developed in the hanging-wall of thrusts due to their slip/propagation rate: A dislocation model, *Journal of Structural Geology*, v. 5, p. 563-571.
- Wojtal, S. F., 1986, Deformation within foreland thrust sheets by populations of minor faults: *Journal of Structural Geology*, v. 8, p. 341-360.

# **Chapter 3 Stable-isotope geochemistry of syntectonic veins in the Livingstone Range anticlinorium and their significance to the thermal and fluid evolution of the southern Canadian Foreland Thrust and Fold Belt.**

Michael A. Cooley, Raymond A. Price, T. Kurtis Kyser & John M. Dixon  
Queen's University, Kingston, Ontario, Canada

## **3.1 Abstract**

The Livingstone Range anticlinorium (LRA) is a long (>65 km) narrow (<5 km) structural culmination of linked en-echelon chevron-style thrust-propagation folds that marks a major hanging-wall ramp across which the Livingstone thrust cuts ~1000 m up-section from a regional décollement in the upper part of Devonian Palliser Formation to a décollement within Jurassic Fernie Formation.

Prior to thrusting and folding, infiltration of Precambrian basement fluids into the Paleozoic strata of the LRA is recorded by deformed jasper+/-fluorite+/-sphalerite veins, and adjacent haloes of altered, dolomitic host rock with high  $^{87}\text{Sr}/^{86}\text{Sr}$  ratios (0.7094 to 0.7100) relative to most host rocks. Basement fluids infiltrating along reactivated basement faults during burial of the Paleozoic carbonate rocks, as well as underlying thick shale units, are possible sources for anomalously radiogenic strontium that occurs in the diagenetically altered Paleozoic carbonate rocks in the LRA and throughout the Western Canada Sedimentary Basin. Early syn-folding fluid flow is recorded by dolomite+/-calcite veins with isotopic compositions that are similar to those of host rocks. It occurred along faults related to thrust-propagation folding, and

also along many tear faults and larger thrust faults. Oxygen-isotope thermometry of four early syn-folding veins indicates they precipitated at anomalously high temperatures (250 +/-50°C). Most have slightly higher  $^{87}\text{Sr}/^{86}\text{Sr}$  ratios relative to adjacent host rocks and are interpreted to have formed from a mixture of formation fluids and hotter basement fluids in a rock-dominated system. The youngest episode of fluid flow along thrust faults and tear faults is recorded by calcite veins with very low  $\delta^{18}\text{O}$  values (-18 to -9‰ PDB), which are interpreted to have precipitated along faults that were active while the LRA was being transported eastward and elevated by underlying thrust faults, and rapidly cooled by infiltrating meteoric water. The conduits along which significant meteoric fluid circulation occurred are marked by visibly altered host rocks that have anomalously low  $\delta^{18}\text{O}$  values and slightly lower  $\delta^{13}\text{C}$  values relative to most host rocks. Evidence for significant meteoric fluid circulation may not be present along the parts of thrust faults and tear faults that contain veins because veins were more likely to have formed where fluid flow became restricted or trapped in thin, discontinuous fractures. Black solid hydrocarbon residues along fault surfaces and between crystals in syntectonic veins, and petroleum-rich fluid inclusions in quartz, calcite and dolomite in syntectonic veins attest to the presence of hydrocarbons within the Carboniferous carbonate rocks in the Livingstone Range anticlinorium at various stages of deformation. Structurally and stratigraphically similar rocks form the reservoir of the prolific Turner Valley field situated nearby in the eastern Foothills.

## 3.2 Introduction

Within the history of deformation of every foreland thrust and fold belt there are concurrent thermal and fluid-flow histories that are integral parts of the tectonic evolution. Fluids transmit heat, facilitate faulting, and transport potentially economic minerals and hydrocarbons.

Hitchon (1984) suggested that high water-table elevations in the areas of high topography along the Canadian Rocky Mountains controlled regional groundwater recharge for the Western Canada Sedimentary Basin, thus providing the hydraulic potential for deep penetration of cold meteoric water that cooled the rocks beneath the deformed belt. Hitchon (1984) also suggested that the deeply infiltrating cold meteoric fluids might have displaced hotter formation fluids at depth, driving them into the undeformed strata beneath the foreland basin, and thus creating the pattern of lower geothermal gradients in the deformed belt and higher geothermal gradients in the prairies that exists today. The pattern of hinterland cooling and foreland heating would have migrated from west to east along with the thrusting and folding deformation (Hitchon, 1984). A similar migrating thermal pattern was recognised in the Idaho-Wyoming thrust belt by Burtner and Nigrini (1994), who inferred that gravity-driven fluid flow during the Sevier Orogeny was responsible for moving large amounts of heat from the depths of the Early Cretaceous foreland basin eastward toward the platform, raising temperatures there and initiating hydrocarbon maturation within the undeformed foreland basin strata. An eastward younging pattern of apatite fission track cooling dates across the Idaho/Wyoming thrust belt indicates that as the thrusting-related deformation migrated eastward, the recently heated rocks were rapidly cooled as they became incorporated into the thrust belt (Burtner and Nigrini, 1994).

The theory that meteoric water penetrated deep into the thrust and fold belt during deformation is generally well supported by studies of the thermal history and fluid flow in the southern Canadian Cordillera (Nesbitt and Muehlenbachs, 1995; Osadetz et al., 2004). A regional

reconnaissance investigation of fluid inclusions and stable isotopes in carbonate and quartz veins by Nesbitt and Muehlenbachs (1995) documented meteoric water signatures in what they interpreted to be primary fluid inclusions in apparently un-deformed syn-tectonic veins across the southern Canadian Cordillera. An investigation of the thermal history of the foreland thrust and fold belt in southern Alberta and British Columbia using apatite fission-track thermochronology and vitrinite reflectance data has shown that rapid cooling of this part of the thrust belt coincided with displacement on the Lewis thrust and other related faults (Osadetz et al., 2004). The widespread occurrence of veins with low  $\delta^{18}\text{O}$  and  $\delta^{13}\text{C}$  values that occur along major thrust faults in the Front Ranges of the Rocky Mountains (Kirschner and Kennedy, 2001) and in thrust-related structures in the subsurface beneath the southern foothills of the Rocky Mountains (Cioppa et al., 2000; Lewchuk et al., 1998; Al-Aasm and Lu, 1994) may be evidence that regionally significant meteoric fluid flow occurred during thrusting; but the absence of alteration along thrust faults and the restricted presence of veins with low  $\delta^{18}\text{O}$  values to within 1 metre of thrusts indicates that only small amounts of fluids flowed along thrust faults in the Front Ranges of the Canadian Rockies (Kirschner and Kennedy, 2001). This implies that the parts of the thrust faults examined by Kirschner and Kennedy (2001) were not significant conduits for meteoric fluid circulation, because the wall rocks of such conduits should have significant host rock alteration if meteoric waters were circulating in sufficient quantities to remove heat from the rock mass.

The concept of a hot thermal event migrating eastward in advance of the thrusting and folding as proposed by Hitchon (1984) and by Burtner and Nigrini (1994) might explain the regional Late Cretaceous pre-thrusting and folding chemical remanent remagnetization observed in the Rocky Mountains and Foothills of southern Alberta and British Columbia (Enkin et al. 2000, Lewchuk et al. 1998, Cioppa et al. 2000). Although this chemical remagnetization might intuitively be attributed to hot fluids that were expelled from the deforming thrust belt, other

evidence to support this fluid event is elusive. No evidence of isotopic or other chemical alteration has been found in the host rocks that would document advective heating prior to or during thrusting deformation, although minor amounts of hot fluids may have entered the undeformed foreland basin prior to thrusting (Machel and Cavell, 1999) and during early stages of thrusting (Bradbury and Woodwell, 1987). It is particularly noteworthy that the Late Cretaceous chemical remanent magnetization is pervasive within the Paleozoic carbonate rocks themselves and is not associated with veins in fractures; moreover, rocks with abundant veins generally have poor paleomagnetic signatures (Enkin et al. 2000).

Detailed analysis of present-day formation fluid salinity data and geothermal data from wells in the Western Canada Sedimentary Basin by Bachu (1995) has shown that the movement of fluids through the undeformed strata of the Western Canada Sedimentary Basin is too slow to be capable of transporting heat by displacing formation fluids. Areas with anomalously high geothermal gradients that exist today in the Alberta foreland basin are not due to lateral flow of hot fluids but are most likely related to heterogeneities in heat production and heat flow from basement rocks underlying the undeformed sedimentary basin (Bachu, 1995). Cioppa et al. (2000) document an increase in magnetic mineral grain size that correlates with recrystallization of microdolomite to mesodolomite in host rock samples from the Turner Valley Formation in the Moose Mountain anticline, indicating that the Cretaceous chemical remagnetization of the rocks is due to recrystallization of in-situ magnetic minerals, a process that could occur simply from increased temperatures without advective heat transport. In addition, comparison of conodont alteration index data to laboratory unblocking temperatures from paleomagnetic studies in the Western Canada Sedimentary Basin have led Symons and Cioppa (2002) to suggest that much of the widespread Cretaceous remagnetization recorded in the strata is likely due to the thermal effects of burial and not orogenic fluid flow.

A principal objective of this project is to investigate the stable-isotope geochemistry of host rocks and syntectonic veins in the LRA and deduce the isotopic compositions of the various fluids that were in equilibrium with host rocks or with vein minerals at subsequent stages of thrusting and folding. Within the LRA, deformation associated with the formation of many carbonate and quartz veins can be linked unequivocally to displacements on specific thrust faults, tear faults, and minor faults. Cross-cutting relationships observed between many vein sets provide relative age constraints between different deformation events and fluid flow. This study combines fluid source information derived from their inferred isotopic compositions, oxygen-isotope thermometry of veins and paleothermal data from nearby coal to establish a thermal, fluid and tectonic history for the LRA, and correlate these with the thermal, fluid and tectonic evolution of the southern Canadian Foreland Thrust and Fold Belt.

### **3.3 Geological Setting**

The Foothills and Rocky Mountains of southwestern Alberta form the eastern margin of the Cordilleran foreland thrust and fold belt. The thrust and fold belt is a northeast-tapering accretionary wedge comprising sedimentary strata that have been scraped off the under-riding Laurentia craton and transported eastward with the over-riding Intermontane terrane, a tectonic collage of oceanic magmatic arc, volcanic and sedimentary rocks that was obducted over and accreted to the western margin of Laurentia during Late Jurassic to Paleocene convergence between Laurentia and subduction zones along its western margin (Monger and Price, 1979; Price, 1981; Price, 1994).

The structure of the accretionary wedge is dominated by east-verging listric thrust faults that flatten with depth and merge into a basal décollement that lies just above the contact between the sedimentary cover and underlying Paleoproterozoic basement. Thrust-propagation folds and

fault-bend folds developed during the thrusting. The displaced and deformed rocks include the Belt-Purcell strata, which accumulated in a Mesoproterozoic intracontinental rift, the Neoproterozoic to Jurassic Cordilleran miogeocline, which accumulated along the western rifted continental margin of Laurentia, the platform cover on Laurentia, which is the lateral equivalent of the miogeocline, and the Jurassic to Eocene synorogenic foreland basin deposits that accumulated in front of the advancing accretionary wedge and were partly incorporated in it. In the Front Ranges imbricate sheets of cratonic platform carbonate strata form conspicuous linear mountain ranges; in the Foothills, thinner imbricate slices of foreland basin siliciclastic strata form more subdued topography, but with isolated linear mountain ranges underlain by local culminations that expose Paleozoic rocks.

### **3.4 Structural Geology of the southern Livingstone Range**

The Livingstone Range anticlinorium (LRA) is a long (65 km) narrow (<5km wide) north-trending horizontally-plunging structural culmination of Carboniferous platformal carbonate rock that stands above the surrounding deformed foreland basin strata of the Foothills belt (Figure 3-1). At the north end, the anticlinorium terminates along the east side of the broad domal Plateau Mountain culmination; at the south end it terminates abruptly in south-plunging conical folds just north of the Crowsnest Pass Highway. The LRA coincides with a major hanging-wall ramp across which the Livingstone thrust cuts ~1000 m up-section from a regional décollement in lime mudstones of the upper part of Devonian Palliser Formation to another regional décollement

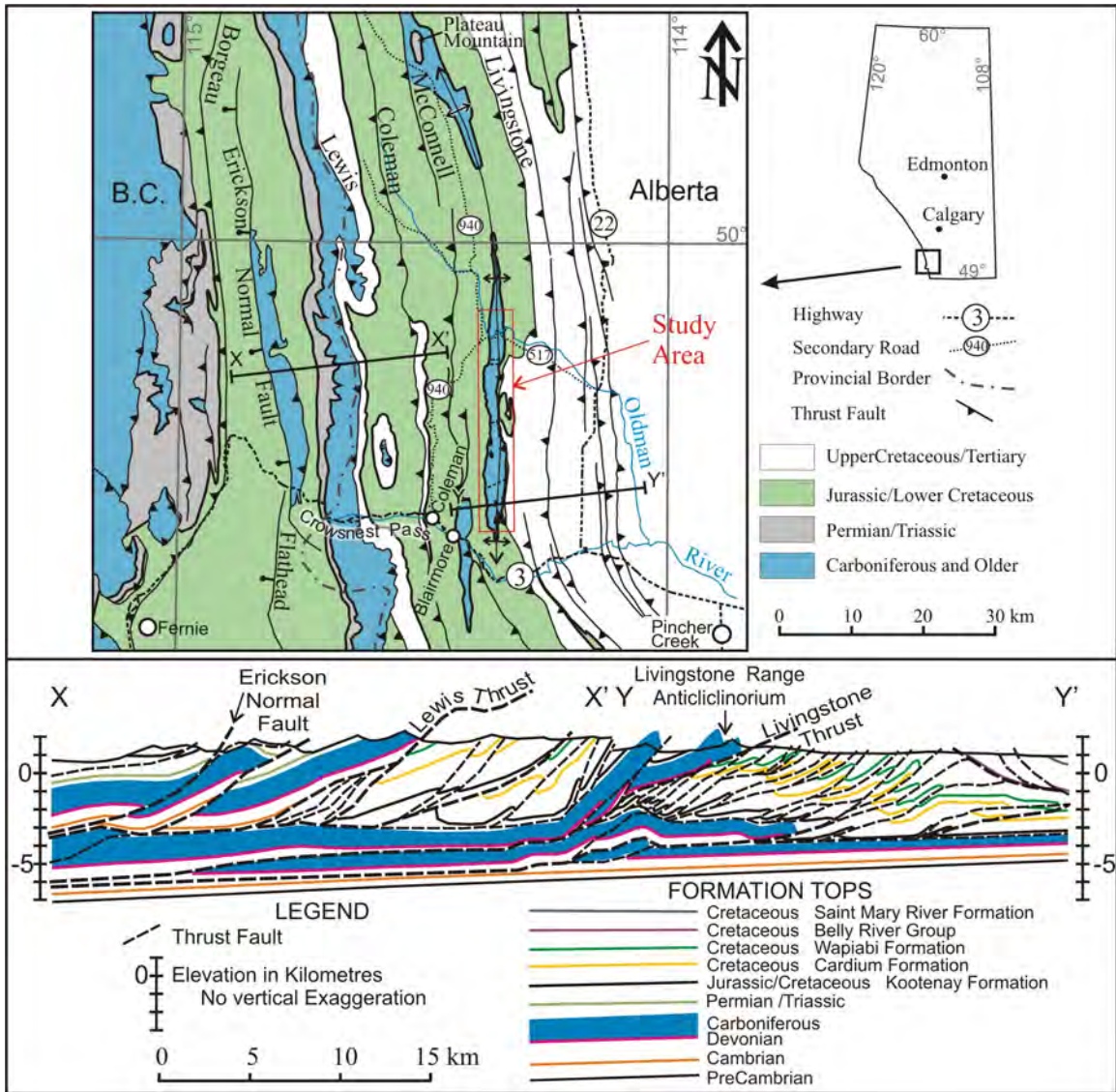


**Figure 3-1.** Regional geological setting of the study area (shown in Figure 2) at the south end of the Livingstone Range, southern Alberta foothills. Map modified from Wheeler and McFeely (1991) and Price (map of Fernie area, in preparation). Cross section X X' modified from Price (cross section of Fernie area, in preparation). Cross section Y Y' modified from unpublished cross section of Paul Mackay.

within marine shale of the Jurassic Fernie Formation. The matching footwall ramp is located more than 30 kilometres to the west, under the Lewis thrust sheet (Price, 1981, 1994). The structure of the Livingstone Range anticlinorium changes along strike as individual anticlines emerge, increase in size, and die out (Figure 3-2). Up to three anticlines occur in various locations. The changes are generally gradual, but locally they occur abruptly across cross-strike discontinuities that coincide with lateral thrust ramps or with northeast-trending “tear faults” that are kinematically linked to slip on the underlying Livingstone thrust. Four cross-strike discontinuities that occur in the study area (Figure 3-2) separate the LRA into five distinct segments, of which four were mapped in detail during this study.

The development of the LRA was dominated by flexural-slip thrust-propagation folding that occurred mainly as the Livingstone thrust was propagating up the ramp through ~1000m of Carboniferous strata during the latest Cretaceous. The resulting chevron-style thrust-propagation folds, which contain conspicuous thrust faults along their hinge zones, were almost fully formed by the time the Livingstone thrust began propagating along the regionally important detachment in the Jurassic Fernie Formation, and began transporting the LRA eastward. The Livingstone Range anticlinorium is an array of linked, en-echelon, mainly chevron-style thrust-propagation folds involving the Devonian-Carboniferous platformal carbonate rocks and overlying Mesozoic siliciclastic foreland basin deposits (Figure 3-2). Each chevron-style anticline is associated with one or more foreland-verging thrust faults that die out upward into the hinge zone. These blind thrusts separate steeply dipping planar east-facing forelimbs from less steeply dipping, west-facing planar backlimbs (Figures 3-3, 3-4, and 3-5). Above the tip lines of the blind thrust faults, the strata in the cores of the anticlines outline concentric, parallel folds. Other minor thrust faults die out downward into the cores of concentric parallel synclines. A more complete description of the structural geology of the study area can be found in Chapter 2.

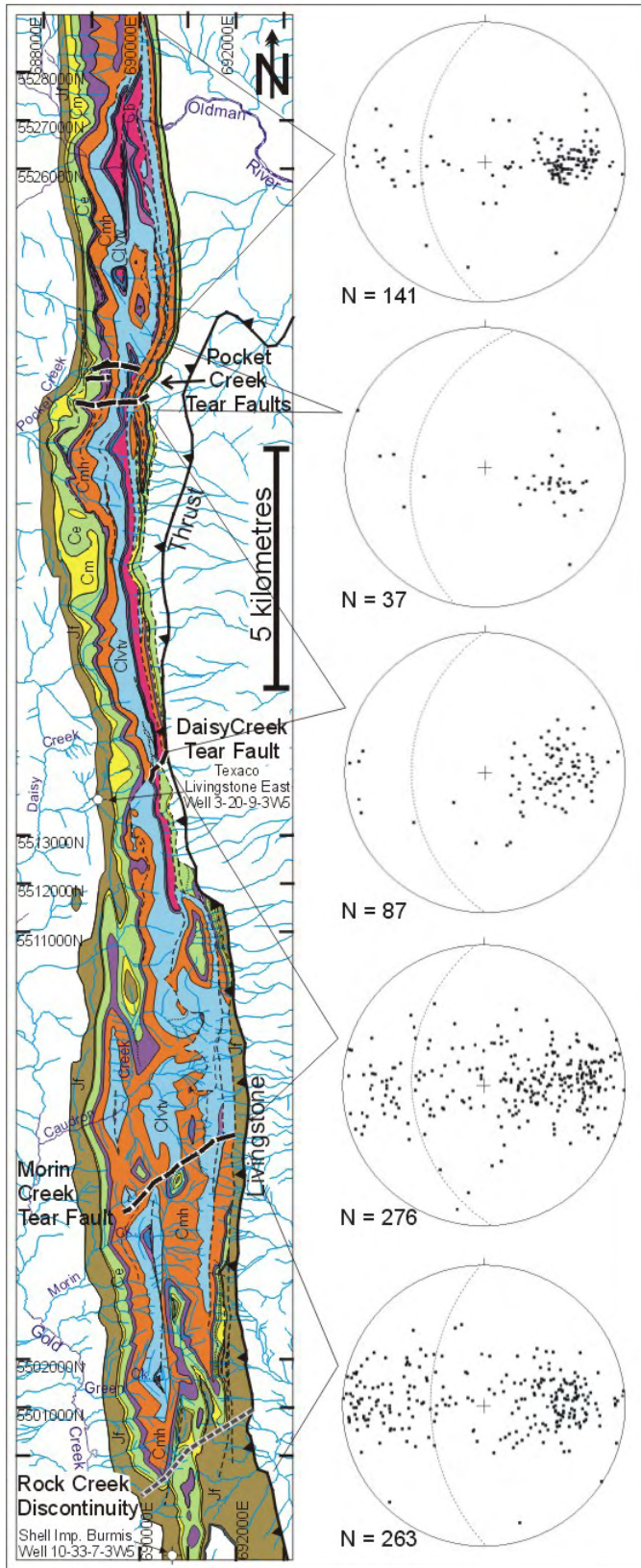


**Figure 3-2.** Geologic map of the study area. Thin dashed lines are thrust faults. Thick dashed lines are tear faults. The location of this map is shown in Figure 3-1. Map units are the same as those in Figure 3-3 and Figure 3-4. The Livingstone Range anticlinorium comprises five straight segments that are separated by regularly spaced cross-strike discontinuities. Bedding orientations within each of the five segments are shown in stereographic projections from the lower hemisphere.

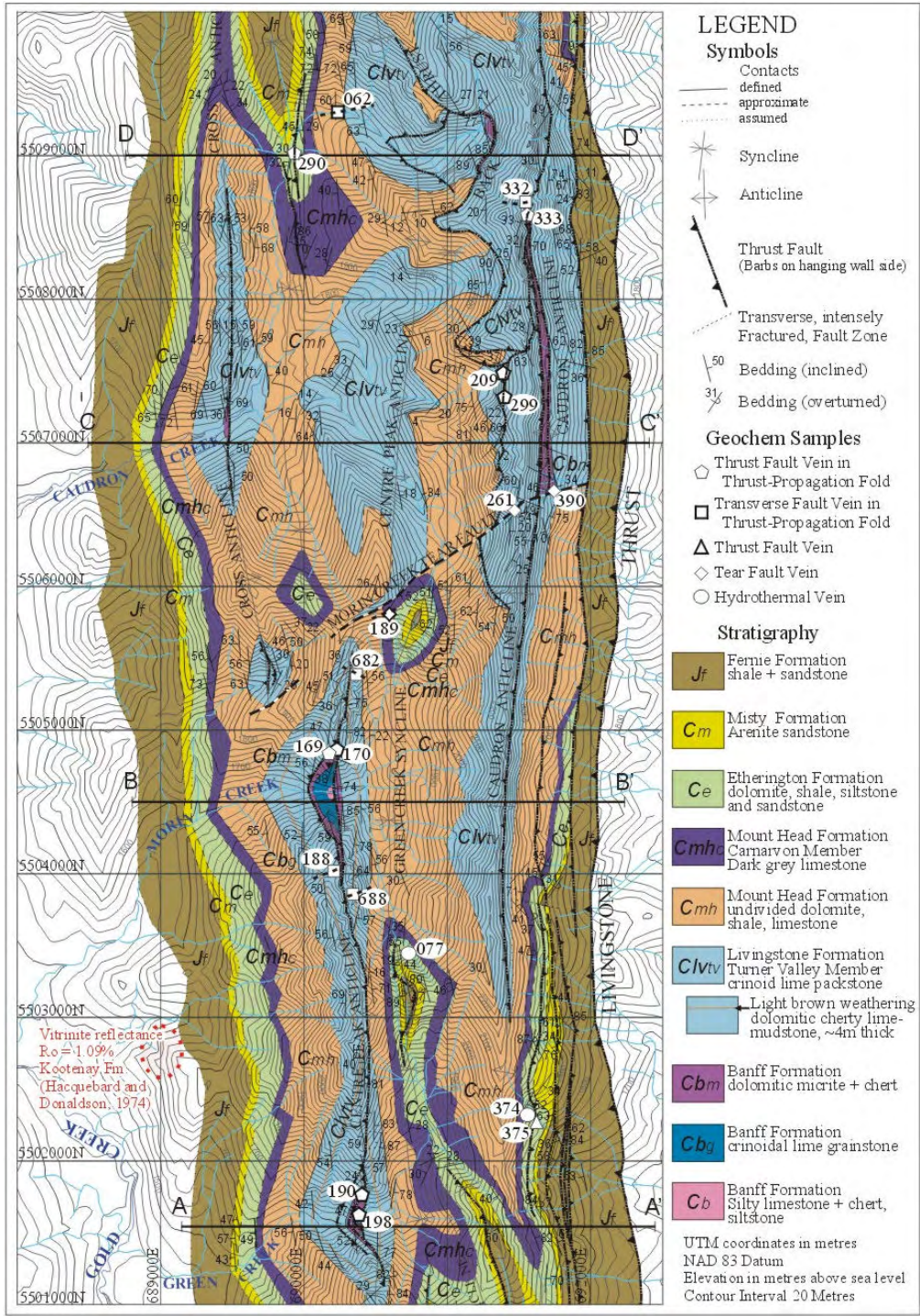


**Figure 3-3.** Geologic map of the southern half of the Livingstone Range anticlinorium study area (based on 1:20000 geological mapping, 2000, 2001, 2002). Sample localities for geochemical analysis are labelled on the map and discussed in the text.

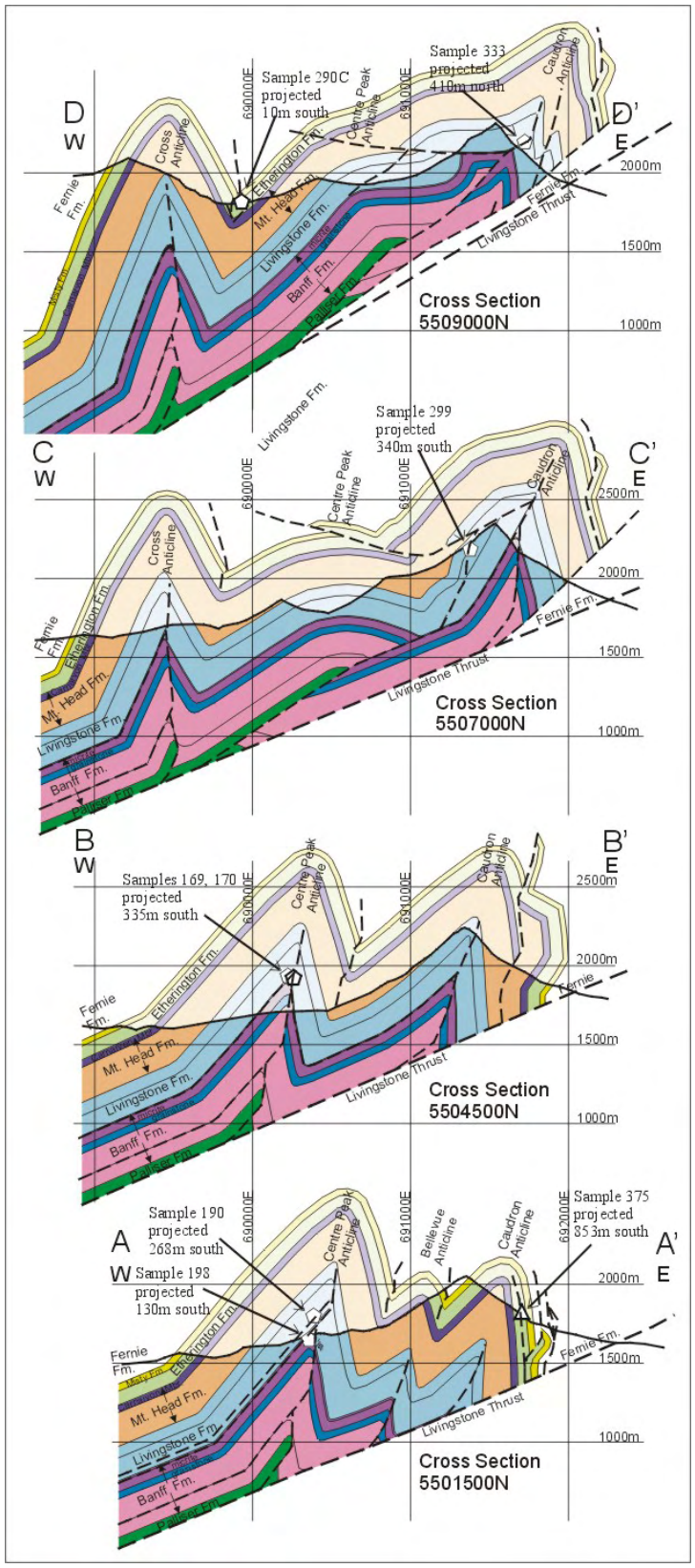


**Figure 3-4.** Geologic cross sections through the southern half of the LRA study area. The locations of cross sections and symbols for geochemical samples are shown on Figure 3-3.



**Figure 3-5.** View south at the core of the Centre Peak anticline, a typical chevron-style thrust-propagation fold in the LRA. The thin solid lines represent stratigraphic contacts. Stratigraphic units (Cbg, Cbm, Clvtv, Clvtv-b and Cmh) are described in the legend in Figure 3-3. The x and x' mark the top of the Banff Formation which has been offset by approximately 250 metres by a thrust fault that propagated out of the back limb of the fold. Thrust faults are represented by thick dashed lines.

During the formation of the Livingstone Range anticlinorium, the Carboniferous carbonate rocks underwent brittle deformation that was conspicuously discontinuous and inhomogeneous at the scale of an individual outcrop (Price, 1967). The deformation involved small displacements along and across a complex array of small contraction and extension faults, inter-bed shear zones, and joints. These brittle fractures bounded individual blocks of rock that underwent large translation and rotation with little or no internal deformation. Substantial dilation occurred during the deformation. Stylolites record pressure solution along some fractures. Precipitation of calcite, dolomite, and quartz in dilatant fracture zones was a widespread but minor component of the deformation. These vein minerals provide the basis for investigating the geochemistry and geothermometry of pore fluids during deformation.

#### ***3.4.1 Southern part of the study area (Green, Morin and Caudron Creeks)***

The southern part of the study area is well exposed in the walls of canyons formed by the creeks (Figure 3-3). Up to three anticlines occur in this area (Figure 3-4). Most are chevron-style flexural-slip thrust-propagation folds; they have planar limbs and angular hinge zones with interlimb angles of  $\sim 60^\circ$ . Each chevron-style anticline has a thrust fault along the hinge zone that dies out upward as a blind thrust (Figure 3-4). In the Centre Peak anticline at Green Creek the hinge zone includes conspicuous jogs associated with thrusts that emerge from bedding detachments in the backlimb and deflect the fold core eastward (Figure 3-5). The east-northeast-trending and steeply dipping dextral Morin Creek tear fault offsets the Centre Peak anticline and the Caudron anticline by  $\sim 250$  metres and  $\sim 130$  metres, respectively (Figure 3-3).

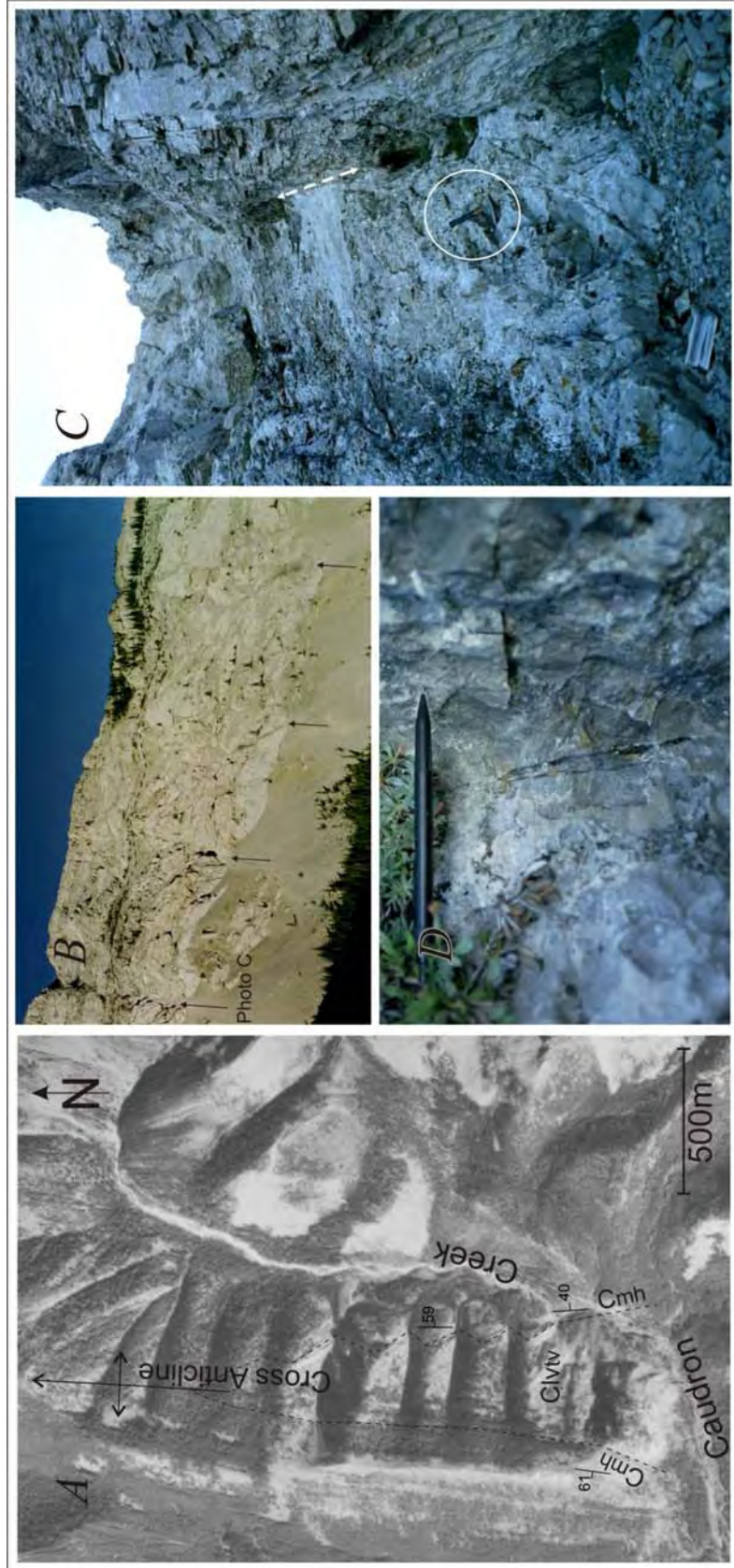
Regularly spaced ( $\sim 150$  metres), east-west striking, steeply dipping zones of intense fracturing and minor faulting transect the north-south striking limbs and hinge zones of chevron-style folds in the vicinity of Green Creek, Morin Creek and Caudron Creek (Figure 3-6). The

transverse zones of intense fracturing, which commonly contain one or more discrete but discontinuous fault surfaces, appear to be restricted mainly to the Livingstone Formation and are commonly marked by gullies that form conspicuous erosion features in the steeper slopes and cliffs (Figure 3-6 A, B). Offsets along transverse fracture zones are commonly 1 metre or less and the sense of displacement varies from one fault to the next. Slickenlines and slickenfibres are rare, and where preserved are generally parallel with the bedding. Solid black hydrocarbon residues are common on fault surfaces and in fractures (Figure 3-6D). In a few transverse fracture zones, cross-cutting calcite and/or dolomite and/or hydrocarbon veins provide evidence of intermittent reactivation of the transverse fracture zones. The transverse zones of intense fracturing and minor faulting appear to have developed during flexural-slip folding by reactivation of a set of pre-existing steeply dipping, east-west-trending mega-joints that had developed preferentially within the Livingstone Formation. These intermittently reactivated fractured zones may have been important conduits for fluid migration before, during and after thrusting and folding; moreover, they provide a good example of the types of small-scale structures that may be important for hydrocarbon migration and accumulation.

#### ***3.4.2 Central part of the study area (Daisy Creek area)***

The central part of the study area is dominated by a westward-dipping homocline of Paleozoic strata in the hanging-wall of the Ernst Creek thrust, which occurs above the Livingstone thrust (Figure 3-7). The steeply dipping, northeast-striking Daisy Creek tear fault (Figure 3-7), which is marked by ~ 160 m of dextral offset of the Ernst Creek thrust, appears to terminate downward against the underlying Livingstone thrust. However, the tear fault transforms

**Figure 3-6.** (following page) Photographs of transverse faults in the LRA. *A* – vertical air photo of the Cross anticline at Caudron Creek. The east-west trending gullies mark the locations of transverse fault zones that cut through Turner Valley Member limestone at regularly spaced intervals in the anticlinal core. Note that most gullies do not extend into the overlying Mount Head Formation. *B* - view westward at the east limb of the Centre Peak anticline south of Morin Creek. The black arrows mark the locations of transverse faults that cut through the east limb. The dashed line marks the surface trace of the hinge of the anticline core. *C* - view westward at intensely fractured limestone within a transverse fault zone visible in Figure 3-6B. Dashed white line with arrows points along the main fault contact. The circle at lower centre of photo outlines a 33 cm-long hammer for scale. *D* is a view to the west at a vertical transverse fault surface at lower centre of photo containing black hydrocarbon residue, a common feature of fault zones. Pencil for scale is 14 cm long.



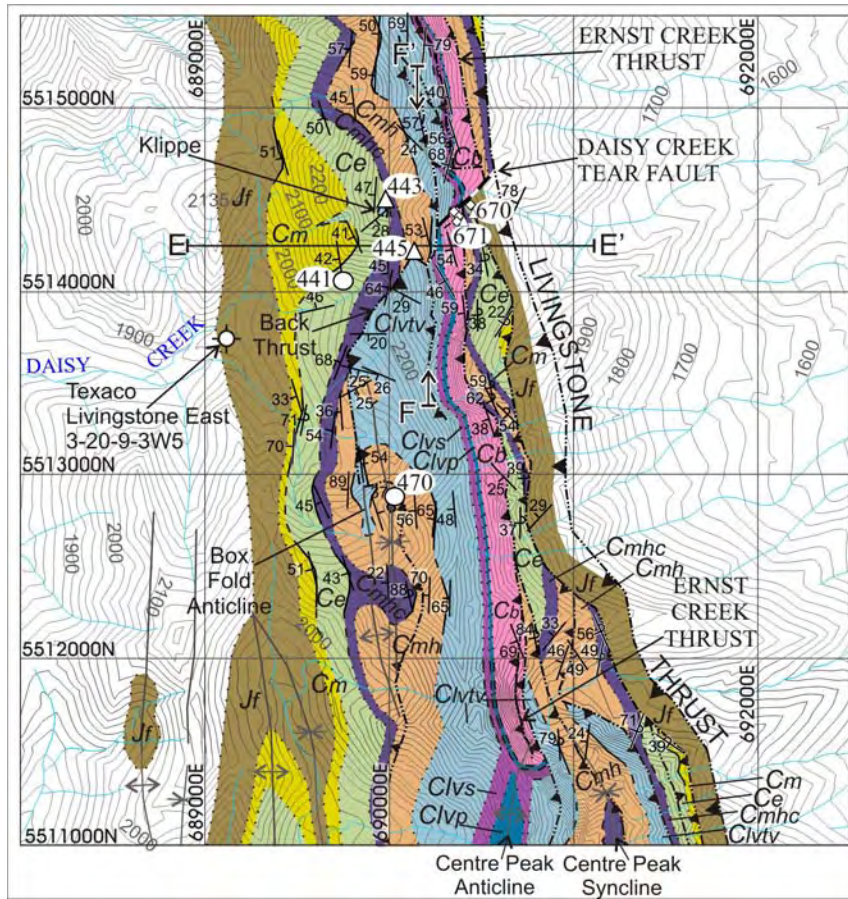


**Figure 3-7.** Geologic map of the Daisy Creek area. The legend for this map is on Figure 3-3. Sample localities for geochemical analysis are labelled on the map and discussed in the text.

upward to form the floor of a thrust wedge that has propagated along a detachment zone in the lower part of the Livingstone Formation (Figure 3-8, sections E E' and F F'). The back thrust that forms the roof of the wedge juxtaposes the Livingstone Formation with the Carnarvon Member of the Mount Head Formation, and the Etherington Formation. A small klippe of Livingstone Formation occurs above the Etherington Formation at the ridge crest, ~200 metres north of cross section E E' (Figure 3-7). The back thrust dies out rapidly southward within the upper part of the Livingstone Formation in the core of a small box fold (Figure 3-7).

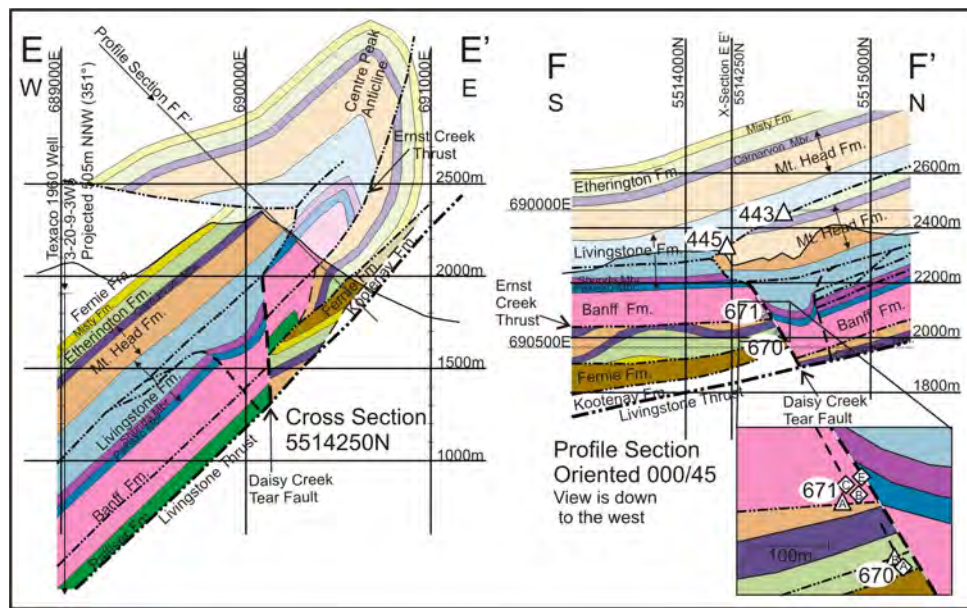


**Figure 3-8.** Cross section E E' and profile section F F' through the Daisy Creek fault system. Profile section F F' is a view down to the west at a plane that strikes north and dips 45 degrees eastward. The locations of the sections are shown on Figure 3-7. Sample localities for geochemical analysis are labelled on profile section F F'.

### **3.4.3 North part of the study area (Pocket Creek area)**

In the Pocket Creek area the structure of the LRA is dominated by the Ernst Creek thrust (Figure 3-9). The west-dipping, north-trending homoclinal panel of Banff Formation and Rundle Group strata in the hanging-wall of the thrust forms the backlimb of the anticlinorium. The thin thrust slices and attenuated folds of Misty, Etherington, Mount Head and upper Livingstone strata in the footwall of the Ernst Creek thrust form the forelimb.

The Ernst Creek thrust and the rest of the LRA are cut by the Pocket Creek tear faults, which are steeply dipping, map-scale, east-west-trending transverse faults (Figures 3-2 and 3-9). They occur within a conspicuous transverse, east-west trending dextral monoclinial flexure that has been superimposed on the entire LRA. The flexure, which is ~1500 m-wide and has an amplitude of ~ 800 m, is situated west of the nose of a north-plunging anticline that involves the Livingstone thrust as well as the Mesozoic rocks in its footwall (Figure 3-9). This anticline is part of a group of folds that deformed the Livingstone thrust and are related to displacements on thrusts that developed below the Livingstone thrust (Douglas, 1950). The two largest tear faults end downward against the Ernst Creek thrust and appear to have been linked kinematically to displacement on it (Figure 3-9). The other smaller tear fault ends downward against a minor thrust that repeats part of the Mount Head Formation within the Ernst Creek thrust slice. All three faults die out upward within the Etherington Formation. Overlying strata, including a minor east-verging backlimb thrust that repeats part of the Etherington and Misty Formations, have been folded by dextral displacement on the southern tear fault. The three tear faults, as a group, deformed at least one minor thrust within the LRA, and they involved small displacements that were linked to displacements on other thrusts within the LRA. The tear faulting evidently occurred during the development of the superimposed dextral transverse monoclinial flexure, and was associated with minor reactivation of pre-existing minor thrusts within the LRA.

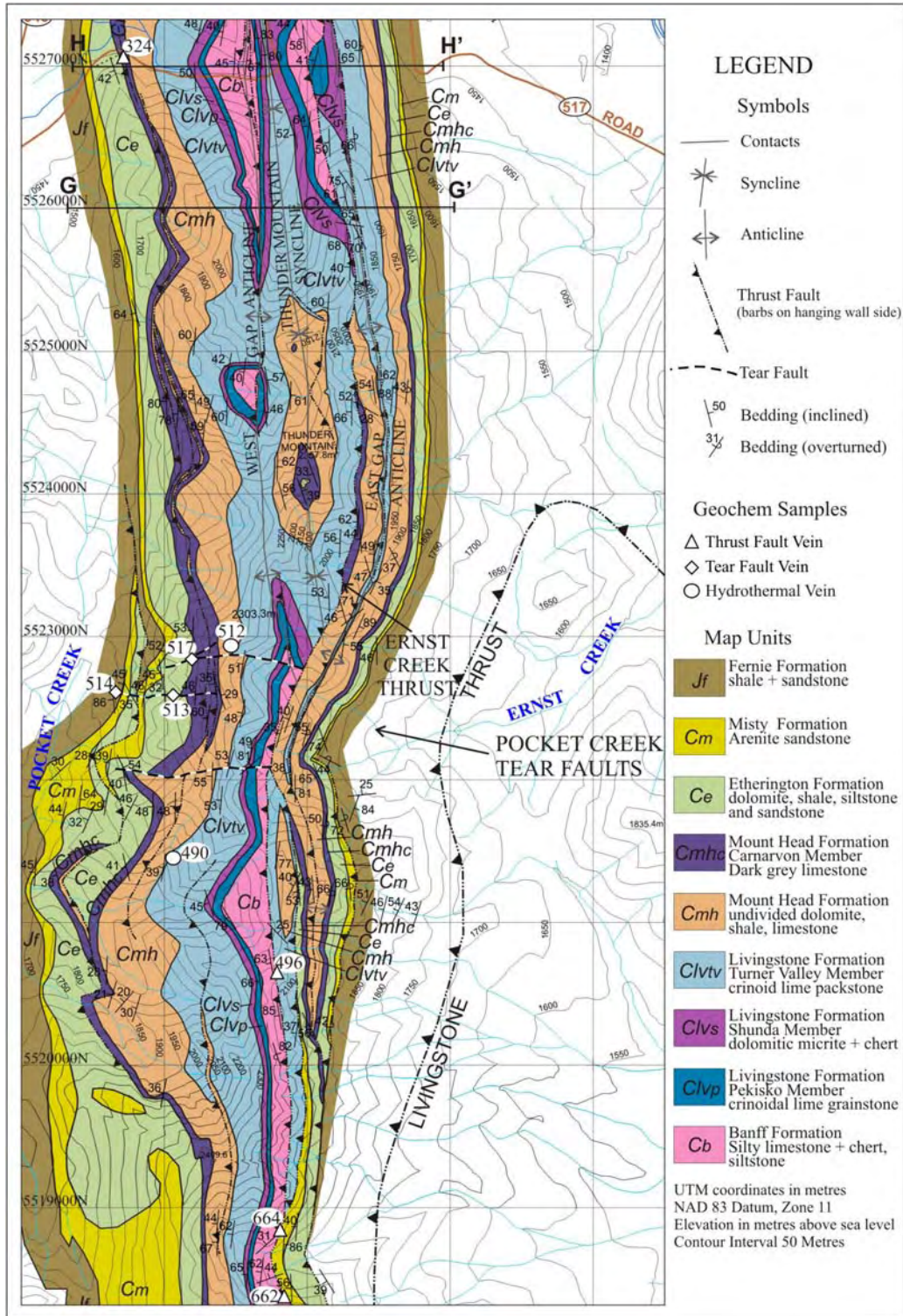


**Figure 3-9.** Geologic map of the northern part of the study area. Three east-west tear faults are associated with a dextral deflection of the LRA at Pocket Creek. Sample localities for geochemical analysis are labelled on the map and discussed in the text.

In the segment of the LRA that extends from the Pocket Creek area northward to the edge of the study area, the structure of the LRA is dominated by Ernst Creek thrust and by the two flexural-slip thrust-propagation anticlines that occur on either side of it, namely, the West Gap anticline and the East Gap anticline (Figure 3-9 and sections G G' and H H' in Figure 3-10). The Ernst Creek thrust, which juxtaposes the Banff Formation over the Rundle Group strata along the west limb of the East Gap anticline is separated from the West Gap anticline by the Thunder Mountain syncline (Figure 3-10).

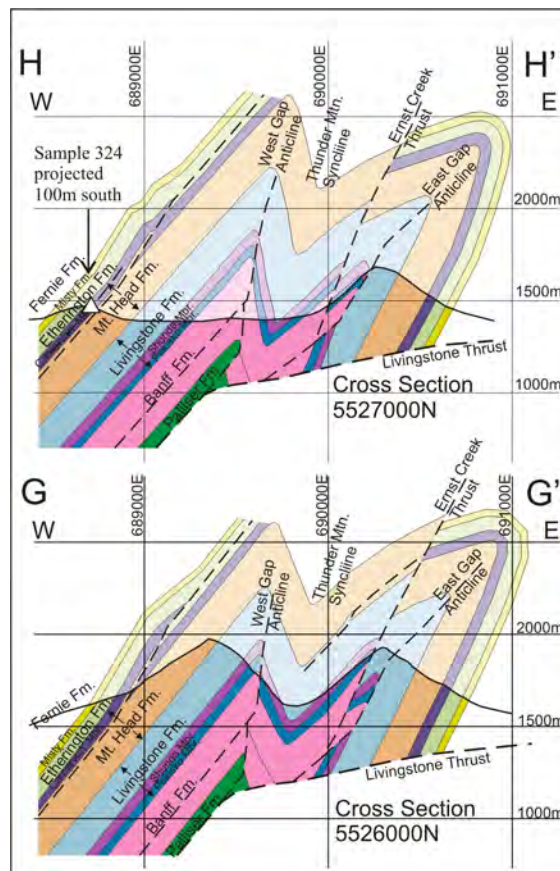


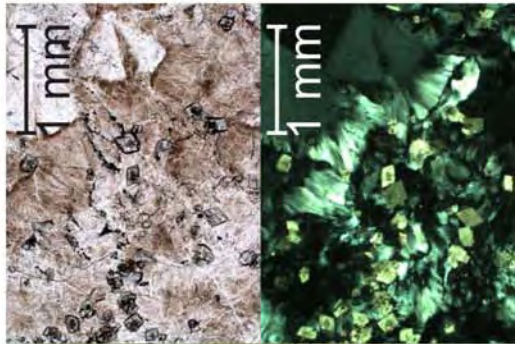
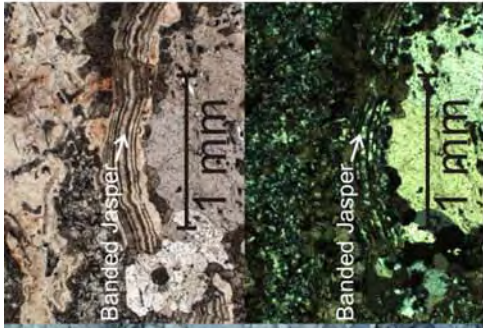
**Figure 3-10.** Cross sections G G' and H H'. The locations of the sections are shown on Figure 3-9.

### 3.4.4 *Descriptions of Veins*

#### 3.4.4.1 *Pre-Thrusting Hydrothermal Veins*

Hydrothermal veins that pre-date thrusting and folding occur locally within the LRA (Figure 3-11). The locations of the hydrothermal veins that were examined during this study are shown on the maps in Figures 3-3, 3-7, and 3-9. All of these veins are fractured, some are cut by stylolites and by younger calcite veins, and some are folded by deformation associated with thrusting and folding. These pre-thrusting hydrothermal veins comprise jasperoid chert +/- fluorite. Traces of sphalerite were found in the hydrothermal veins at sample location 490 (Figure 3-9). Vein quartz is commonly cherty with some jasperoid layers and nodules that commonly replace host rocks. Most nodules are ~1 cm in diameter and consist of concentric layers of chert (Figure 3-11 A). Two samples contain nodules that consist of concentric layers of alternating chert and fluorite (Figure 3-11 B). In some thin sections, jasperoid chert contains euhedral dolomite rhombs (Figure 3-11 C). Narrow alteration haloes adjacent to the veins are only observed rarely. They comprise decimetre-wide zones of lighter-coloured dolomitic host rock (Figure 3-11 A), which is locally silicified. Euhedral to subhedral rhombs of pale purple fluorite are common within late calcite along the margins of remnants of dolomitized host rock. Bedding-parallel hydrothermal veins are common within a red shale unit within the lower part of the Etherington Formation (samples 077 and 374; Figure 3-3, sample 441; Figure 3-7). Bedding-parallel veins are also present in one outcrop of Carnarvon Member of the Mount Head Formation (sample 470; Figure 3-7 and Figure 3-11 C). Bedding-perpendicular veins generally strike ESE or NNW when local bedding orientations are restored to horizontal. Bedding-perpendicular veins are generally less than 3 centimetres thick and less than one metre long. At sample location 490 (Figure 3-9 and Figure 3-11 D), three parallel hydrothermal veins, which strike 101 degrees, lie en-echelon and are right-stepping along a zone that trends 110 degrees, which implies a sinistral sense of shear.

**Figure 3-11.** (following page) Photographs of hydrothermal veins that pre-date thrusting and folding. *A* – The flat surface facing the field of view is an east-dipping bedding surface cut by orthogonal hydrothermal veins with narrow alteration haloes in surrounding siltstone (Sample locality 374, Figure 3-3). Inset microphotographs in *A* show thinly-banded jasperoid chert cut by younger calcite. *B* - view northward at west-dipping Etherington Formation. The hammer lies on an irregular bedding surface along which brecciated hydrothermal vein fragments are cemented by calcite as shown in detail in the inset photo in the lower right corner (Sample locality 441, Figure 3-7). *C* - view southward at a west-dipping bedding-parallel hydrothermal vein cut by a near-vertical stylolitic surface. Inset microphotographs show euhedral dolomite crystals included in jasperoid chert (Sample locality 470, Figure 3-7). *D* - view eastward at a west-dipping bedding surface of dolomitic mudstone near the top of the Livingstone Formation. Three steeply dipping, en-echelon hydrothermal veins lie along an ESE-trending sinistral-sense shear zone (Sample locality 490, Figure 3-9).

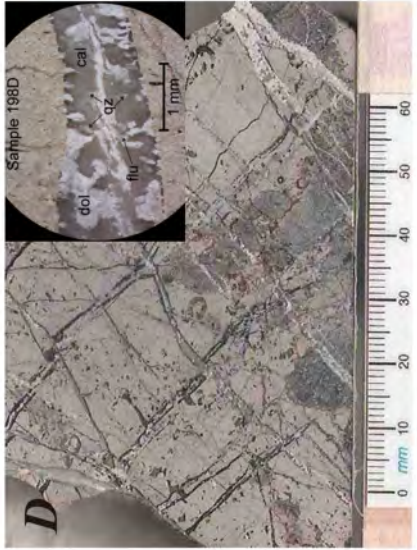
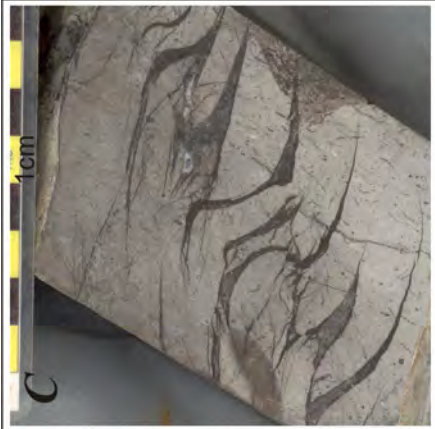
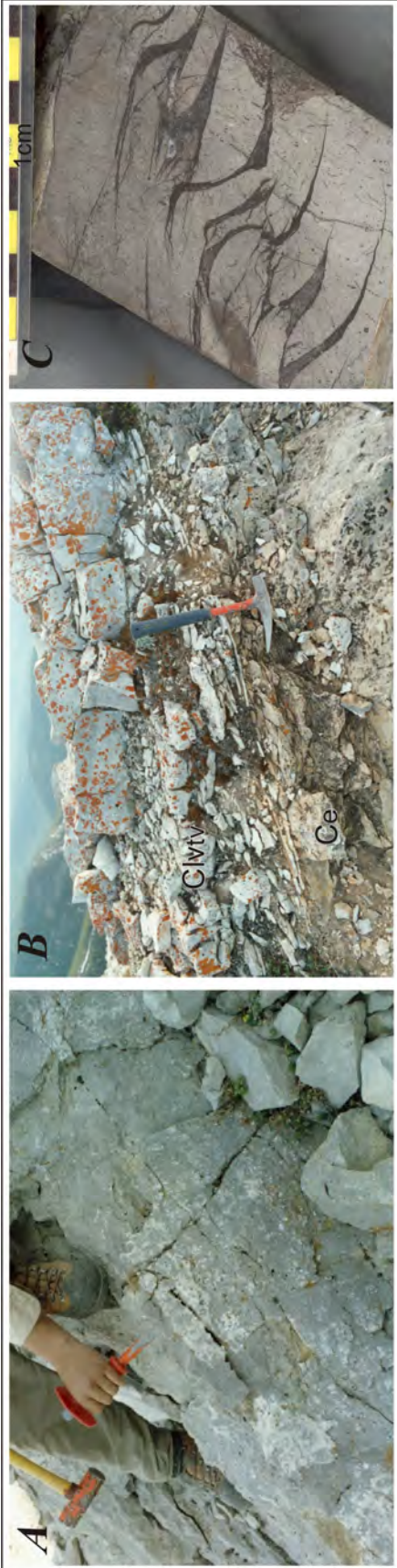


#### 3.4.4.2 *Veins in fault zones*

Veins occur but are rarely observed in fault zones in the study area. The veins are commonly < 2 mm wide and < 30 cm long. Vein and host rock samples for isotopic analysis were collected from outcrops where the veins were clearly kinematically related to specific fault zones. The types of veins collected include: encrustations on fault surfaces that exhibit shear steps and slickenfibres or slickenlines (Figure 3-12A); layered veins that record several periods of dilation and vein growth on fault surfaces (Figure 3-12B); sigmoidal en-echelon tension gashes that are kinematically related to movement on adjacent faults (Figure 3-12C); cross-cutting veins that occur in intensely fractured and tightly folded hinge zones of thrust-related folds (Figure 3-12D, E); and breccias comprising clasts of host rock cemented by vein minerals that are present in dilatant zones along faults (Figure 3-12F). Brecciation was observed within a few transverse faults and tear faults but not along thrust faults.

Veins that occur within fractured host rocks within thrust fault zones generally consist of at least two sets. The earlier vein set commonly occurs as subhorizontal to irregular networks of thin (<1mm wide) veinlets of dark grey to black calcite +/- dolomite that contain abundant intercrystalline black hydrocarbon residue. These veins fill fractures that formed during an earlier episode of locally intense brittle deformation along the fault zone. These are commonly cut by younger white to light grey calcite +/- dolomite veins that are steeply dipping, thick (1– 13 mm wide), few in number, and widely spaced (cm to dm spacing). These younger veins commonly contain minor traces of hydrocarbon residue. Syn-tectonic vein quartz is very rare, but where present it generally occurs within faults that cut silica-rich host rocks, such as chert-bearing carbonate rocks or sandstone.

**Figure 3-12.** (following page) Veins associated with fault zones in the LRA. *A* - view northward at the footwall of the Daisy Creek back thrust. Down-dip trending slickenlines are defined by white calcite encrusting the fault surface. *B* - view westward at calcite veins (black dashed line) that lie along the surface of the Daisy Creek back thrust, where Turner Valley Member of Livingstone Formation (Clvtv) has been thrust over Ethernington Formation (Ce). *C* - view northward at an oriented sample of micritic limestone of Lower Turner Valley showing thrust-sense sigmoidal en-echelon calcite veins that developed in a duplex structure in the core of the Centre Peak anticline at Morin Creek. *D* - polished slab of dolomitic limestone and chert of the micrite unit of the top of the Banff Formation cut by two generations of calcite veins. The inset photo in *D* is a close-up view of the younger vein set which contains dolomite, calcite and quartz. *E* - view westward at the outcrop where the sample in photo *D* was taken. This fractured rock occurs within a duplex structure in the core of the Centre Peak anticline at Green Creek. *F* - view southward at a transverse fault zone marked by breccia and massive white calcite veining that cuts through Upper Mount Head Formation in Caudron Creek.



## 3.5 Isotope Geochemistry

### 3.5.1 Analytical Methods

Calcite, dolomite and quartz in veins and in host rocks were readily identified in hand specimens by etching surfaces with 10% HCl. Calcite readily dissolves to form vitreous dull grey recessive patches, whereas white dolomite crystals and colourless euhedral quartz crystals stand out in relief. Mineral growth textures were also examined in thin sections with a petrographic microscope, and with cathodoluminescence to confirm that there was no apparent zonation within individual crystals.

Powdered samples of calcite and dolomite were collected from individual veins and from host rocks using a dental drill. Quartz was collected from one vein by dissolving the calcite and dolomite in HCl and hand-picking residual quartz crystals.

$\delta^{18}\text{O}$  and  $\delta^{13}\text{C}$  values for calcite or dolomite in veins and in host rocks were measured in  $\text{CO}_2$  released from 5 to 10 mg powdered samples reacted with 100% phosphoric acid, following a method modified from that of McCrea (1950). Nine samples consisting of mixtures of both calcite and dolomite were processed by differential dissolution to separate the  $\text{CO}_2$  evolved from each mineral. The accuracy of this method was verified for one sample for which the calcite and dolomite were separated manually. Isotopic compositions were measured on a Finnigan Mat 252 isotope ratio mass spectrometer at the Queen's Facility for Isotope Research. An additional 99 analyses were done using a Thermo-Finnigan gas bench continuous flow apparatus connected to a Thermo Finnigan Delta Plus XP isotope ratio mass spectrometer at the Queen's Facility for Isotope Research using helium as the carrier gas. For this procedure 0.5 mg of pure calcite or pure dolomite was reacted with 100% anhydrous phosphoric acid at 75°C.

$\delta^{18}\text{O}$  values of quartz samples were measured using bromine pentafluoride (Clayton and Mayeda, 1963).  $\delta^{18}\text{O}$  values were measured on a Finnigan Mat 252 isotope ratio mass spectrometer at the Queen's Facility for Isotope Research.

$\delta^{18}\text{O}$  and  $\delta^{13}\text{C}$  values for carbonates and  $\delta^{18}\text{O}$  values for quartz are reported relative to Vienna Pee Dee belemnite (VPDB) using delta ( $\delta$ ) notation in units of permil (‰).  $\delta = [(R_{\text{sample}}/R_{\text{standard}}) - 1] \times 1000$  where R represents  $^{13}\text{C}/^{12}\text{C}$  or  $^{18}\text{O}/^{16}\text{O}$ . Replicate analyses indicate a reproducibility of +/- 0.2‰ for both  $^{13}\text{C}/^{12}\text{C}$  and  $^{18}\text{O}/^{16}\text{O}$ .

Temperatures of vein formation were calculated for oxygen-bearing mineral pairs that were assumed to have precipitated together in equilibrium using the calcite-water fractionation factors of O'Neil et al. (1969), dolomite-water fractionation factors of Matthews and Katz (1977), and quartz-water fractionation factors of Clayton et al. (1972). For each mineral pair, the two corresponding fractionation factor equations were combined to cancel the water terms and solve for temperature. Temperature calculations have an associated error of approximately +/- 50 °C, which represents an uncertainty of +1.9‰/-2.5‰ for  $\delta^{18}\text{O}$  value of the water from which the minerals precipitated.

Sample preparation for strontium isotopic analyses involved dissolving ~20 mg of powdered sample in 10% HCl, centrifuging, evaporating the solute and redissolving it in sufficient 2% nitric acid solution to bring the Sr content to a suitable concentration for analysis. Strontium isotope ratio measurements were done with a NEPTUNE HR-ICP-MS (ThermoFinnigan, Bremen, Germany) at the Queen's Facility for Isotope Research. Sample inlet is via an Elemental Scientific PFA nebulizer (100 $\mu\text{l}/\text{min}$ ) with a cyclonic/Scott spray chamber with aluminum cones. Typical operating conditions produce a beam of ca.  $7.5 \times 10^{-11}$  amperes for  $^{88}\text{Sr}$  from a 300 ppb Sr solution. Typical operating parameters were: RF power, 1200; Guard Electrode, on; Cool Gas, 16.00 L/m; Aux Gas, 1.00 L/m; and Nebulizer Gas, 1.00 L/m. Each sample measurement consisted of 7 blocks with 9 cycles/block and an integration time of 8.389

sec. Peak centre was at the beginning of each sample and amplifiers were rotated and baselines measured (0.5 amu) for each block.  $^{83}\text{Kr}$  is measured to correct for Kr interference on  $^{84}\text{Sr}$  and  $^{86}\text{Sr}$ , and  $^{85}\text{Rb}$  is measured to correct for  $^{87}\text{Rb}$  interference on  $^{87}\text{Sr}$ . Measurements of standard reference material NIST SRM987 had a value of 0.710240, and replicate analyses indicate a precision of  $\pm 0.00010$  ( $2\sigma$ ).

### 3.5.2 Results

Carbonate samples of 35 host rocks and 33 veins were analysed for their oxygen and carbon isotopic compositions (Table 1 and Figure 3-13).

#### 3.5.2.1 Host Rocks

$\delta^{18}\text{O}$  values of thirty-five host rock samples range from  $-12.3$  to  $-0.7\text{‰}$  (Figure 3-13). Thirteen of these samples consist of diagenetic dolomite, and 19 consist of either pure calcite or the calcite component of weakly dolomitized host rock. These  $\delta^{18}\text{O}$  values, which are lower than the proposed value of approximately  $0\text{‰}$  for Mississippian seawater carbonate (Killingly, 1983; Muehlenbachs, 1997), are similar to those determined for diagenetically altered Carboniferous carbonate host rocks that occur along strike to the north and south in the Foothills of the Rocky Mountains (Cioppa et al. 2000, Lewchuk et al., 1998, Al-Aasm and Lu, 1994).

$\delta^{13}\text{C}$  values of strata that are older than the Carnarvon Member of the Mount Head Formation (these include the Banff Formation, Livingstone Formation and the lower part of the Mount Head Formation) range from  $+0.8$  to  $+3.1\text{‰}$  (Figure 3-13, Table 1). These values are similar to those determined by Veizer et al. (1998) for host rocks of equivalent age from Bochum, Germany, and Ottawa, Canada.

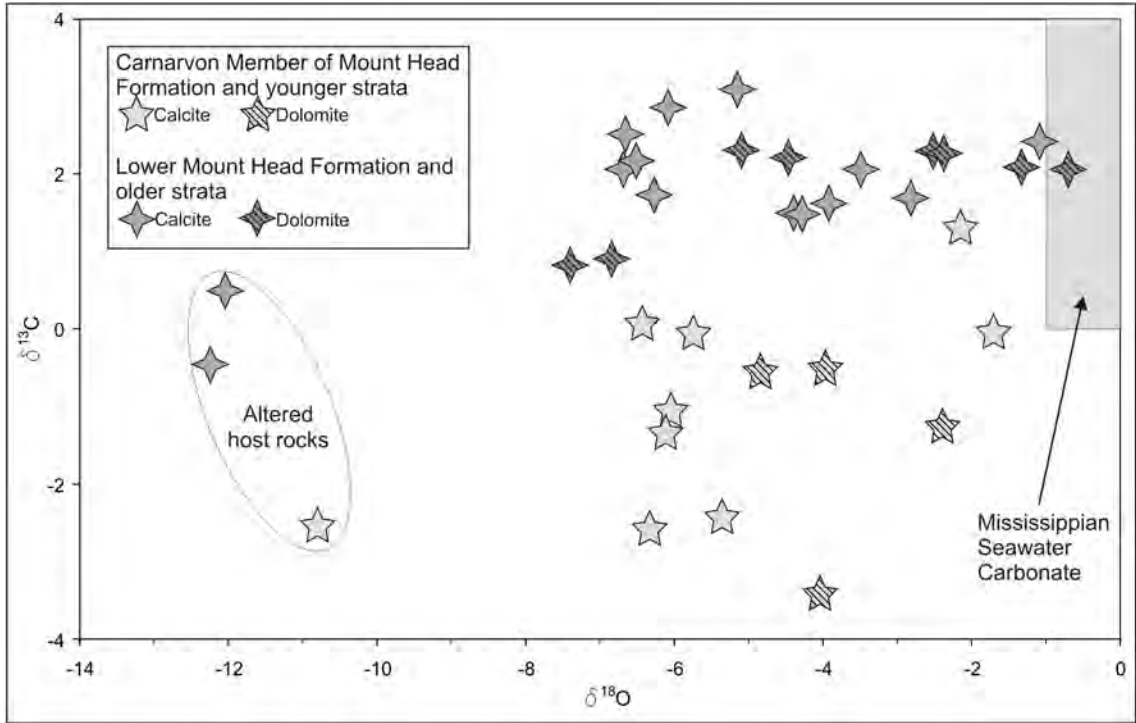


**Figure 3-13.**  $\delta^{18}\text{O}$  versus  $\delta^{13}\text{C}$  values of host rock samples collected from the LRA study area. Host rocks from the top member of the Mount Head Formation and younger units have  $\delta^{13}\text{C}$  values that are consistently lower than those of older units. Three host rock samples with  $\delta^{18}\text{O}$  values  $< -10$  ‰ are from thrust fault zones where host rocks have been recrystallized. The shaded box represents proposed Mississippian Seawater carbonate composition, where the  $\delta^{18}\text{O}$  range is based on Killingly (1983) and Muehlenbachs (1998) and the  $\delta^{13}\text{C}$  range is based on Veizer et al. (1999).

**Table 1.** Isotopic compositions of host rocks and veins collected from the LRA.  $\delta^{18}\text{O}$  and  $\delta^{13}\text{C}$  values are reported relative to VPDB. Host rocks are denoted by sample numbers that end with R, Rcal, or Rdol. Vein sample numbers end with V, V1, V2, etc, where V2 indicates a younger cross-cutting vein set. Three hydrothermal vein samples are mentioned in the text but were not analyzed (374, 441, 470).

SAMPLE	Mineral	EastUTM	NorthUTM	$\delta^{13}\text{C}$	$\delta^{18}\text{O}$	$^{87}\text{Sr}/^{86}\text{Sr}$	Structure	Host Rock Strata
062C-R	DOLOMITE	690220	5509314	2.2	-4.5	0.70908	Tear Fault	Cmh
062C-V1	CALCITE	690220	5509314	-3.0	-4.4	0.70896	Tear Fault	
062C-V2	CALCITE	690220	5509314	-1.0	-2.4	0.70906	Tear Fault	
077A-R	DOLOMITE	690661	5503452	-0.6	-4.8	0.70990	Pre-deformation hydrothermal alteration	Ce lower
077A-V	CALCITE	690661	5503452	-6.7	-16.9	0.70914	Thrust Fault	
077B-R	DOLOMITE	690661	5503452	1.3	-2.1	0.71002	Pre-deformation hydrothermal alteration	Ce lower
169A-R	CALCITE	690205	5504835	1.5	-4.3		Thrust Fault in Thrust-Propagation Fold	Clvtv lower
169A-V	CALCITE	690205	5504835	0.9	-5.4		Thrust Fault in Thrust-Propagation Fold	
170A-R	CALCITE	690222	5504835	1.5	-4.4	0.70812	Thrust Fault in Thrust-Propagation Fold	Clvtv lower
170A-V1	CALCITE	690222	5504835	1.4	-4.7		Thrust Fault in Thrust-Propagation Fold	
170A-V2	CALCITE	690222	5504835	0.1	-6.1	0.70837	Thrust Fault in Thrust-Propagation Fold	
188A-Rcal	CALCITE	690220	5504030	2.1	-6.5	0.70862	Transverse Fault in Thrust-Propagation Fold	Clvtv lower
188A-Rdol	DOLOMITE	690220	5504030	3.0	-5.9		Transverse Fault in Thrust-Propagation Fold	Clvtv lower
188A-V1	CALCITE	690220	5504030	2.3	-6.6		Transverse Fault in Thrust-Propagation Fold	
188A-V2cal	CALCITE	690220	5504030	-1.1	-5.3	0.70877	Transverse Fault in Thrust-Propagation Fold	
188A-V2dol	DOLOMITE	690220	5504030	-0.2	-4.3		Transverse Fault in Thrust-Propagation Fold	
189A-R	CALCITE	690556	5505856	0.0	-6.4		Tear Fault Morin Creek	Cmh
189A-V1	CALCITE	690556	5505856	-0.3	-6.3		Tear Fault Morin Creek	
189C-R	CALCITE	690556	5505856	-0.1	-5.8		Tear Fault Morin Creek	Cmh
189C-V3	CALCITE	690556	5505856	-2.1	-4.5		Tear Fault Morin Creek	
190A-R	CALCITE	690400	5501768	2.1	-3.5		Thrust Fault in Thrust-Propagation Fold	Cbm
190A-V2cal	CALCITE	690400	5501768	0.7	-6.0		Thrust Fault in Thrust-Propagation Fold	
190A-V2dol	DOLOMITE	690400	5501768	1.9	-4.8		Thrust Fault in Thrust-Propagation Fold	
198B-R	CALCITE	690381	5501617	1.7	-2.8	0.70907	Thrust Fault in Thrust-Propagation Fold	Cbm
198B-V1	CALCITE	690381	5501617	1.4	-4.7	0.70886	Thrust Fault in Thrust-Propagation Fold	
198B-V2cal	CALCITE	690381	5501617	0.5	-6.2	0.70889	Thrust Fault in Thrust-Propagation Fold	
198B-V2dol	DOLOMITE	690381	5501617	0.9	-5.1	0.70889	Thrust Fault in Thrust-Propagation Fold	
198B-V2dol	DOLOMITE	690381	5501617	1.0	-5.0		Thrust Fault in Thrust-Propagation Fold	
198D-R	DOLOMITE	690381	5501617	2.3	-2.4		Thrust Fault in Thrust-Propagation Fold	Cbm
198D-V1	CALCITE	690381	5501617	1.4	-4.7		Thrust Fault in Thrust-Propagation Fold	
198D-V2cal	CALCITE	690381	5501617	1.3	-5.3		Thrust Fault in Thrust-Propagation Fold	
198D-V2dol	DOLOMITE	690381	5501617	2.4	-4.0		Thrust Fault in Thrust-Propagation Fold	
198D-V2qz	QUARTZ	690381	5501617		-3.0		Thrust Fault in Thrust-Propagation Fold	
261-R	CALCITE	691481	5506537	2.1	-6.7	0.70863	Tear Fault Morin Creek	Clvtv middle
261-V	CALCITE	691481	5506537	0.2	-6.5	0.70880	Tear Fault Morin Creek	
209-R	CALCITE	691359	5507445	0.51	-12.03		Thrust Fault in Thrust-Propagation Fold	Clvtv upper
290C-R	DOLOMITE	689925	5509008	-1.2	-2.4	0.70857	Thrust Fault in Thrust-Propagation Fold	Ce upper
290C-V1cal	CALCITE	689925	5509008	-2.4	-5.7	0.70908	Thrust Fault in Thrust-Propagation Fold	
290C-V1dol	DOLOMITE	689925	5509008	-1.9	-5.2		Thrust Fault in Thrust-Propagation Fold	
299B-Rdol	DOLOMITE	691362	5507340	2.1	-0.7	0.70822	Thrust Fault in Thrust-Propagation Fold	Clvtv upper
299B-V1	CALCITE	691362	5507340	-1.5	-5.2	0.70860	Thrust Fault in Thrust-Propagation Fold	
299B-V2	CALCITE	691362	5507340	-0.7	-4.9	0.70858	Thrust Fault in Thrust-Propagation Fold	
324Z-R	CALCITE	688654	5527100	-0.1	-1.7		Tear Fault	Cmh
324Z-V2	CALCITE	688654	5527100	-4.4	-8.3		Tear Fault	
332B-R	CALCITE	691566	5508672	1.6	-3.9	0.70846	Transverse Fault in Thrust-Propagation Fold	Clvtv lower
332B-V2	CALCITE	691566	5508672	-0.8	-3.5	0.70897	Transverse Fault in Thrust-Propagation Fold	
333B-R	CALCITE	691559	5508590	2.9	-6.1		Thrust Fault in Thrust-Propagation Fold	Clvtv lower
333B-V1	CALCITE	691559	5508590	1.7	-7.5		Thrust Fault in Thrust-Propagation Fold	
333B-V2	CALCITE	691559	5508590	1.8	-7.9		Thrust Fault in Thrust-Propagation Fold	
375A-V	CALCITE	691587	5502353	-5.9	-17.8	0.70848	Thrust Fault	
390A-V	CALCITE	691722	5506652	-0.5	-3.7		Tear Fault Morin Creek	
390B-R	CALCITE	691722	5506652	0.9	-6.8		Tear Fault Morin Creek	Cbm
443-V1	CALCITE	689967	5514481	-21.6	-16.1		Thrust Fault	
443-V2	CALCITE	689967	5514481	-19.0	-17.1		Thrust Fault	
445C-Rdol	DOLOMITE	690122	5514194	1.9	4.9		Thrust Fault	Cmh
445-V1centre	CALCITE	690122	5514194	-15.3	-18.0	0.70845	Thrust Fault	
445-V2margin	CALCITE	690122	5514194	-13.8	-17.6	0.70874	Thrust Fault	
490A-V cal	CALCITE	689019	5521440	0.7	-9.3	0.70927	Pre-deformation hydrothermal alteration	
490B-R dol	DOLOMITE	689019	5521440	2.1	-1.3	0.70937	Pre-deformation hydrothermal alteration	Clvtv upper
496-R	CALCITE	689771	5520654	-0.4	-12.3		Thrust Fault	Clvtv middle
496-V	CALCITE	689771	5520654	-1.3	-5.2		Thrust Fault	
503-V	CALCITE	688740	5522057	-0.47	-9.58		Tear Fault Pocket Creek	
505-V	CALCITE	688893	5522057	-5.18	-6.56		Tear Fault Pocket Creek	

Table 1 (cont'd).

SAMPLE	Mineral	EastUTM	NorthUTM	$\delta^{13}\text{C}$	$\delta^{18}\text{O}$	$^{87}\text{Sr}/^{86}\text{Sr}$	Structure	Host Rock Strata
512-R	DOLOMITE	689489	5522886	2.3	-2.5	0.71012	Pre-deformation hydrothermal alteration	Cmh
513-R	DOLOMITE	689020	5522599	-3.4	-4.1		Tear Fault Pocket Creek	Ce middle
513-V1	CALCITE	689020	5522599	-10.5	-11.5		Tear Fault Pocket Creek	
513-V2	CALCITE	689020	5522599	-5.5	-11.8		Tear Fault Pocket Creek	
514-R	CALCITE	688658	5522634	-1.2	-6.4		Tear Fault Pocket Creek	Jf
514-V	CALCITE	688658	5522634	-2.1	-10.5		Tear Fault Pocket Creek	
517A-R	CALCITE	689185	5522850	-2.6	-6.3		Tear Fault Pocket Creek	Cmh
517A-V	CALCITE	689185	5522850	-11.2	-13.1		Tear Fault Pocket Creek	
662B-breccia	CALCITE	689839	5518301	-1.3	-6.1		Thrust Fault	Ce middle
662B-V	CALCITE	689839	5518301	-4.1	-8.7		Thrust Fault	
662C-R	CALCITE	689839	5518301	1.2	-5.3		Thrust Fault	Ce middle
662C-V1	CALCITE	689839	5518301	0.2	-6.8		Thrust Fault	
662C-V2	CALCITE	689839	5518301	-2.6	-12.3		Thrust Fault	
662D-R	DOLOMITE	689839	5518301	2.4	-1.1		Thrust Fault	Cb upper
662D-V	DOLOMITE	689839	5518301	1.3	-5.1		Thrust Fault	
664A-V1	CALCITE	689809	5518833	-7.1	-9.7		Thrust Fault	
670A-V1	DOLOMITE	690435	5514459	-3.0	0.4	0.70983	Tear Fault Daisy Creek	
670B-R	CALCITE	690435	5514459	-2.5	-10.8	0.70981	Tear Fault Daisy Creek	Ce middle
670B-V2	CALCITE	690435	5514459	-4.5	-16.2	0.70885	Thrust Fault	
670B-V3	CALCITE	690435	5514459	-12.1	-16.5	0.70923	Thrust Fault	
671A-R	DOLOMITE	690400	5514442	0.9	-7.4		Thrust Fault	Cb upper
671A-V1	CALCITE	690400	5514442	0.8	-6.4		Thrust Fault	
671A-V2	CALCITE	690400	5514442	-3.3	-10.7		Thrust Fault	
671B-R	CALCITE	690400	5514442	1.7	-6.3		Tear Fault Daisy Creek	Cb upper
671B-V	CALCITE	690400	5514442	-0.2	-7.0		Tear Fault Daisy Creek	
671C-V	CALCITE	690400	5514442	-0.6	-4.2		Tear Fault Daisy Creek	
671E-V	CALCITE	690400	5514442	-2.1	-7.1		Tear Fault Daisy Creek	
682A-R	CALCITE	690360	5505393	3.1	-5.1		Thrust Fault in Thrust-Propagation Fold	Cltv upper
682A-V	CALCITE	690360	5505393	0.9	-5.5		Thrust Fault in Thrust-Propagation Fold	
688A-R	CALCITE	690349	5503866	2.5	-6.7		Transverse Fault in Thrust-Propagation Fold	Cltv middle
688A-V1	CALCITE	690349	5503866	1.4	-6.0		Transverse Fault in Thrust-Propagation Fold	
688A-V2cal	CALCITE	690349	5503866	-0.6	-5.8		Transverse Fault in Thrust-Propagation Fold	
688A-V2dol	DOLOMITE	690349	5503866	1.8	-4.6		Transverse Fault in Thrust-Propagation Fold	

$\delta^{13}\text{C}$  values of host rocks from the Carnarvon Member of the Mount Head Formation, and from the overlying Etherington Formation, range from  $-3.4$  to  $+1.3\text{‰}$  (Figure 3-13). This range of  $\delta^{13}\text{C}$  values is at least  $1.7\text{‰}$  lower than the value of approximately  $+3.0\text{‰}$  shown by data presented by Veizer et al. (1999) for seawater carbonate rocks of equivalent age.

Three host rock samples have aberrantly low  $\delta^{18}\text{O}$  values from  $-12.3$  to  $-10.8\text{‰}$  (Figure 3-13). These three host rocks, which occur along thrust faults, are lighter in colour than the surrounding rocks, are weakly stained with iron oxides and have sandy, granular textures in outcrop and milky, translucent to opaque textures in thin sections, all consistent with rocks that

have been hydrothermally altered. Two of the altered host rocks are from the Turner Valley Member of the Livingstone Formation and have  $\delta^{13}\text{C}$  values of +0.5‰ and -0.4‰, which are at least 1‰ lower than the  $\delta^{13}\text{C}$  values of other samples of the Turner Valley Member (Table 1).

### 3.5.2.2 Veins

Thrust-propagation folding in the LRA involved displacements along thrust faults and transverse faults within fold hinges and fold limbs. Veins from both of these fault zone types have  $\delta^{18}\text{O}$  and  $\delta^{13}\text{C}$  values that plot within a narrow range that overlaps the lower  $\delta^{18}\text{O}$  range of most host rocks (Figure 3-14). Veins from thrust fault zones within thrust-propagation folds have  $\delta^{18}\text{O}$  values that range from -7.9 to -4.0‰ and  $\delta^{13}\text{C}$  values that range from -2.4 to +2.4‰ (Figure 3-14, Table 1). Vein samples collected from transverse faults that formed within fold limbs during thrust-propagation folding have  $\delta^{18}\text{O}$  values that range from -6.0 to -3.5‰ and  $\delta^{13}\text{C}$  values that range from -1.1 to +1.8‰ (Figure 3-14, Table 1).

Nineteen vein samples from major tear faults that cut across the LRA have  $\delta^{18}\text{O}$  values that range from -13.1 to -2.4‰ and  $\delta^{13}\text{C}$  values that range from -10.5 to -0.2‰. Ten of these veins have  $\delta^{18}\text{O}$  and  $\delta^{13}\text{C}$  values that are similar to those of host rock values (Figure 3-14).

Veins from major and minor thrust fault zones that are not related to thrust-propagation folding have the lowest  $\delta^{18}\text{O}$  values that range from -18.0 to -4.4‰ and low  $\delta^{13}\text{C}$  values that range from -21.6 to +1.3‰. However, three vein samples from thrust faults have  $\delta^{18}\text{O}$  and  $\delta^{13}\text{C}$  values that lie within the range of host rock isotopic compositions (Figure 3-14, Table 1).

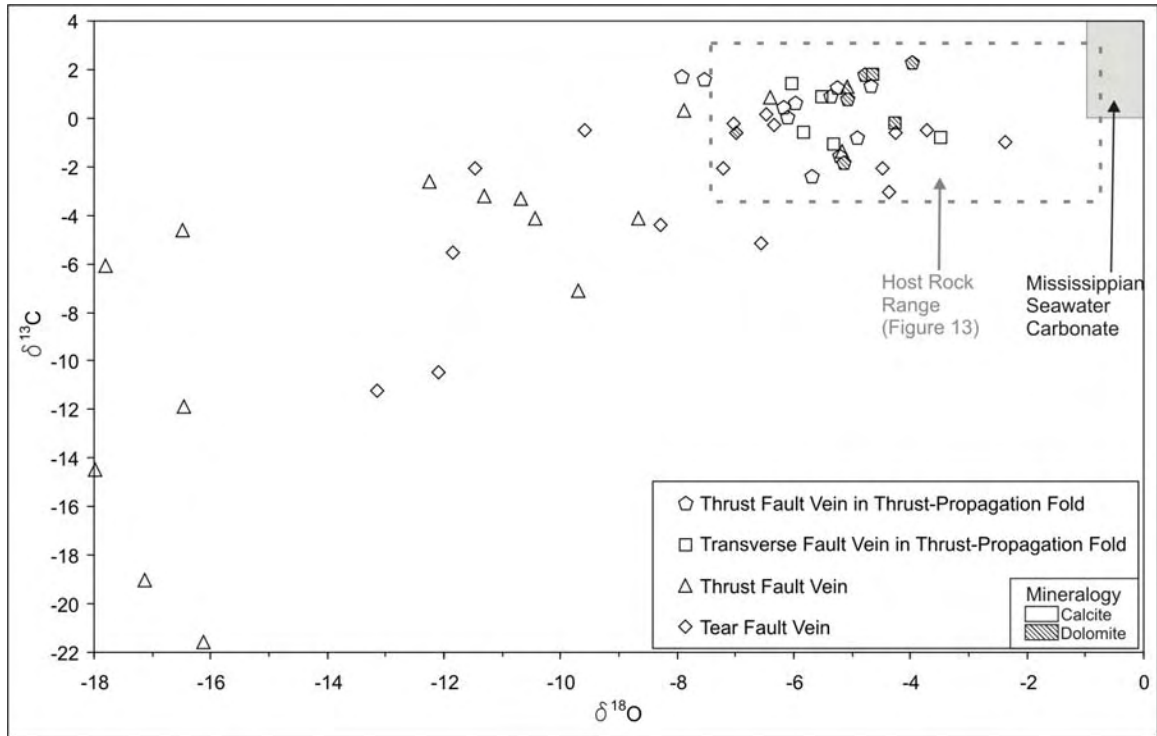


**Figure 3-14.**  $\delta^{18}\text{O}$  versus  $\delta^{13}\text{C}$  values of carbonate veins collected from different types of structures in the LRA study area. The majority of veins associated with thrust-propagation folding have compositions that lie within the range of host rock compositions, represented by the box with the dashed outline. The shaded box represents proposed Mississippian Seawater carbonate composition, where the  $\delta^{18}\text{O}$  range is based on Killingly (1983) and Muehlenbachs (1998) and the  $\delta^{13}\text{C}$  range is based on Veizer et al. (1999).

### 3.5.2.3 Stable Isotope Thermometry

Temperatures of vein-formation were calculated for five samples from fault zones within the Centre Peak anticline that are interpreted to have been active during thrust-propagation folding (Table 2). Coexisting oxygen-bearing minerals within these veins are assumed to have precipitated in isotopic equilibrium with each other and coeval water. The temperature error of  $\sim\pm 50^\circ\text{C}$  represents a range in  $\delta^{18}\text{O}$  values for water of  $+1.7/-2.3\text{‰}$  for calcite/water, and  $+1.9/-2.5\text{‰}$  for dolomite/water. Calcite and dolomite in these veins have irregular intergrowth textures that show no evidence of sequential growth; neither calcite nor dolomite preferentially grew along vein margins and there are no vein centrelines consisting of only one mineral (Figure 3-12D). Quartz in veins at sample locality 198 occurs as randomly oriented, subhedral radiating crystal aggregates or euhedral doubly terminating single crystals that are in contact with either calcite or dolomite (Figure 3-12D).

**Table 2.** Apparent equilibration temperatures and coeval water compositions calculated from  $\delta^{18}\text{O}$  values of calcite, dolomite +/- quartz in veins in fault zones in the Centre Peak anticline. The error associated with the temperature calculation is approximately  $\pm 50^\circ\text{C}$ , which represents a range in  $\delta^{18}\text{O}$  values for coeval water of  $+1.7/-2.3\text{‰}$  for calcite/water, and  $+1.9/-2.5\text{‰}$  for dolomite/water (\*).

Sample	Structure	Calcite $\delta^{18}\text{O}$	Dolomite $\delta^{18}\text{O}$	Quartz $\delta^{18}\text{O}$	Water $\delta^{18}\text{O}$ ( $+1.7/-2.3\text{‰}$ )	Temperature ( $\pm 50^\circ\text{C}$ )
198B-V2	Thrust Fault in Thrust-Propagation Fold	-6.2	-5.0		-13.0	250
		-6.2	-5.1		-12.6	260
198D-V2	Thrust Fault in Thrust-Propagation Fold	-5.3		-3.0	-12.1	250
			-4.0	-3.0	* -11.5	260
		-5.3	-4.0		-12.9	230
		-5.2		-3.0	-11.7	260
		-5.2	-4.0		-11.9	250
190-V2	Thrust Fault in Thrust-Propagation Fold	-6.0	-4.8		-12.8	250
688A-V2	Transverse Fault in Thrust-Propagation Fold	-5.8	-4.6		-12.7	250
188A-V2	Transverse Fault in Thrust-Propagation Fold	-5.3	-4.3		-10.9	280
		-5.4	-4.3		-11.9	260

In the hanging wall of the thrust fault that cuts along the hinge zone of the Centre Peak anticline at Green Creek, a set of late, east-west-trending, steeply dipping veins cut across the hinge zone of a tightly folded thrust duplex of lime mudstone and chert of the top of the Banff Formation (sample location 198; Figure 3-3 and cross section A A' in Figure 3-4). Oxygen isotopic compositions of calcite and dolomite from sample 198B-V2 provide apparent equilibrium temperatures near 250°C, and an average  $\delta^{18}\text{O}$  value of coeval water of -12.8‰ (Table 2). A second vein sample (198D-V2), which was collected less than one metre south of 198B-V2, has calcite, dolomite and quartz with equilibration temperatures also averaging 250°C, and an average  $\delta^{18}\text{O}$  value for coeval water of -12.0‰ (Table 2).

Veins that are steeply dipping and north-south-trending and that lie in the hanging wall of a thrust fault in the hinge zone of the Centre Peak anticline on the north side of Green Creek canyon (sample locality 190; Figure 3-3 and cross section A A' in Figure 3-4) contain calcite and dolomite that have an apparent equilibrium temperature of 250°C and a  $\delta^{18}\text{O}$  value for coeval water of -12.8‰ (Table 2). Similarly, carbonate veins from a transverse fault zone that cuts the forelimb of the Centre Peak anticline, approximately 760 metres south of Morin Creek (sample locality 688; Figure 3-3), contain calcite and dolomite that have an apparent equilibrium temperature of 250°C and a  $\delta^{18}\text{O}$  value for coeval water of -12.7‰ (Table 2).

Carbonate veins within a transverse fault zone that cuts across the backlimb of the Centre Peak anticline occur approximately 600 metres south of Morin Creek (sample locality 188, Figure 3-3). Calcite and dolomite from sample 188A-V2 provide apparent equilibration temperatures of 280°C and 260°C and an average  $\delta^{18}\text{O}$  value for coeval water of -11.4‰ (Table 2).

The similarity of these apparent equilibration temperatures and inferred  $\delta^{18}\text{O}$  values for coeval water (Table 2) implies that the thermal and fluid conditions were constant along the southern part of the Centre Peak anticline during the formation of these veins. The veins at sample locality 198 in particular are inferred to have formed during the later stages of thrust-

propagation folding because they cut across the hinge zone of a tightly folded thrust duplex in the core of the Centre Peak anticline and are themselves only weakly deformed.

#### 3.5.2.4 Strontium isotopic ratios

Host rocks that are cut by pre-thrusting hydrothermal jasperoid chert veins are generally composed of dolomite with relatively high  $^{87}\text{Sr}/^{86}\text{Sr}$  ratios ranging from 0.70937 to 0.71012 (Table 1, Figure 3-15). Host rocks from fault zones in thrust-propagation folds have lower  $^{87}\text{Sr}/^{86}\text{Sr}$  ratios that range from 0.70812 to 0.70909 (Table 1, Figure 3-15). The  $^{87}\text{Sr}/^{86}\text{Sr}$  ratios of all host rocks are higher than the expected range of 0.70767 to 0.70799 for Lower Carboniferous seawater carbonate rocks (Veizer et al., 1999), indicating that they have been altered by fluids with high  $^{87}\text{Sr}/^{86}\text{Sr}$  ratios.

The  $\delta^{18}\text{O}$  values of most host rocks are similar, regardless of the type of fault in which they occur, except for one altered host rock (670B-R) from a tear fault zone cut by thrust fault. This sample consists of recrystallized calcite with a very low  $\delta^{18}\text{O}$  value of -10.8‰ and a high  $^{87}\text{Sr}/^{86}\text{Sr}$  ratio of 0.70981 (Table 1, Figure 3-15).

Veins from fault zones in thrust-propagation folds have  $^{87}\text{Sr}/^{86}\text{Sr}$  ratios that range from 0.70837 to 0.70908 (Table 1, Figure 3-15), similar to the range of 0.70812 to 0.70909 for  $^{87}\text{Sr}/^{86}\text{Sr}$  ratios of the local host rocks. However, most individual veins in thrust-propagation folds have slightly higher  $^{87}\text{Sr}/^{86}\text{Sr}$  ratios than the host rock with which they occur (Figure 3-15).

Calcite veins from thrust faults that are inferred to have been active during later stages of thrusting deformation have very low  $\delta^{18}\text{O}$  values that range from -18.0 to -16.5‰. The  $^{87}\text{Sr}/^{86}\text{Sr}$  ratios of these late calcite veins, which range from 0.70845 to 0.70923, are similar to the  $^{87}\text{Sr}/^{86}\text{Sr}$  ratios of most host rocks.



The calcite veins that have the highest  $^{87}\text{Sr}/^{86}\text{Sr}$  ratios and lowest  $\delta^{18}\text{O}$  values are from young thrust faults that cut through host rocks with very high  $^{87}\text{Sr}/^{86}\text{Sr}$  ratios (Samples 670 and 070A, Figure 3-15), indicating that the  $^{87}\text{Sr}/^{86}\text{Sr}$  ratios of veins are strongly influenced by local host rock. Sample 670 is one location where an early vein with a high  $\delta^{18}\text{O}$  value and a high  $^{87}\text{Sr}/^{86}\text{Sr}$  ratio (Figure 3-15) is cut by a younger vein with a much lower  $\delta^{18}\text{O}$  value and a lower  $^{87}\text{Sr}/^{86}\text{Sr}$  ratio (Figure 3-15; sample 670B-V2).

The  $^{87}\text{Sr}/^{86}\text{Sr}$  ratios for most veins lie within the range of the host rock, suggesting that the source of the strontium was the host rocks.

### **3.6 Interpretation**

The isotopic compositions of the host rocks and veins from different structures show distinct patterns that can be used to infer the types of fluids that were flowing through the structures at various tectonic stages. The  $\delta^{18}\text{O}$  values are especially important for elucidating the thermal and fluid flow history (Figure 3-16).

#### ***3.6.1 Pre-thrusting dolomitization and diagenesis***

Most Carboniferous carbonate rocks in the LRA contain dolomite that has replaced the matrix of the original rock. This is especially evident within the fine-grained carbonate mudstones. The matrix-replacement dolomite is interpreted to have formed during diagenesis at early stages of burial and lithification (Machel, 2004) and is a common feature in carbonate rocks within the Western Canada Sedimentary Basin (Cioppa et al. 2000, Lewchuk et al., 1998, Al-Aasm and Lu, 1994). Diagenesis may also be indicated by the relatively low  $\delta^{18}\text{O}$  values of both calcite and dolomite within many host rocks in the LRA, relative to the expected value of approximately 0‰ (Killingly, 1983; Muehlenbachs, 1997).

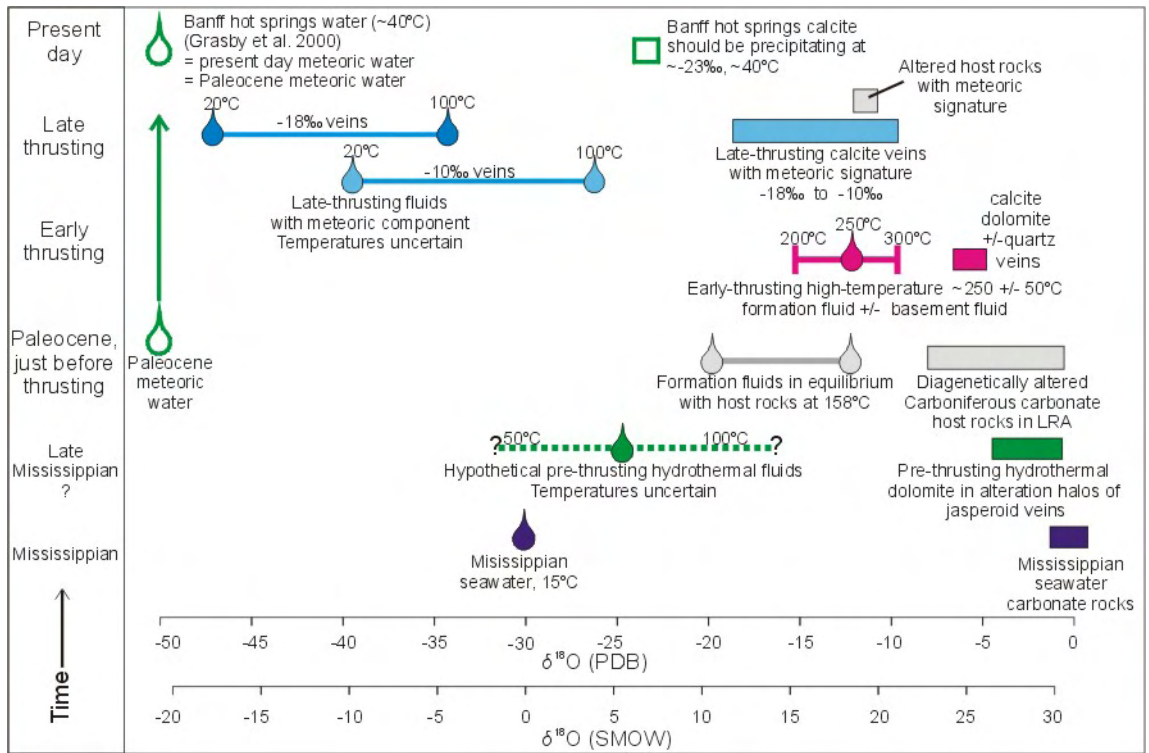


**Figure 3-16.** The thermal and fluid evolution in the LRA deduced from  $\delta^{18}\text{O}$  values of host rocks and veins.

A progressive decrease in  $\delta^{18}\text{O}$  values of the carbonate host rocks, and a progressive increase in the  $\delta^{18}\text{O}$  values of formation fluids would be expected to occur because of fractionation during isotopic exchange between the fluids and adjacent rocks at progressively higher temperatures. Host rocks in the LRA also have relatively high  $^{87}\text{Sr}/^{86}\text{Sr}$  ratios, which may indicate that an allochthonous fluid with radiogenic strontium was circulating through the rocks during this pre-thrusting dolomitization and diagenesis. The allochthonous fluid could have originated from the thick shale units of the underlying Banff and Exshaw Formations, or from the underlying Paleoproterozoic crystalline basement.

### ***3.6.2 Pre-thrusting hydrothermal fluids***

The high  $^{87}\text{Sr}/^{86}\text{Sr}$  ratios present in dolomite in alteration haloes that envelope hydrothermal jasper +/-fluorite+/-sphalerite veins (Figure 3-15) record the presence of allochthonous fluids in the Carboniferous rocks of the LRA. The temperatures at which these veins formed, and the  $\delta^{18}\text{O}$  values of the fluids that formed them are not known, however, displayed on Figure 3-16 is a hypothetical range of possible  $\delta^{18}\text{O}$  values for the hydrothermal fluids of  $-30$  to  $-20\%$ , based on a possible temperature range of  $50$  to  $100^\circ\text{C}$  and actual  $\delta^{18}\text{O}$  values of  $-4.8$  to  $-1.3\%$  for hydrothermal dolomite in alteration haloes. These fluids could have been basin fluids circulating through shales, or fluids migrating up from the Paleoproterozoic crystalline basement, and the high  $^{87}\text{Sr}/^{86}\text{Sr}$  ratios of vein haloes (Figure 3-15) are consistent with both interpretations. A basement source for the fluids is supported in the LRA by the probable structural relationship between the ESE and NNW strikes of the horizontally restored bedding-perpendicular hydrothermal veins which are symmetrically distributed about the ENE-trending tear faults and transverse faults within the LRA. The ENE-trending faults probably follow pre-existing regional joints or minor faults. The Morin Creek tear fault (Figure 3-3), the Daisy Creek

tear fault (Figure 3-7), and the smaller transverse faults in the limbs of the anticlines (Figure 3-6A) all terminate upward within the lower part of the Mount Head Formation, which may indicate that these fractures formed in the Late Mississippian, during deposition of the Mount Head Formation. However, the youngest strata found to contain pre-thrusting jasperoid veins are of the Late Mississippian Etherington Formation, which suggests that reactivation of the faults and upward flow of basement fluids could have continued into the Late Carboniferous (Figure 3-17). Many of the veins in the Etherington Formation are parallel to bedding, suggesting that they formed at a time when the Etherington Formation was at a relatively shallow depth of burial.

The underlying Paleoproterozoic basement of western Canada and United States is composed of a collage of continental blocks separated by ancient fault zones and sutures. The Vulcan structure of southern Alberta is one such structure. It is marked by a conspicuous ENE-trending regional negative bouguer gravity anomaly, and paired negative and positive aeromagnetic anomalies that are interpreted to mark an ENE-trending fault structure between the Medicine Hat Block to the south and the Loverna Block to the North (Eaton et al., 1999; Clowes et al., 2002). Palinspastic restoration of the LRA ~40 km westward to its approximate original pre-thrusting location aligns this part of the Livingstone Range above the southwest trend of the Vulcan Low. The ENE-trending transverse faults within the LRA may be related to fractures that were once controlled by the underlying Vulcan structure, which was probably active during Late Mississippian, and may have been associated with upward migration of hydrothermal fluids with high  $^{87}\text{Sr}/^{86}\text{Sr}$  ratios from the Paleoproterozoic crystalline basement.

An Early Cretaceous timing of basement fault reactivation and local hydrothermal activity is also a possibility (Figure 3-17). Early Cretaceous reactivation of basement structures, which has been attributed to thrust loading along the continental margin of western North America, has been documented elsewhere in the Canadian Cordillera (Hart and Plint, 1993; Lemieux, 1999).



### **3.6.3 Early syn-thrusting formation fluid flow +/- basement fluids**

Thrust-propagation folding occurred early in the evolution of the LRA as the Livingstone thrust propagated through the ramp separating the regional detachments in the Palliser Formation and the Fernie Formation. Most thrust-propagation folds in the LRA are chevron folds, a fold style that develops rapidly once initiated (Ramsay, 1974). The rapid dilation accompanying brittle chevron-style flexural-slip thrust-propagation folding would have caused formation fluids to be drawn into the dilatant zones in the folds.

Vein samples collected from fault zones that are interpreted to have been active during thrust-propagation folding have  $\delta^{18}\text{O}$  and  $\delta^{13}\text{C}$  values that are similar to those of the local host rocks (Figure 3-14), which suggests that the veins formed from fluids that were isotopically influenced by local lithology. The consistently lower  $\delta^{13}\text{C}$  values of all veins relative to host rocks are interpreted to be due to the addition of carbon from oxidized hydrocarbons. The presence of hydrocarbons in the vein-forming fluids is supported by the abundant occurrence of hydrocarbon fluid inclusions in the vein calcite and dolomite.

Oxygen isotope thermometry of coexisting calcite and dolomite +/- quartz from five veins from near the top of the Banff Formation in the core of the Centre Peak anticline (Table 2) show that these veins formed at  $\sim 250 \pm 50^\circ\text{C}$ . This is at least  $40^\circ\text{C}$  higher than the paleotemperature of  $\sim 158^\circ\text{C}$  estimated for the top of the Banff Formation, which was calculated assuming a geothermal gradient of  $25^\circ\text{C}/\text{km}$ , an average surface temperature of  $20^\circ\text{C}$  and a depth of 5.5 km. The reasons for selecting these thermal constraints and the strata thickness of 5.5 km are explained below.

The geothermal gradient of  $25^\circ\text{C}/\text{km}$  predicted for the LRA prior to thrusting deformation may be a conservative upper limit for the actual geothermal gradient during the Paleocene, if one assumes that the geothermal gradient pattern in southwest Alberta has not changed significantly

since the Paleocene. The present geothermal gradient in the un-deformed sedimentary basin rocks of southwestern Alberta, just east of the thrust and fold belt, averages between 20 and 25°C/km (Bachu and Burwash, 1994). The pre-thrusting geothermal gradient that Osadetz et al. (2005) estimated for the Lewis Thrust sheet was 20°C/km.

A source of error in estimating the temperature of the top of the Banff Formation just prior to thrusting and folding comes from the uncertainty in estimating the thickness of strata that lay above the Banff Formation prior to erosion, which is dependant on the age at which displacement began along the Livingstone Thrust. The next major thrust to the west, the Lewis Thrust, which has a maximum displacement of approximately 140 km (Sears, 2001) began moving at ~74 Ma and stopped at ~59 Ma (Osadetz et al. 2004, Sears, 2001). Assuming both the Lewis thrust and Livingstone thrust had similar displacement rates and both stopped moving at ~59 Ma, the Livingstone Thrust, which has a displacement of approximately 40 km, would have begun moving at ~64 Ma, during deposition of thick sand beds of the Paleocene Porcupine Hills Formation. At this time, the Banff Formation strata that was about to be deformed by the Livingstone thrust was overlain by Carboniferous Livingstone Formation to Cretaceous Lower Belly River Group strata that is still preserved near the LRA today, and by the upper part of the Cretaceous Belly River Group and overlying younger strata that have since been removed by erosion. The thickness of the eroded strata can be roughly estimated by extrapolating the thickness of the Cretaceous Belly River Group and overlying units, up to the base of the Paleocene Porcupine Hills Formation, which are currently preserved beneath the prairies to the east of the thrust and fold belt. The extrapolation of these thicknesses requires that the units gradually thicken westward, which occurs within all stratigraphic units in the Western Canada Sedimentary Basin. Using this method of extrapolating stratigraphic thickness, an estimated total thickness of approximately 5.5 km of strata lay above the Banff Formation just prior to initial displacement on the Livingstone thrust. This method of estimating the amount of strata removed

by erosion is not precise, however, even if one assumes that the strata that lay above the Banff Formation prior to thrusting was as thick as 7 km, the temperature near the top of the Banff Formation would have been at most 195°C, which would still be below the ~250 +/- 50°C temperature range calculated by isotope thermometry of veins from the Centre Peak anticline core, especially when considering that the geothermal gradient used is likely a conservatively high limit.

The estimated paleotemperature of ~158°C for the top of the Banff Formation is in agreement with an inferred temperature calculated from vitrinite reflectance values of coal in the Kootenay Formation, which lies ~1km above the top of the Banff Formation in the LRA. A reflectance value of  $R_o = 1.09\%$  (Hacquebard and Donaldson, 1974) for the Kootenay Formation coal that lies to the west of the southern part of the Livingstone Range (Figure 3-3) gives a calculated temperature estimate of 135°C, using the method of Middleton (1982). A similar temperature, ~133°C, is obtained by using the geothermal gradient of 25°C/km, a surface paleotemperature of 20°C, but a burial depth of approximately 4.5 km.

The >40°C difference between the expected ~158°C host rock temperature and the ~250 +/- 50°C vein temperatures suggests that some of the fluid that formed these veins probably ascended from depths of >2 km below the top of the Banff Formation. A basement-derived source for these hot fluids is also supported by the generally higher  $^{87}\text{Sr}/^{86}\text{Sr}$  ratios of most veins relative to their adjacent host rocks (Figure 3-15, Table 1). The  $\delta^{18}\text{O}$  values of the waters/fluids that formed these early syn-folding veins for which temperatures of vein formation are known range from -10.9 to -13.0‰ (Table 2, Figure 3-16). Host rocks at the expected temperature of ~158°C are inferred to have been in equilibrium with associated formation fluids with  $\delta^{18}\text{O}$  values that range from -19 to -12‰ (Figure 3-16).

Many samples of veins from tear faults and thrust faults that are not related to thrust-propagation folding have  $\delta^{18}\text{O}$  values that are similar to host rock compositions but  $^{87}\text{Sr}/^{86}\text{Sr}$

ratios that are sometimes higher, which indicates that early movement along many of these faults occurred when the structures were occupied by formation- and basement-derived fluids. In a few cases the fault zones contain two sets of veins, an earlier vein with a high  $\delta^{18}\text{O}$  value and a younger vein with a much lower  $\delta^{18}\text{O}$  value (Table 1, sample locations 670 and 671).

The isotopic compositions of veins that are related to thrust-propagation folding have a lower  $\delta^{18}\text{O}$  limit of  $\sim -8.0\text{‰}$  and a lower  $\delta^{13}\text{C}$  limit of  $\sim -2.4\text{‰}$  (Figure 3-14). These values are interpreted to represent the lowest probable isotopic compositions of veins that formed from formation fluids and basement fluids. In the LRA, any vein with a  $\delta^{18}\text{O}$  value lower than  $-9\text{‰}$  is interpreted to have precipitated from fluid that was not buffered by the host rock system, resulting in low  $\delta^{18}\text{O}$  values. Such low  $\delta^{18}\text{O}$  fluids would likely be of meteoric origin. The absence of veins with very low  $\delta^{18}\text{O}$  values in the fault zones that were active during thrust-propagation folding indicates that these faults were relatively inactive by the time meteoric water began infiltrating.

#### **3.6.4 Late syn-thrusting meteoric fluid flow and vein formation**

After an initial stage of thrust-propagation folding, the Livingstone thrust propagated eastward along a detachment in the Fernie Formation, and the LRA began to be transported eastward. Veins that formed within the LRA along thrust faults and tear faults that were active during this later stage of deformation have very low  $\delta^{18}\text{O}$  values and  $\delta^{13}\text{C}$  values (Figure 3-14) and are interpreted to have precipitated from fluids that contained a significant component of meteoric water. These faults include the Pocket Creek tear faults in the north part of the study area (Figure 3-9), which contain veins with very low  $\delta^{18}\text{O}$  values (Samples 503, 513, 514, 517; Table 1, Figure 3-9) indicating a substantial component of meteoric water. The Pocket Creek tear faults formed during late stages of thrusting when the LRA became folded by activity of younger underlying thrusts.

The fluids that were circulating through the strata during later stages of thrusting are interpreted to have contained a significant component of meteoric water that was ultimately responsible for cooling the rock mass. The temperatures at which veins were forming at this time were likely quite variable, with locally low or high temperature zones being controlled by abundance or absence of fault networks that were open to fluid flow. The thrust belt was a dynamic fluid flow system in which fluid conduits likely changed abruptly through time; while deformation caused some faults to open, elsewhere it caused other faults to close and restrict fluid flow, which may have been accompanied by the precipitation of vein-forming minerals that sealed off conduits. According to the thermal and tectonic model presented in Figure 3-18, these veins would have precipitated at temperatures below 100°C. If one assumes the temperatures of the circulating meteoric fluids ranged between 20 to 100°C, the corresponding  $\delta^{18}\text{O}$  values of the waters would have ranged between -40 to -25‰ (Figure 3-16).

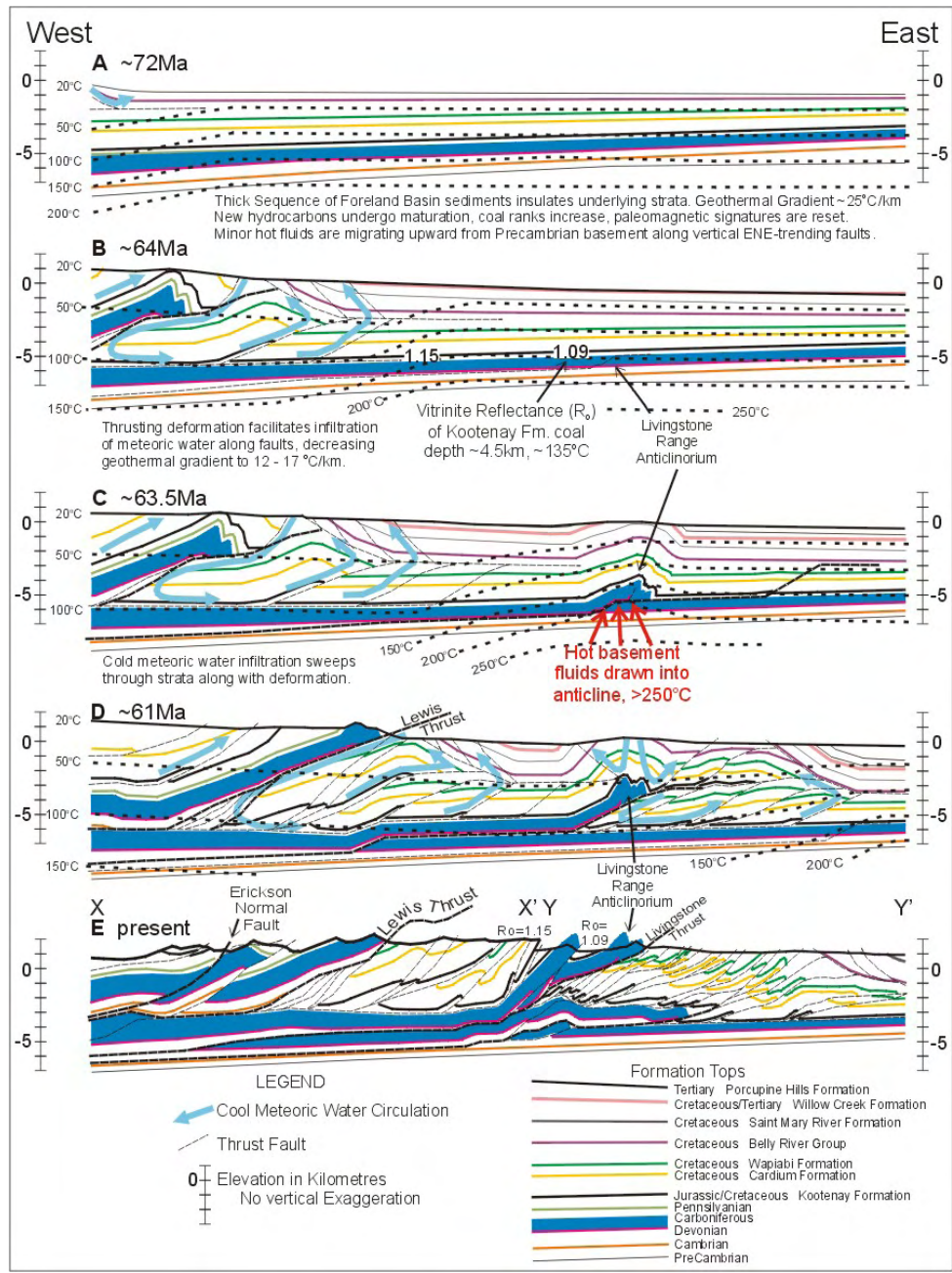


**Figure 3-18.** Hypothetical sequential palinspastic reconstruction of a composite balanced cross section showing the thermal, fluid, and deformation history of the southern Canadian Front Ranges and Foothills. Cross section X X' is modified from R. A. Price (cross section of Fernie map, in preparation). Cross section Y Y' is modified from an unpublished cross section of Paul Mackay. Cross section locations are shown on Figure 3-1. All ages are approximate, and are based on the assumption that initial movement of Livingstone thrust occurred at ~64Ma (see text for discussion).

### 3.7 Regional Implications of the Isotopic Data

#### 3.7.1 *Regional dolomitization and infiltration of basement fluid*

In the Western Canada Sedimentary Basin, pervasive dolomitization affected much of the Paleozoic carbonate strata during diagenesis, which occurred in several stages, beginning shortly after deposition and continuing after burial (Cioppa et al. 2000, Lewchuk et al., 1998, Al-Aasm and Lu, 1994). Diagenesis involved the systematic formation of new dolomite with successively lower  $\delta^{18}\text{O}$  values with each event, and it included the incorporation of variable amounts of radiogenic strontium (Cioppa et al. 2000, Lewchuk et al., 1998, Al-Aasm and Lu, 1994). In the LRA,  $^{87}\text{Sr}/^{86}\text{Sr}$  ratios in most carbonate host rocks are higher than the ratios expected from unaltered Early Carboniferous carbonates (Veizer et al., 1999), but the highest  $^{87}\text{Sr}/^{86}\text{Sr}$  ratios are in dolomitized host rock in alteration haloes that surround the pre-thrusting hydrothermal veins. The fractures in which the hydrothermal veins developed represent the conduits through which basement fluids may have been migrating during diagenesis, possibly providing the radiogenic strontium that became incorporated into the diagenetic dolomite.

The east-northeast-trending Morin Creek tear fault, Daisy Creek tear fault, and the smaller transverse faults in the limbs of the anticlines likely originated as regional fractures or faults related to reactivation of underlying basement faults during Late Carboniferous. The spatial coincidence of the southern part of the LRA with the ENE-trending Vulcan Structure in the underlying Paleoproterozoic basement suggests that basement faults were important conduits for infiltration of fluids into other parts of the Western Canada Sedimentary Basin as well, and they may have been responsible for the initiation of the vertical surfaces that became reactivated as tear faults in the thrust and fold belt.

### ***3.7.2 Pre-thrusting hot thermal event***

The temperature increase that occurred in the foreland strata prior to thrusting and folding is interpreted by Bachu (1995) and Symons and Cioppa (2002) to result from sedimentary burial, rather than to advective heating by displaced deep basin fluids as predicted by Hitchon (1984). The heating of underlying strata produced by the temporary insulating effect of a thick blanket of overlying foreland basin sediments accumulating ahead of the deformation front resulted in increased maturation of coal and other hydrocarbons, and the Late Cretaceous chemical remagnetization of the Paleozoic rocks (Symmons and Cioppa, 2002; Enkin et al., 2000).

The effects of this process on the rocks of the LRA are illustrated in Figure 3-18A and 3-18B. From Late Jurassic to Paleocene, more than 4.5 km of strata accumulated in the foreland basin in the area that was eventually to become the LRA (Figure 3-18B). In the LRA the insulating blanket of foreland basin sediment continued to insulate the LRA during its earliest stage of thrust-propagation folding, temporarily allowing the Carboniferous carbonate rocks to maintain the high temperatures of approximately 158°C proposed for the top of Banff Formation.

### ***3.7.3 Initial syn-thrusting fluid flow***

As the Livingstone thrust propagated up through the Paleozoic strata, the dilation associated with brittle deformation during the rapid formation of thrust-propagation folds caused formation fluids and hot basement fluids to be drawn into the faults and folds (Figure 3-18C). Veins that precipitated in the thrust faults and transverse faults that were active during thrust-propagation folding formed at anomalously high temperatures (250 +/-50°C, Table 2). These veins have higher  $^{87}\text{Sr}/^{86}\text{Sr}$  ratios relative to those of adjacent host rocks (Table 1, and Figure 3-

15), consistent with a significant portion of the vein-forming fluids having come from the underlying Paleoproterozoic crystalline basement. However, the  $\delta^{18}\text{O}$  and  $\delta^{13}\text{C}$  values of these veins were evidently buffered by the adjacent host rocks, indicating small volumes of fluids in a rock-dominated system.

Regional infiltration of hot basement-derived fluids into thrust-related dilatant zones could have occurred along the entire thrust and fold belt as thrust faults were propagating eastward and incorporating new, previously undeformed strata into the deformation belt. Intermittently reactivated structures that cut up through the Paleozoic strata from the underlying Paleoproterozoic crystalline basement probably contained fluids that flowed through basement rocks. Machel and Cavell (1999) in their assessment of “squeegee” fluid flow suggested that relatively small amounts of basement fluids or fluids from Cambrian clastics entered the foreland basin in central Alberta during thrusting and folding deformation. Basement-derived fluids could have been infiltrating during all stages of thrusting and folding; however, during later thrusting-dominated stages, any isotopic evidence of basement fluids would have been masked by the circulation of meteoric water.

#### ***3.7.4 Regional syn-thrusting meteoric fluid infiltration***

Infiltration of meteoric water in the fault zones of the LRA is recorded by calcite veins with  $\delta^{18}\text{O}$  values that are lower than -9‰. These veins occur in fault zones that are interpreted to have been active during the thrust-transport deformation that followed the initial stage of thrust-propagation folding. Veins with very low  $\delta^{18}\text{O}$  values have been documented in thrust faults in the southern Canadian Rocky Mountains that are exposed in the Front Ranges (Kirschner and Kennedy, 2001) and in other thrusts that are penetrated by petroleum exploration boreholes in subsurface thrust-related structures in the Foothills (Cioppa et al. 2000, Lewchuk et al., 1998, Al-

Aasm and Lu, 1994). The thrust-transport deformation, which was marked by large displacements that included uplift and erosional exhumation, evidently coincided with deep penetration of meteoric fluids and advective cooling (Figure 3-18D) that left a regional isotopic record in the form of tectonic veins in fault zones with low  $\delta^{18}\text{O}$  values.

An investigation of the thermal history of the foreland thrust and fold belt in southern Alberta and British Columbia based on apatite fission-track thermochronology and vitrinite reflectance data has shown that rapid cooling of this part of the thrust belt coincided with displacement on the Lewis thrust and other related faults (Osadetz et al., 2004). The geothermal gradient in the Lewis thrust sheet changed from approximately 20°C/km prior to thrusting to 8-12°C/km during thrusting. This change has been attributed to deep infiltration of cool meteoric water driven by high topography and facilitated by enhanced permeability due to brittle deformation (Osadetz et al., 2004).

The abrupt cooling of rocks that are incorporated into the thrust and fold belt above propagating thrust faults may explain the increase in vitrinite reflectance values of coal with depth in thrust repeats of Kootenay Formation coals intersected in many hydrocarbon exploration wells, as shown by Hacquebard and Cameron (1989). Although Hacquebard and Cameron (1989) attribute the increase of vitrinite reflectance with depth to be mainly due to post-deformation coalification in the Kootenay Formation, they acknowledge the same pattern is possible from the thrusting of coal with low rank over coal with a higher rank. If the observations of Osadetz et al. (2004) are applicable to the rest of the thrust and fold belt, coal-bearing strata would have been cooled by infiltrating meteoric water and coalification would have ceased soon after they became incorporated into the thrust and fold belt. As thrusting proceeded, coal-bearing strata that were insulated by relatively thin foreland basin deposits became faulted, folded, transported, elevated and rapidly cooled by infiltrating meteoric water. Coal at the same stratigraphic level further east in the undeformed foreland basin would thus have been blanketed by thicker foreland basin

deposits and would therefore have attained a higher rank than the coal that was about to be thrust over it. A similar process of eastward-migrating foreland basin sedimentation affecting coalification has been proposed for the Grande Cache area of west central Alberta by Kalkreuth and McMechan (1984, 1996) to explain the relatively higher vitrinite reflectance values of coals that occur in the Alberta syncline relative to successively lower ranks of equivalent coal strata that exist to the west and east. Kalkreuth and McMechan (1984, 1996) propose that deposition of the coal-bearing sediments was at least partly synchronous with the uplift of the Cordillera to the west. As a consequence, the western part of the coal-bearing sequences was not buried as deeply or for as long a period of time as the eastward extension of these beds along the axis of the Alberta syncline.

The large volumes of water that must have circulated through the strata in sufficient quantities to remove heat and decrease geothermal gradients must have flowed along conduits that should be visible today by some degree of hydrothermal alteration or karstification of adjacent host rock. Locally, however, the lack of alteration along thrust faults examined by Kirschner and Kennedy (2001) in the Front Ranges of the Rocky Mountains, and the absence of low  $\delta^{18}\text{O}$  values in veins that occur  $> 1$  metre away from thrust faults, led them to infer that only small volumes of meteoric fluids had passed through the faults that they examined.

Hot springs that flow in the Rocky Mountains today may be analogous to the type of deeply penetrating meteoric fluid flow systems that once cooled the rock mass during thrusting and folding. The very low  $\delta^{18}\text{O}$  values of these hot spring waters show that they are meteoric waters (Grasby et al., 2000). Water flowing from the hot springs in Banff, Alberta, are slightly saturated with respect to carbonate, and they should be precipitating calcite with  $\delta^{18}\text{O}$  values of  $\sim -24\%$  (Figure 3-16) (calculated using data of Grasby et al., 2000). If veins were forming at depth along major conduits for meteoric fluid circulation during thrusting and folding, their isotopic compositions should be around  $\sim -24\%$ . However, the lowest  $\delta^{18}\text{O}$  values in calcite veins are –

18‰ in the LRA, ~-15 ‰ in the Front Range thrusts (Kirschner and Kennedy, 2001), -17‰ in the subsurface Moose Mountain structure (Cioppa et al., 2000), -12 ‰ in the subsurface Waterton Gas Field (Lewchuck et al., 1998) and -12‰ in the subsurface Quirk Creek gas field (Al-Aasm and Lu, 1994). These  $\delta^{18}\text{O}$  values are higher than ~-24‰ and therefore likely represent meteoric fluids that had partly equilibrated with host rocks before precipitating veins, and hence were unlikely to have formed along the main conduits for meteoric fluid circulation. Evidence for significant meteoric fluid circulation perhaps may not be expected along the parts of thrust faults and tear faults that contain veins because veins are more likely to have formed where fluid flow became restricted or trapped in thin, discontinuous fractures, allowing the meteoric fluids to partially equilibrate with the host rocks.

In the LRA, three host rocks have anomalously low  $\delta^{18}\text{O}$  values and slightly lower  $\delta^{13}\text{C}$  values relative to most host rocks (Table 1, samples 209-R, 670B-R and 496-R, and Figure 3-13). These host rocks are generally lighter in colour than the surrounding rocks, they are weakly to strongly stained with limonite and they have sandy, granular textures in outcrop and milky, translucent to opaque textures in thin sections that indicate these rocks have been hydrothermally altered. Their very low  $\delta^{18}\text{O}$  values (-10.8 to -12.2‰, Figure 3-13, Table 1) relative to all other host rocks analysed in the LRA indicates that they were altered by meteoric waters and may have once been located along major conduits of meteoric fluid circulation.

The cooling of the thrust sheets is therefore inferred to have occurred by local circulation of significant volumes of meteoric fluid through relatively few major conduits, and the cooling of the rest of the rocks mass was by conduction, analogous to the water-cooling system of the common internal combustion engine. Large volumes of meteoric fluids did not flush through the entire rock mass through every crack, fracture and pore space. As thrusting deformation progressed from west to east, the region of infiltrating meteoric fluids and rapid cooling also migrated along with the deformation (Figure 3-18A-D), flushing out the heat that had been

contained by the thick insulating shale-bearing foreland basin deposits, abruptly and significantly lowering the regional geothermal gradient.

### **3.8 Conclusions**

Deformed jasper +/-fluorite+/-sphalerite veins, and adjacent dolomitic alteration haloes with high  $^{87}\text{Sr}/^{86}\text{Sr}$  ratios and high  $\delta^{18}\text{O}$  values relative to most host rocks, record the pre-thrusting and folding infiltration of Paleoproterozoic crystalline basement fluids into the Paleozoic strata of the LRA along reactivated basement faults that cut Paleozoic rocks. Similar basement-derived fluids may also have provided the radiogenic strontium that is recorded by the anomalously high  $^{87}\text{Sr}/^{86}\text{Sr}$  ratios within diagenetically altered Paleozoic carbonate host rocks in the LRA and elsewhere in the Western Canada Sedimentary Basin, however a shale basin source for the strontium is also very probable. Most tear faults that cut through the Livingstone thrust sheet, and the transverse faults that preferentially cut the Livingstone Formation in the cores of the anticlines, can be interpreted as fractures that originated during the Carboniferous during movement along underlying basement faults and that were subsequently reactivated during thrusting and folding.

Prior to the formation of the LRA, the actively deforming parts of the thrust belt to the west were becoming thickened by thrust faults, elevated and exposed to erosion. As sediment was shed eastward from the emerging thrust belt, approximately 4.5 km of strata accumulated in the foreland basin above the Paleozoic rocks that would eventually be incorporated into the LRA. The geothermal gradient was likely no greater than 25°C/km at this time, and the top of the Banff Formation, which was buried under ~5.5 km of strata, achieved a maximum temperature of ~158°C.

The rapid dilation accompanying brittle chevron-style flexural-slip thrust-propagation folding caused formation fluids and small amounts of basement fluids to be drawn into the dilatant zones in the folds, and into tear faults and larger thrust faults that were active at this early stage of deformation. Veins that formed at this time precipitated at anomalously high temperatures (250 +/-50°C) that were not in thermal equilibrium with the surrounding strata, which would have been ~158°C. These veins have  $\delta^{18}\text{O}$  values that are similar to those of adjacent host rocks, which support a formation fluid origin, but they have slightly higher  $^{87}\text{Sr}/^{86}\text{Sr}$  ratios that indicate small components of fluid from the underlying crystalline basement. Host rocks and veins from these early-formed structures have  $\delta^{18}\text{O}$  values that range from -7.92‰ to -1.08‰. The structural hydrocarbon traps that developed during this time would have been too hot for oil or gas preservation, and strata that were down-dip to the west would also have been over-mature and therefore could not have been a hydrocarbon source. Hydrocarbons could only have accumulated in the LRA during later stages of thrusting deformation when it became juxtaposed over Mesozoic source rocks in the footwall of the Livingstone thrust.

Younger veins with low  $\delta^{18}\text{O}$  values (-18 to -9‰) in thrust faults and tear faults are interpreted to have formed from meteoric fluid that infiltrated during later stages of deformation while the LRA was being transported eastward and elevated by displacements on the Livingstone thrust and on underlying thrust faults. As thrusting deformation progressed from west to east, the region of infiltrating meteoric fluids and rapid cooling also migrated along with the deformation (Figure 3-18A-D), flushing out the heat that had been contained by the thick insulating layer of shaley foreland basin deposits.

The thrust belt was a dynamic fluid flow system in which fluid conduits likely changed abruptly through time; while deformation caused some faults to open, elsewhere it caused other faults to close and restrict fluid flow, which may have been accompanied by the precipitation of vein-forming minerals that sealed off conduits.

The conduits along which significant meteoric fluid circulation occurred within the LRA are indicated in a few locations along faults where host rocks have been strongly altered and have anomalously low  $\delta^{18}\text{O}$  values (-10.8 to -12.2‰).

Rapid cooling due to deep infiltration into the shallow brittle surface of the deforming earth is almost certainly not restricted to thrust and fold belts, nor is its thermal effect necessarily restricted to the upper few kilometers. This model for fluid flow has significant implications for predicting thermal conditions in deep metamorphic rocks that lie beneath the brittle crust, the most obvious effect being to push down the brittle/ductile transition zone, which would enhance even deeper meteoric fluid circulation and cause the deflection of underlying isotherms. With such a model, previous ideas of simple, gradual cooling histories from uplift and erosion of an orogen might actually be preceded by a brief period of rapid cooling right at the beginning of deformation.

### **3.9 Acknowledgements**

This research has been supported by NSERC research grants to Raymond Price, Kurt Kyser and John Dixon. We gratefully acknowledge the financial assistance of the sponsors of the Fold Fault Research Project. Geochemical analyses were conducted under the invaluable supervision of Kerry Klassen and Don Chipley of the Queen's University Facility for Isotope Research. Field work benefited greatly from the field assistance of Greg Cameron, Scott Conley and Kyle Larson. We are grateful for the constructive criticisms of Margot McMechan and Timothy Diggs. Digital topography has been provided by AltaLIS Ltd., and access to well logs was provided by Nexen.

### 3.10 References

- Al-Aasm, I. S.; Lu, F., 1994. Multistage dolomitization of the Mississippian Turner Valley Formation, Quirk Creek Field, Alberta; chemical and petrologic evidence. *Memoir - Canadian Society of Petroleum Geologists*, v.17, p.657-675.
- Bachu, S. (1995). Synthesis and model of formation-water flow, Alberta Basin, Canada. *AAPG Bulletin*, v. 79, No 8, p. 1159-1178.
- Bachu, S. and Burwash, R. A., 1994. Geothermal Regime in the Western Canada Sedimentary Basin, Chapter 30 in *Geological Atlas of the Western Canada Sedimentary Basin*, G.D. Mossop and I. Shetson (comp.), Canadian Society of Petroleum Geologists and Alberta Research Council, Calgary, Alberta.
- Bradbury, J.H., Woodwell, G.R., 1987. Ancient fluid flow within foreland terrains. In: Goff, J.C., Williams, B.P.J. (Eds.), *Fluid Flow in Sedimentary Basins and Aquifers*. Geol. Soc. London Spec. Publ. 34, 87–102.
- Burtner, R. L. and Nigrini, A., 1994. Thermochronology of the Idaho-Wyoming Thrust Belt during the Sevier Orogeny: a new, calibrated, multiprocess thermal model. *AAPG bulletin*, v. 78, (10) p. 1586, 1612.
- Cioppa, M. T.; Al-Aasm, I. S.; Symons, D. T. A.; Lewchuk, M. T.; Gillen, K. P., 2000. Correlating paleomagnetic, geochemical and petrographic evidence to date diagenetic and fluid flow events in the Mississippian Turner Valley Formation, Moose Field, Alberta, Canada. *Sedimentary Geology*, vol.131, no.3-4, pp.109-129.
- Clayton, R N; O'Neil, J R; Mayeda, T K, 1972. Oxygen Isotope Exchange between Quartz and Water. *Journal of Geophysical Research*, vol.77, no.17, p.3057-3067.

- Clowes, R. M., Burianyk M. J. A., Kanasewich, E. R and Gorman, A. R, 2002. Crustal velocity structure from SAREX, the Southern Alberta Refraction Experiment1. *Canadian Journal of Earth Sciences* v. 39, p. 351–373.
- Cooley, M. A., Price, R. A., Dixon, J. M. and Kyser, T. K. (in review). Chevron-style, flexural-slip thrust-propagation folding, Livingstone Range anticlinorium, southern Alberta Foothills, Canada. Submitted to *AAPG Bulletin*.
- Douglas, R. J. W., 1950. Callum Creek, Langford Creek and Gap map-area, Alberta, *Geological Survey of Canada Memoir* 255.
- Eaton, D. W.; Ross, G. M and Clowes, R. M., 1999. Seismic-reflection and potential-field studies of the Vulcan structure, Western Canada; a Paleoproterozoic Pyrenees? *Journal of Geophysical Research*, v.104, no. B10, p.23,255-23,269.
- Enkin, R.J., Osadetz, K.G., Baker, J. & Kisilevsky, D., 2000. Orogenic remagnetizations in the front ranges and inner foothills of the Southern Canadian Cordillera: chemical harbinger and thermal handmaiden of Cordilleran deformation, *GSA Bulletin.*, v. 112, p. 929-942.
- Grasby, S. E., Hutcheon, I., and Krouse, H.R., 2000. The influence of water-rock interaction on the chemistry of thermal springs in western Canada *Applied Geochemistry*, v. 15, p. 439 – 454.
- Hacquebard, P. A.; and Cameron, A. R., 1989. Distribution and coalification patterns in Canadian bituminous and anthracite coals. *International Journal of Coal Geology*, v.13, no.1-4, p.207-260.
- Hacquebard, P. A., Donaldson, J. R., 1974. Rank studies of coals in the Rocky Mountains and Inner Foothills Belt, Canada. *Geological Society of America, Special Paper* 153, p. 75-94.

- Hart, B.S. and Plint, A.G., 1993. Tectonic influence on deposition and erosion in a ramp setting: Upper Cretaceous Cardium Formation, Alberta Foreland Basin. *American Association of Petroleum Geologists Bulletin*, v. 77, p. 2092-2107.
- Hitchon, B., 1984. Geothermal gradients, hydrodynamics, and hydrocarbon occurrences, Alberta, Canada. *American Association of Petroleum Geologists Bulletin*, v.68, p.713-743.
- Kalkreuth, W., and McMechan, M. E., 1984. Regional pattern of thermal maturation as determined from coal rank-studies, Rocky Mountain Foothills and Front Ranges north of Grande Cache, Alberta – implications for petroleum exploration. *Bulletin of Canadian Petroleum Geology* v. 32, no. 3, p. 249-271.
- Kalkreuth, W., and McMechan, M. E., 1996. Coal rank and burial history of Cretaceous-Tertiary strata in the Grande Cache and Hinton areas, Alberta, Canada: implications for fossil fuel exploration. *Canadian Journal of Earth Science*, v. 33, p. 938-957.
- Katz, A; Matthews, A., 1977. The dolomitization of CaCO<sub>3</sub> (sub 3); an experimental study at 252-295 degrees C. *Geochimica et Cosmochimica Acta*, v.41, no.2, p. 297-308.
- Killingly, J. S., 1983. Effects of diagenetic recrystallization on <sup>18</sup>O <sup>13</sup>C values of deep-sea sediments. *Nature*, v. 301, p. 594-597.
- Kirschner, D. L.; Kennedy, L. A., 2001. Limited syntectonic fluid flow in carbonate-hosted thrust faults of the Front Ranges, Canadian Rockies, inferred from stable isotope data and structures. *Journal of Geophysical Research, B, Solid Earth and Planets*, v.106, no.5, p.8827-8840.
- Langenberg, C.W, Beaton, A. and Berhane, H. 2002. Regional Evaluation of the Coalbed Methane Potential of the Foothills/Mountains of Alberta (Second Edition) Alberta Geological Survey EUB/AGS Earth Sciences Report 2002-05.

- Lemieux, S., 1999. Seismic reflection expression and tectonic significance of Late Cretaceous extensional faulting of the Western Canada sedimentary basin in southern Alberta. *Bulletin of Canadian Petroleum Geology*, v. 47; no. 4; p. 375-390.
- Lewchuk, M. T., Al-Aasm, I. S., Symons, D. T. A. and Gillen, K. P., 1998. Dolomitization of Mississippian carbonates in Shell Waterton gas field, southwestern Alberta: insights from paleomagnetism, petrology and geochemistry, *Bulletin of Canadian Petroleum Geology*, v. 46, 3, p. 387-410.
- Machel, H. G., 2004. Concepts and models of dolomitization; a critical reappraisal. *Geological Society Special Publications*, vol.235, p.7-63.
- Machel, H. G., and Cavell, P. A., 1999. Low-flux, tectonically-induced squeegee fluid flow (“hot flash”) into the Rocky Mountain Foreland Basin. *Bulletin of Canadian Petroleum Geology*. v. 47, 4, p. 510-533.
- Matthews, A., Katz, A., 1977. Oxygen isotope fractionation during dolomitization of calcium carbonate. *Geochimica et Cosmochimica Acta* 41, 1431– 1438.
- McCrea, J.M., 1950, On the isotopic chemistry of carbonates and a paleotemperature scale. *Journal of Chemical Physics*, v. 18, p. 849–857.
- Middleton, M. F., 1982. Tectonic history from vitrinite reflectance. *Geophysical Journal of the Royal Astronomical Society*, v. 68, no. 1, p. 121–132.
- Monger, J. W. H.; Price, R. A., 1979. Geodynamic evolution of the Canadian Cordillera; progress and problems. *Canadian Journal of Earth Sciences*, v.16, 3, p.771-791.
- Muehlenbachs, K., 1998. The oxygen isotopic composition of the oceans, sediments and the seafloor. *Chemical Geology* v. 145, p. 263–273.

- Nesbitt, B. E. and Muehlenbachs, K., 1995. Geochemistry of syntectonic, crustal fluid regimes along the Lithoprobe Southern Canadian Transect. *Canadian Journal of Earth Sciences*, v. 32, p. 1699-1719.
- O'Neil, J. R., Clayton, R. N., Mayeda, T. K., 1969. Oxygen isotope fractionation in divalent metal carbonates. *The Journal of Chemical Physics*, v.51, no.12, p.5547-5558.
- Osadetz, K. G., Kohn, B. P., Feinstein, S., and Price, R. A., 2004. Foreland belt thermal history using apatite fission-track thermochronology: Implications for Lewis thrust and Flathead fault in the southern Canadian Cordilleran petroleum province, in Swennen, R., Roure, F., and Granath, J. W., eds., *Deformation, fluid flow, and reservoir appraisal in foreland fold and thrust belts: AAPG Hedberg Series, No. 1*, American Association of Petroleum Geologists, Tulsa, U.S.A., p. 21–48.
- Price, R. A., 1967. The tectonic significance of mesoscopic subfabrics in the southern Rocky Mountains of Alberta and British Columbia. *Canadian Journal of Earth Sciences* v. 4, no. 1, p.39-70.
- Price, R. A., 1981. The Cordilleran foreland thrust and fold belt in the southern Canadian Rocky Mountains, in McClay, K. R., and Price, N. J., eds., *Thrust and nappe tectonics*, The Geological Society of London, p. 427-448.
- Price, R. A., 1994. Cordilleran tectonics and the evolution of the Western Canada sedimentary basin, in Mossop, G. D., and Shetsen, I., eds., *Geological Atlas of Western Canada*: Calgary, Canadian Society of Petroleum Geologists/Alberta Research Council, p. 13-24.
- Price, R. A., Osadetz, K. A., Kohn, B. P., Feinstein, S., 2001. Deep refrigeration of an evolving thrust and fold belt by enhanced penetration of meteoric water; the Lewis thrust sheet, southern Canadian Rocky Mountains. *Abstracts with Programs - Geological Society of America*, v. 33 (6), p. 52.
- Ramsay, J. G., 1974. Development of chevron folds. *Geological Society of America Bulletin*, v. 85, no. 11, p. 1741-1754.

- Sharma, T., and Clayton, R. N., 1965. Measurement of O-18/O-16 ratios of total oxygen of carbonates. *Geochimica et Cosmochimica Acta*, vol.29, no.12, p.1347-1353.
- Sibson, R. H., and Poulson, K. H., 1988. High angle reverse faults, fluid pressure cycling, and mesothermal gold-quartz deposits. *Geology*, v. 16, p. 551-555.
- Symons, D. T. A., Cioppa, M. T., 2002. Conodont CAI and magnetic mineral unblocking temperatures: implications for the Western Canada Sedimentary Basin. *Physics and Chemistry of the Earth* v. 27, p. 1189–1193.
- Veizer, J., Ala, D., Azmy, K., Bruckschen, P., Buhl, D., Bruhn, F., Carden, G. A. F., Diener, A., Ebner, S., Godderis, Y., Jasper, T., Korte, C., Pawellek, F., Podlaha, O. G., Strauss, H., 1999.  $^{87}\text{Sr}/^{86}\text{Sr}$ ,  $\delta^{13}\text{C}$  and  $\delta^{18}\text{O}$  evolution of Phanerozoic seawater. *Chemical Geology* v. 161, p. 59–88.

## **Chapter 4 Conclusions and recommendations for further work**

### **4.1 Structural geology conclusions**

The Livingstone Range anticlinorium is a detached and displaced hanging-wall-ramp thrust-propagation fold. It developed as the eastward propagating Livingstone thrust cut upward through ~1000 m of well bedded, shallow-water, Upper Paleozoic carbonate strata to form a ramp between extensive regional detachments in the lime mudstones of the upper part of the Upper Devonian Palliser Formation and in the marine shales of the Jurassic Fernie Formation. The anticlinorium consists of an array of linked, asymmetric chevron folds that have planar limbs and blind thrust systems within the fold hinge zones.

The distinctive pattern of ramp-flat thrusting that occurs along the hinge zone thrust system of the asymmetric chevron-style Centre Peak anticline consists of a series of stacked detachment thrusts, each of which emerges from a different zone of interbed slip in the backlimb of the anticline and deflects the hinge zone eastward. Each detachment thrust consists of two contrasting segments. The lower segment, which is parallel to bedding in the less steeply dipping backlimb of the fold, juxtaposes a hanging-wall flat with a footwall ramp. The upper segment, which is sub-parallel with the steeply-dipping forelimb, juxtaposes a hanging-wall ramp with what roughly approximates a footwall flat. Each successively lower detachment thrust dies out in the hinge zone at approximately the same stratigraphic level that an overlying detachment thrust fault emerges from a bedding detachment zone in the backlimb. Successively higher bedding detachment thrusts deflect the hinge zone eastward and therefore displacement along each of them is interpreted to have occurred after the displacement on the underlying thrust. The growth of the anticline was arrested with the final displacement on the highest bedding detachment thrust, which terminates in the core of a concentric, parallel, flexural-slip fold. It provides an

actualistic model for the configuration/geometry of the structure prior to the development of each of the underlying detachment thrusts that deflect the hinge zone.

The chevron-style thrust-propagation folding that produced the Centre Peak anticline differs fundamentally from models described by Dahlstrom, (1969 and 1970); Williams and Chapman (1983) Jamieson (1987), Suppe and Medwedeff (1990), Wickham (1995), and Allmendinger (1998). Although the initial stages may have been the same as in the models, the Centre Peak anticline underwent additional deformation involving the propagation of thrust faults that emerged from bedding detachment zones in the backlimb and deflected the hinge zone. This additional thrust-propagation folding tightened the fold hinge to an interlimb angle of ~60 degrees and lengthened the fold limbs, effectively doubling the amplitude of the anticline and producing its distinctive chevron style; moreover, it involved approximately 30 degrees of shear that was mainly distributed along a few detachment horizons via inter-bed slip throughout the >1km thick backlimb of the fold, which implies that a similar degree of shear occurred throughout the Livingstone thrust sheet to the west. The significant shearing that occurred within the Livingstone thrust sheet likely also occurred in other thrust sheets within the foreland thrust and fold belt, and in other thrust belts around the world. This distributed shearing should be considered in all palinspastic restorations of thrust belts to make cross section interpretations more correct.

Locally important bedding detachment zones occur in the lower part of the Banff Formation, in the micrite unit at the top of the Banff Formation and near the base of the Turner Valley Member of the Livingstone Formation. These local detachments may be regionally important as well. Most of the individual chevron-style thrust-propagation folds in the anticlinorium originated above the minor ramps that developed along the hanging-wall of the Livingstone thrust as it propagated up-section from one bedding-parallel detachment zone to another. Notable exceptions are the tight chevron-style Cross anticline which formed above a

thrust splay that branched upward from the Livingstone thrust, and one short segment of the Centre Peak anticline that formed a broad open fault-bend fold.

Along-strike changes in the structure of the Livingstone Range anticlinorium are generally gradual, but locally they occur abruptly across cross-strike discontinuities. These are associated with dextral tear faults (or lateral thrust ramps) that are kinematically linked to slip on the Livingstone thrust. The Morin Creek and Daisy Creek tear faults, which die out upward near the top of the Livingstone Formation, may have originated by reactivation of pre-existing east-northeast-trending steeply dipping faults that were active prior to deposition of the Mount Head Formation. The Pocket Creek tear faults, which trend east-west and cut through Mount Head Formation and younger strata, are interpreted to have formed much later when a dextral transverse fault-bend fold flexure was superimposed on the anticlinorium as the Livingstone thrust sheet was being transported eastward on underlying thrusts.

## **4.2 Isotope-geochemistry Conclusions**

Deformed jasper+dolomite+/-fluorite+/-sphalerite veins and adjacent haloes of altered host rock with high  $^{87}\text{Sr}/^{86}\text{Sr}$  ratios and high  $\delta^{18}\text{O}$  values relative to most host rocks record the pre-deformation infiltration of allochthonous fluids into the Paleozoic strata of the LRA. These allochthonous fluids, which probably originated in the Paleoproterozoic crystalline basement of the Western Canada Sedimentary Basin, provided the radiogenic strontium that is presently recorded by the anomalously high  $^{87}\text{Sr}/^{86}\text{Sr}$  ratios within Paleozoic carbonate rocks in the LRA and elsewhere in the Western Canada Sedimentary Basin.

Prior to the formation of the LRA, tectonic thickening, rock uplift, and vigorous erosion were occurring in the actively deforming parts of the thrust belt to the west. Sediment shed eastward from the emerging thrust belt accumulated to a depth of approximately 4.5 km in the

foreland basin above the Paleozoic rocks that would eventually be incorporated into the LRA. The geothermal gradient was approximately 28°C/km at this time, and the temperature of the Paleozoic rocks in the LRA should have been approximately 170°C.

Formation fluids and small amounts of basement fluids were present within the LRA while the Livingstone thrust was propagating up a ramp through the Paleozoic strata to a décollement in the Jurassic Fernie Formation. These fluids were drawn by dilation during deformation into the faults and fractures that formed within thrust-propagation folds, and into tear faults and larger thrust faults that were active at this early stage of deformation. Veins that formed at this time precipitated at anomalously high temperatures ( $\geq 250^\circ\text{C}$ ). They were not in thermal equilibrium with the surrounding strata, which would have been at approximately 170°C. These early formed veins have  $\delta^{18}\text{O}$  values that are similar to those of adjacent host rocks, which indicates that they originated as formation fluids, but they have  $^{87}\text{Sr}/^{86}\text{Sr}$  ratios that are slightly higher than adjacent host rocks, which indicates they include some amount of basement fluid. Calcite in host rocks and veins from these early-formed structures have  $\delta^{18}\text{O}$  values that range from  $-7.9$  to  $-1.1\%$ .

Most of the tear faults that cut through the Livingstone thrust sheet, and the transverse faults that preferentially cut Livingstone Formation and older strata in the cores and limbs of the anticlines, are interpreted to be faults and fractures that originated during the Carboniferous and that were subsequently reactivated during thrusting and folding. Host rocks along these vertical structures have slightly lower  $\delta^{18}\text{O}$  values relative to the  $\delta^{18}\text{O}$  values of host rocks along thrust faults, which indicate that the host rocks along the vertical faults may have been slightly more affected by diagenesis due to the presence of fluids along these ancient vertical conduits. The slightly lower  $\delta^{18}\text{O}$  values of host rocks in transverse faults and tear faults could also be attributed to wall rock alteration by the greater presence of fluids that were circulating through these vertical conduits during thrust-propagation folding.

In a few locations, older veins, with  $\delta^{18}\text{O}$  values that are similar to host rock values, are cut by younger veins with  $\delta^{18}\text{O}$  values that are much lower (<-9‰). These younger veins are interpreted to have precipitated from fluids containing a significant component of meteoric water that infiltrated downward during later stages of deformation, while the LRA was being transported eastward and upward along the Livingstone thrust and along underlying thrust faults. Infiltration of meteoric water rapidly cooled the Livingstone thrust sheet and any other strata that became incorporated into the thrust and fold belt.

The low  $\delta^{18}\text{O}$  values of veins within the Pocket Creek tear faults indicate they formed while the Livingstone thrust sheet was being infiltrated by meteoric water. This occurred while the LRA was being folded due to displacements along younger underlying thrust faults. Unlike other northeast-trending tear faults, the Pocket Creek tear faults trend east-west and they occur within a conspicuous transverse, east-west trending dextral monoclinial flexure that has been superimposed on the entire LRA.

Conduits along which significant meteoric water circulation occurred within the LRA are indicated by a few locations along faults where host rocks have been strongly altered and have anomalously low  $\delta^{18}\text{O}$  values (-10.8 to -12.2‰).

The thermal and fluid processes that coincided with deformation of the Livingstone Range anticlinorium during Paleocene thrusting likely occurred along the entire length of the Foreland Thrust and Fold Belt in the southern Canadian Cordillera, and in other similar thrust belts around the world. Rock type and weather patterns may also play important roles in the application of this model to other thrust and fold belts. In a thick shale-dominated basin, permeability of fault zones would likely be greatly reduced by the ductile behaviour of the shale, as compared to the brittle deformation associated with carbonate rocks or sandstone. In arid regions such as the Tian Shan mountains of western China or the Zagros Mountains of Iran, the lack of rainfall would likely reduce the cooling effects during deformation.

Rapid cooling due to deep infiltration of meteoric water into the shallow brittle surface of the deforming earth is almost certainly not restricted to thrust and fold belts, nor is its thermal effect necessarily restricted to the upper few kilometers. This model for fluid flow has significant implications for predicting thermal conditions in deep metamorphic rocks that lie beneath the brittle crust, the most obvious effect being to push down the brittle/ductile transition zone, which would enhance even deeper meteoric fluid circulation and cause the deflection of underlying isotherms. With this model, previous interpretations of simple, gradual cooling histories from proposed uplift and erosion of an orogen might actually be preceded by a brief period of rapid cooling right at the beginning of deformation.

### **4.3 Summary of Hydrocarbon Exploration Significance**

The LRA is a well-exposed analogue to similar but buried hanging-wall ramp anticlines such as the Turner Valley anticline, which is a prolific hydrocarbon-bearing structure that underlies the foothills ~40 km south of Calgary.

Broad anticlinal culminations occur between cross-strike discontinuities in the LRA. The cores of the doubly-plunging folds are occupied by brittle, strongly fractured and porous limestone of the Livingstone Formation, forming an ideal reservoir rock. Overlying the thick limestones are less deformed, shale-dominated strata of the Mount Head and Etherington Formations, which form the cap rock of the structure.

The relationships observed between the locations of fold culminations and cross-strike discontinuities in the LRA may provide actualistic models for interpreting deeply-buried prospective petroleum reservoir structures, which commonly are difficult to interpret with seismic reflection imaging. Along-strike changes in the structures are generally gradual in the LRA, but locally they occur abruptly across cross-strike discontinuities. The complicated geometry of

linked thrust-propagation folds and their abrupt termination or offsets at tear faults as shown in the LRA shows the complexity that can be expected in subsurface plays, where along-strike deep-drilling that may intend to intersect an anticline crest may not work out if the new exploration hole is on the other side of an unanticipated transverse structure. Many transverse structures in the LRA, the largest of which consistently occur as dextral-sense tear faults, are interpreted to be reactivated ancient faults, hence the recognition and understanding of pre-existing structures and their potential effects on younger thrust-related structures is key to predicting how and where to explore for more potential along-strike in a reservoir.

The abundant fractures that occur along the Centre Peak anticline in the Green Creek/Morin Creek area have relatively heterogeneous orientations and do not show a consistent pattern that can be related simply to folding. Fracture patterns are instead dominated by east-west trending transverse zones of intense fracturing that cut through the hinge zone and fold limbs. These zones formed during reactivation of a widely spaced (~150 metres) pre-existing fracture set that trends ENE. The transverse fracture zones are especially well developed within Livingstone Formation strata in the forelimbs of the anticlines in the LRA, which would have made this the most permeable part of the structure during hydrocarbon migration and trapping. The lack of young veins with meteoric signatures in these transverse structures may indicate that they were well-sealed beneath their shale cap rock. There may have been no through-put of meteoric fluids, but immiscible hydrocarbons could still migrate up into these structures. These transverse fracture zones do not extend up into the overlying shale-bearing Mount Head Formation, which may have served as a seal that prevented the upward migration of fluids.

Fluid flow during the earliest stages of thrust-propagation folding did include hydrocarbon gas; hydrocarbon fluid inclusions are preserved within many of the earliest veins. However, at this stage the structure was too deep and too hot to preserve hydrocarbons in

structural traps. Potential source rocks down-dip would also have been over-mature and could never have contributed hydrocarbons to the LRA structural traps at any time.

Hydrocarbons could only have accumulated in the LRA after it had been transported eastward and upward by underlying thrust faults and cooled by the circulation of meteoric water. At this stage the LRA was juxtaposed over Mesozoic source rocks in the footwall of the Livingstone thrust. At this time the LRA would still have been buried under several kilometres of strata.

Hydrocarbons likely persisted in the Carboniferous carbonate rocks within the cores of the anticlines in the LRA until they became breached by erosion and the hydrocarbons leached away. The past presence of oil is indicated by the ubiquitous presence of black, dry solid hydrocarbon residues in fault zones, and by the strong petroleum odor that can be detected in freshly broken rocks from most fault zones.

#### **4.4 Recommendations for further work**

##### ***4.4.1 Analogue modelling of bedding-detachment thrust-propagation folding***

The chevron style thrust-propagation folds in the LRA, with their angular hinges and narrow interlimb angles, differ from previous analogue models of which the author is aware. The conspicuous jogs in the hinge zone, that formed from bedding detachment thrusts propagating out of the backlimb, need to be understood better regarding their relative timing. Did these fault form sequentially from bottom to top as folding extended the anticline upward, or were all the detachment thrusts active at the same time as the entire fold tightened?

#### ***4.4.2 Direct dating of veins (and deformation) using Sm-Nd in fluorite.***

The ages of deformation events that occurred in the LRA are primarily based on stratigraphic arguments, which only provide approximate ages. Absolute age dates are generally not possible in thrust and fold belts due to a lack of datable material in the deformed stratigraphic succession. A possible dating method, which uses samarium and neodymium in fluorite (Chesley et al., 1994), may have potential in the LRA and elsewhere in the Canadian Cordillera because many of the early veins in the LRA contain fluorite.

#### ***4.4.3 Fluid inclusion study of veins.***

Fluid inclusion analyses would help constrain the temperatures at which veins formed, providing invaluable information regarding thermal evolution of the study area. Such a study would be challenging, however, as most veins are composed of dolomite and calcite, which generally show evidence of having been affected by later deformation. The author has made many thin section slides for fluid inclusion analyses and found only hydrocarbon-bearing inclusions (they fluoresce in UV light), with which it is difficult to work with. A focused fluid inclusion study may find primary hydrous fluid inclusions in undeformed parts of veins, which are crucial for determining the conditions at which the veins first precipitated.

#### ***4.4.4 Recognition and documentation of major conduits of meteoric fluid circulation.***

The major conduits along which abundant meteoric fluids may have circulated through the LRA, and that were ultimately responsible for cooling the rock mass, are recognised by areas along faults that have been visibly recrystallized, that generally have a conspicuous pale colour,

and that have anomalously low  $\delta^{18}\text{O}$  values relative to all other host rocks. These features were largely overlooked in the LRA because fieldwork was focused on finding veins as indicators of fluid flow. Ironically, the presence of veins may actually represent zones of minor fluid circulation and should be avoided, unless they are cross-cut by later meteoric fluid alteration. Additional descriptive and isotopic work needs to be done on the major conduits to document the extent of the alteration haloes and to determine their timing of formation relative to deformation events.

#### **4.5 References**

- Allmendinger, R. W., 1998. Inverse and forward modelling of trishear fault-propagation folds. *Tectonics*, v. 17, p. 640-656.
- Chesley, J T; Halliday, A N; Kyser, T K; Spry, P G, 1994. Direct dating of mississippi valley-type mineralization; use of Sm-Nd in fluorite. *Economic Geology and the Bulletin of the Society of Economic Geologists*, v.89, no.5, p.1192-1199.
- Dahlstrom, C. D. A., 1969. Balanced cross sections: *Canadian Journal of Earth Sciences*, v. 6, p. 743-757.
- Dahlstrom, C. D. A., 1970, Structural geology in the eastern margin of the Canadian Rocky Mountains: *Bulletin of Canadian Petroleum Geology*, v. 18, p. 332-406.
- Jamison, W. R., 1987, Geometric analysis of fold development in overthrust terranes: *Journal of Structural Geology*, v. 9, no. 2, p. 207-219.
- Suppe, J., and Medwedeff, D. A., 1990. Geometry and kinematics of fault-propagation folding. *Ecologiae Geologicae Helvetiae*, v. 83, p. 409-454.

Wickham, J., 1995, Fault displacement-gradient folds and the structure at Lost Hills, California (U.S.A.): *Journal of Structural Geology* v. 17, no. 9, p. 1293-1302.

Williams, G., and Chapman, T., 1983, Strains developed in the hanging-wall of thrusts due to their slip/propagation rate: A dislocation model, *Journal of Structural Geology*, v. 5, p. 563-571.

THE STRUCTURAL, THERMAL, AND FLUID EVOLUTION OF THE LIVINGSTONE RANGE ANTICLINORIUM, AND ITS REGIONAL SIGNIFICANCE TO THE SOUTHERN ALBERTA FORELAND THRUST AND FOLD BELT  
 Geologic Map and Cross Sections of the Southern Livingstone Range

Michael A. Cooley, PhD. thesis, Queen's University, November 2007

